



January 2013

Modeling Arsenic, Antimony, And Selenium Partitioning During Coal Combustion

David W. James

Follow this and additional works at: <https://commons.und.edu/theses>

Recommended Citation

James, David W., "Modeling Arsenic, Antimony, And Selenium Partitioning During Coal Combustion" (2013). *Theses and Dissertations*. 1439.
<https://commons.und.edu/theses/1439>

This Dissertation is brought to you for free and open access by the Theses, Dissertations, and Senior Projects at UND Scholarly Commons. It has been accepted for inclusion in Theses and Dissertations by an authorized administrator of UND Scholarly Commons. For more information, please contact zeinebyousif@library.und.edu.

MODELING ARSENIC, ANTIMONY, AND SELENIUM PARTITIONING
DURING COAL COMBUSTION

by

David William James
Bachelor of Science, Brigham Young University, 2006
Master of Science, Brigham Young University, 2011

A Dissertation

Submitted to the Graduate Faculty

of the

University of North Dakota

In partial fulfillment of the requirements

for the degree of

Doctor of Philosophy

Grand Forks, North Dakota
August
2013

Copyright © 2013 David W. James

This dissertation, submitted by David James in partial fulfillment of the requirements for the Degree of Doctor of Philosophy from the University of North Dakota, has been read by the Faculty Advisory Committee under whom the work was performed, and is hereby approved.

Gautham Krishnamoorthy

Wayne Seames

Steven Benson

Frank Bowman

Evguenii Kozliak

This dissertation is being submitted by the appointed advisory committee as having met all of the requirements of the Graduate School at the University of North Dakota and is hereby approved.

Wayne Swisher
Interim Dean of the Graduate School

Date: _____

PERMISSION

Title Modeling Arsenic, Antimony, and Selenium Partitioning During Coal Combustion

Department Chemical Engineering

Degree Doctor of Philosophy

In presenting this dissertation in partial fulfillment of the requirements for a graduate degree from the University of North Dakota, I agree that the library of this University shall make it freely available for inspection. I further agree that permission for extensive copying for scholarly purposes may be granted by the professor who supervised my dissertation work or, in his absence, by the Chairperson of the department or the dean of the Graduate School. It is understood that any copying or publication or other use of this dissertation or part thereof for financial gain shall not be allowed without written consent. It is also understood that due recognition shall be given to me and to the University of North Dakota in any scholarly use which may be made of any material in my dissertation.

David James

Date 18 July 2013

ACKNOWLEDGMENTS

I express gratitude for those who have provided resources and support for this undertaking. This research was funded in part by each of the following groups or organizations.

- North Dakota Experimental Program to Stimulate Competitive Research Infrastructure Improvement Program
- U.S. Department of Energy EPSCoR RII Program
- University of North Dakota, College of Engineering and Mines, Department of Chemical Engineering
- North Dakota SUNRISE
- University of North Dakota, Graduate School

My sincere appreciation is expressed for members of my advisory committee for their time, guidance, and support during my experience in the doctoral program at the University of North Dakota. Furthermore, the faculty and staff in the UND Department of Chemical Engineering have made all the difference in this experience.

I furthermore take this opportunity to express my deepest appreciation for the support of my wife, our two sons, our extended family members, and the divine inspirations that have come, which have made completion of this undertaking possible.

David W. James

ABSTRACT

Even though greenhouse gas emissions have gained widespread recent attention, they are not the only form of pollution associated with coal. Several trace elements liberated from the coal matrix during combustion represent additional pollutants that must be understood and controlled. These elements have a variety of ways in which they are associated within coal, which impacts how they may be released into the environment. Namely, trace elements are classified as “included,” “excluded,” or “organically bound.” Specific elements—arsenic, antimony, and selenium—are of particular interest due to their semi-volatile nature.

Modeling the partitioning of semi-volatile elements—arsenic, antimony, and selenium—is the focus of this undertaking. Programming was done in C⁺⁺ with particle-time-temperature inputs from computational fluid dynamics software. The developed program is unique in that it combines previous mathematical approaches in conjunction with only recently available experimentally determined speciation details to determine the release of trace elements from organically bound forms and pyritic family minerals. The distribution of mineral inclusions is achieved using a semi-random combination approach in conjunction with computer controlled scanning electron microscopy data sets. Exclusions are taken directly from the data sets and organically bound elemental distribution was achieved by mass balance.

Temperature profiles were correlated with data from a 19kW down-fired furnace burning a Powder River Basin subbituminous coal using the chemical percolation devolatilization model. Particles used in the model have a range of properties that include pure mineral grains, pure coal

particles, coal particles with included mineral grains, and excluded mineral particles. Pyritic family mineral inclusions with larger initial diameters were found to retain a greater fraction of the initial trace elements present than smaller particles. Arsenic and antimony show similar trace element release trends for particles of similar size and temperature profile. Calculations indicate that a larger fraction of the initial selenium contained in pyritic family minerals were released than either arsenic or antimony for both inclusions and exclusions

By rigorously accounting for thermochemical equilibrium, kinetics, and transport experienced by the various associated forms of trace elements inside the coal, this developed model can be used to visualize aspects related to trace element release from pyritic family mineral groups during pulverized coal combustion.

Keywords: *coal, modeling, partitioning, arsenic, antimony, selenium*

TABLE OF CONTENTS

LIST OF TABLES	xv
LIST OF FIGURES	xvii
NOMENCLATURE.....	xxi
1. INTRODUCTION.....	1
1.1. Background.....	1
1.2. Motivation for this Dissertation.....	3
1.3. General Statement of the Problem.....	4
1.4. Scope of Dissertation.....	6
2. LITERATURE REVIEW	9
2.1. Coal Definitions.....	10
2.1.1. TE Partitioning Overview.....	11
2.1.2. TE Partitioning Pathways.....	13
2.1.3. Included, Excluded, and Organically Associated TEs.....	15
2.1.4. Coal Mineral Types and Chemical Analysis.....	18
2.1.5. Trace Element Volatility.....	23
2.2. The Importance of Pyrite.....	26
2.3. Coal Rank Considerations.....	29
2.4. Select TE Species.....	32
2.4.1. Arsenic.....	33
2.4.2. Antimony.....	33

2.4.3. Selenium	34
2.4.4. Impact of Other Elements	34
2.5. Modeling.....	38
2.5.1. Swelling and Shrinking Behavior	38
2.5.2. Fragmentation	39
2.5.3. Partitioning Approaches.....	40
2.5.4. Transition from Microscopic Environment to Flue Gas Environment	41
2.5.5. Modeling History	42
2.6. Summary.....	44
3. MODEL FUNDAMENTALS.....	45
3.1. Assumptions/Limitations	46
3.2. Boundary Conditions	47
3.3. Model Design.....	48
3.3.1. ASTM Analysis	49
3.3.2. CCSEM Mineral Associations.....	50
3.3.3. Mass Balance and Associations	51
3.3.4. Coal PSD.....	51
3.4. ANSYS Fluent	51
3.4.1. Other CFD Package Options.....	52
3.4.2. Gaseous Species.....	53
3.4.3. Primary Pyrolysis.....	54
3.4.4. Char Burnout.....	55
3.4.5. Devolatilization.....	56

3.4.6. Particle Temperature Profile	57
3.4.7. Particle Tracks	57
3.5. Object Oriented C++	58
3.6. Data Solver – The Black Box Explained	59
3.6.1. Particle Size Distribution Development.....	59
3.6.2. Mass Transfer.....	66
4. TEMPERATURE VALIDATION	75
4.1. UND Furnace Specifications	75
4.1.1. Furnace Geometry.....	75
4.1.2. Boundary Conditions/Fluent Specifications	77
4.1.3. Coal Details.....	78
4.2. UND Furnace Temperature Profiles	79
4.3. UND Furnace Volatile and Char Mass Fractions	84
5. MODEL RESULTS AND DISCUSSION	89
5.1. Select Parameter Sensitivities.....	89
5.1.1. Particle Temperature	89
5.1.2. Pulse Duration.....	90
5.2. Inclusions	93
5.3. Exclusions.....	98
5.4. Inclusion/Exclusion Comparisons	101
5.5. Organically Bound.....	102
5.6. (PM10) Fraction.....	103
6. RECOMMENDATIONS AND CONCLUSIONS.....	107

6.1. Recommendations.....	107
6.2. Cautionary Considerations.....	109
6.3. Conclusions.....	110
7. APPENDICES.....	113
Appendix A Excerpts from the C ⁺⁺ Program Operations Manual.....	115
Appendix B Sample Input Files.....	143
Appendix C Sample Output Files	153
Appendix D UND Furnace Diagrams.....	159
Appendix E Other Relationships Used	161
8. REFERENCES.....	165

LIST OF TABLES

Table 2-1 Major minerals found in coal and some related inorganic oxides from ash analysis	21
Table 3-1 Heterogeneous surface reaction kinetic rate data	56
Table 3-2 Melting points of idealized pure components of several minerals typically found in coals	67
Table 3-3 Raoultian activity coefficient of various species	73
Table 4-1 Fuel/carrier gas inlet parameters	77
Table 4-2 Secondary air inlet parameters	78
Table 4-3 Proximate analysis of Southern PRB subbituminous coal	78
Table 4-4 Ultimate analysis of Southern PRB subbituminous coal.....	78
Table 4-5 Ash composition of the Southern PRB subbituminous coal	79
Table 7-1 Idealized formulas of the various mineral groups	121
Table 7-2 TEPCO Jehoshaphat required input file names	133

LIST OF FIGURES

Figure 2-1 Illustration depicting a typical pulverized coal combustion system and related equipment.....	13
Figure 2-2 Behavior of impurities in coal.....	14
Figure 2-3 Illustration of modes of occurrence of inorganic constituents in coal: inclusions, exclusions, and organically bound materials in a porous char	15
Figure 2-4 Relative enrichment and volatility of selected coal trace elements	24
Figure 2-5 Pyrite transformation during combustion	27
Figure 3-1 Developed C++ program model algorithm.....	48
Figure 3-2 Weight percent on a mineral basis of select mineral groups, by mineral particle size, detected by CCSEM for the Southern PRB subbituminous coal.....	61
Figure 3-3 Example Southern PRB subbituminous coal particle size distribution and calculated mineral-free volume particle size distribution equivalent	63
Figure 3-4 Example of calculated results of the number of coal particles generated during the program as well as the number of those particles that actually have any combination of pyrite, pyrrhotite, or oxidized pyrrhotite minerals within those coal particles for a given pulse duration	64
Figure 3-5 Vaporization processes for TEs	68
Figure 4-1 UND 19kw down-fired furnace configuration.....	76
Figure 4-2 Illustration of the differences between devolatilization models predicted temperature profiles and the 19kw down-fired UND furnace burning a Southern PRB subbituminous coal	80
Figure 4-3 Illustration of the ANSYS Fluent modeled static temperature profile described as part of the current investigation for the CPD model	81
Figure 4-4 Plots (a) through (h) of the difference in particle and static temperatures versus particle path length using the CPD model as part of the current investigation	83

Figure 4-5 Modeled UND down-fired furnace volatile mass fractions as a function of time and bin number for all the particle tracks of a Southern PRB subbituminous coal.....	84
Figure 4-6 Modeled UND down-fired furnace time of moisture + devolatilization release as a function of time coal particle size range and bin number for all the particle tracks of a Southern PRB subbituminous coal.....	85
Figure 4-7 Modeled UND down-fired furnace duration of devolatilization as a function of coal particle size range and bin number for all the particle tracks of a Southern PRB subbituminous coal.....	86
Figure 4-8 Modeled UND down-fired furnace particle char mass fractions as a function of path length for all the particle tracks for a Southern PRB subbituminous coal.....	87
Figure 5-1 Plot depicting the fraction of combined total number of coal particles containing pyritic family minerals by particle track bin number	91
Figure 5-2 Plot depicting the fraction of combined included pyritic family mineral surface area by particle track size range and bin number.....	92
Figure 5-3 Contour plot of predicted arsenic released from pyritic family mineral inclusions for UND furnace; darker colors represent higher localized concentrations	94
Figure 5-4 Contour plot of predicted antimony released from pyritic family mineral inclusions for UND furnace; darker colors represent higher localized concentrations	95
Figure 5-5 Contour plot of predicted selenium released from pyritic family mineral inclusions for UND furnace; darker colors represent higher localized concentrations	95
Figure 5-6 Plot depicting the overall arsenic, antimony, and selenium fractions released from pyritic family mineral inclusions found within each of the coal particle bins and size ranges indicated.....	97
Figure 5-7 Plot depicting the overall arsenic, antimony, and selenium fractions released from pyritic family mineral exclusions found within the mineral particle size ranges indicated	99
Figure 5-8 Plot depicting the cumulative percent of the total arsenic released from exclusions based on initial mineral size, μm , and distance from the top of the furnace	100

Figure 5-9 Plot depicting the cumulative percent of the total selenium released from exclusions based on initial mineral size, μm , and distance from the top of the furnace	101
Figure 5-10 Contour plot of predicted initially organically bound arsenic released for UND furnace; darker colors represent higher localized concentrations.....	103
Figure 5-11 Graph of PM10 for full assimilation of mineral inclusions, no assimilation of inclusions, and experimentally determined outlet fly ash sizes (as taken by other graduate students) for the UND furnace with the localized-measured- high temperatures shown.	104
Figure 7-1 TEPCO Jehoshaphat program icon	132
Figure 7-2 Opening program example screen.....	132
Figure 7-3 Program example display of number of particles in each size bin.....	134
Figure 7-4 Program example display of coal organically bound elemental total mass for pulse and mass fraction of organically associated metals.....	135
Figure 7-5 Program example screen to determine if the trace element and organically bound sections of the program should be executed	136
Figure 7-6 Program example screen to determine if the inclusion section should be continued.....	137
Figure 7-7 Example console messages shown from the program depicting k values of arsenic release from the specified particle.....	137
Figure 7-8 Program example screen to determine if the exclusion section should be executed	138
Figure 7-9 Example mesh of the UND 19kW down-fired furnace inlet.....	159
Figure 7-10 Illustration of the UND 19kW down-fired furnace	160

NOMENCLATURE

Abbreviations

ASTM	American Society for Testing and Materials
CCSEM	Computer Controlled Scanning Electron Microscopy
CFD	Computational Fluid Dynamics
CPD	chemical percolation model
DOE	Department of Energy
EPSCOR IIP	Experimental Program to Stimulate Competitive Research Infrastructure Improvement Program
hhv	higher heating value
PRB	Powder River Basin
PSD	particle size distribution
SCR	Selective Catalytic Reduction
TEs	trace element(s)
TEPCC	Trace Element Partitioning During Pulverized Coal Combustion

Chemical Species

Al	aluminum
As	arsenic
Ba	barium
C	carbon
Ca	calcium
Cl	chlorine
Cu	copper
F	fluorine
Fe	iron
H	hydrogen
K	potassium
Mg	magnesium

Na	sodium
Ni	nickel
O	oxygen
P	phosphorus
Si	silicon
S	sulfur
Sr	strontium
Ti	titanium
CO	carbon monoxide
CO ₂	carbon dioxide
H ₂	hydrogen
H ₂ O	water
N ₂	nitrogen
O ₂	oxygen
SO ₂	sulfur dioxide
vol	volatile component of coal particle

Symbol and Meaning,

L = length, t = time, T = temperature, M = mass

<i>A, B</i>	coefficients for various correlations	-
<i>A</i>	Arrhenius rate expression pre-exponential factor	
<i>C_{i,b}</i>	bulk concentration of solute i in the melt	mole/L ³
<i>C_i</i>	concentration of gas i in bulk	mole/L ³
<i>d_p</i>	diameter of particle	L
<i>D_{αβ}</i>	Binary diffusivity for the pair α-β in a multi-component system	L ² /t
<i>D_i</i>	effective Knudsen diffusivity	
<i>D_{oxy}</i>	diffusivity of oxygen in the bulk gas	
<i>D_m</i>	diffusivity of element i in the bulk gas	
<i>E</i>	activation energy	
<i>J_i</i>	overall mass transport rate	mole/L ³ t
<i>J_i</i>	molar flux	mole/L ²
<i>k</i>	overall mass transfer coefficient	
<i>k_L</i>	mass transfer coefficient through melt	
<i>k_E</i>	mass transfer coefficient at surface	
<i>k_U</i>	mass transfer coefficient through pores	
<i>k</i>	Arrhenius rate constant	
<i>M_i</i>	molecular weight of species i	M/mole
<i>n</i>	moles	mole
<i>P</i>	pressure	M/Lt ²
<i>P_i^o</i>	vapor pressure of the pure element	
<i>r_i</i>	inclusion radius	
<i>R</i>	gas constant	moleL ² /t ² T
<i>SA</i>	surface area	L ²
<i>t</i>	time	t

	T	absolute temperature	T
	V	volume	L^3
	V_m	Mineral grain volume	L^3
	V_{mfree}	Mineral free volume	L^3
	X_i, Y_i	mole fraction of species i	-
	Y_i	mole fraction of solute i in melt	-
 <i>Greek Symbols</i>			
alpha	α	relative volatility	
alpha	α'	re-condensation coefficient	
gamma	γ_i	Raoultian activity coefficient of solute i in the infinitely dilute solution	
kappa/epsilon	κ/ϵ	Lennard-Jones parameter	T
mu	μ_γ	viscosity of gas	M/Lt
Pi	π	3.14159....	-
rho	$\rho_s, \rho_l, \rho_p, \rho_g$	density solid, liquid, particle, gas	M/L^3
sigma	σ	collision diameter	L
phi	$\Phi_{\alpha\beta}$		
omega	$\Omega_{\mu}, \Omega_k, \Omega_D$	collision integrals	-

1. INTRODUCTION

1.1. Background

Fossil fuels supplied more than 82% of the United States energy in 2011 (U.S. Department of Energy 2013). Coal is a robust fossil fuel that provides ~37% of the United States electric power sector's net generation. It is anticipated that even though other forms of electric power generation are being developed, the usage of coal will continue to develop and increase over the next few years (Freese 2010). However, governmental legislations—including the Utility – Mercury and Air Toxics Standards – Act (U.S. Environmental Protection Agency 2011), the endangerment finding provided by the US Environmental Protection Agency (2009), as well as the previously enacted Clean Air Act and its related amendments (Clean Air Act 1963)—have put the economic viability of coal use into question. Federal, academic, and industrial energy sectors are working collaboratively to find viable means of clean power generation technologies that will avoid economic losses that may ensue as a result of regulations.

Some may envision a future of non-fossil fuel energy generation; however, technology and infrastructure are not in place to make this aspiration the present reality (Baxter 2009). Coal and other fossil-fuel-based energy sources provide relatively inexpensive power, which is desirable to nations facing increasing financial burdens. The ability to economically transition from current power systems to new, reliable technologies is seen as primary issue affecting the sustainability of coal as a main source of energy (Seames 2005, 2008). Even though greenhouse

gas emissions have gained widespread recent attention, they are not the only form of pollution associated with coal. *Trace elements* (TEs) liberated from the coal matrix during combustion may represent the source of additional pollutants that must be controlled. Although some elements are listed as hazardous air pollutants they can be essential to life. Selenium is an example of a life essential element that if it is present in too great a quantity it can be harmful. In addition, impurities within coal impact the reliability of advanced power systems that are being developed to aid in carbon capture and sequestration technologies (Seames 2008). Arsenic has the noted potential of causing deactivation of catalysts used in selective catalytic reduction systems for NO_x control (Senior et al. 2006; Baxter 2005).

Trace elements have a variety of ways in which they are associated within coal that will determine how they are partitioned during combustion. This will eventually impact their size distribution and determine if they exit the combustion system in vapor form or as particulate matter. This, in turn, determines the effectiveness of pollution control devices in capturing TEs. Namely, TEs can be related to coal as inclusions and exclusions or can be organically bound in the coal matrix (Finkelman 1994).

Specific elements, including arsenic, antimony, and selenium, are elements of particular interest due to their semi-volatile nature. These elements have known associations with pyritic family minerals. Each type of TE association within coal must be understood so that improvements in technology such as new configurations, operating modes, and remediation processes may continue to be developed.

Understanding the impact of the mode of occurrence on TE liberation can be accomplished through modeling. Modeling coal combustion behavior is not a new field.

However, in part due to the complexity of the multifarious nature of coal, publically available codes that describe TE liberation seem to be unavailable. Trace element modeling represents an area in which improvements can be made to help ensure the viability of the coal industry for the foreseeable future, especially if the models are versatile enough to account for multiple environments. Furthermore, as new energy conversion technologies such as oxy-combustion and gasification are being investigated, a fundamental understanding of how the changes in the operating conditions will impact partitioning should be determined.

Understanding TE behavior is important for several reasons. Primarily, TEs released during coal combustion may be hazardous environmental pollutants. Additionally, they pose the risk of poisoning emission control catalysts. Released TEs also have the potential to cause unwanted equipment corrosion. Trace element partitioning is also important at this time as TEs have the potential to greatly affect carbon capture and sequestration technologies. By being able to identify when, where, and how a TE is released from the coal matrix, methods of remediation can be put into place.

1.2. Motivation for this Dissertation

Within the combustion zone, environmental properties vary as a function of time and space due to inherent temperature and kinetic dependencies and due to the presence of both oxidative and reducing environments that are within and surrounding a particle. Quantitative determination of partitioning during pulverized coal combustion processes is not available in current publically available modeling programs. It requires detailed kinetic, heat transfer, and mass transfer relationships within individual coal particles, which may have previously been too computationally expensive.

Analytical solutions have been limited due to the mathematical complexity of the process as well the persistent kinetic rate, elemental speciation, and mass transfer data information gaps that are needed to describe the behavior of TE species. A computer model is needed to help users visualize and see trends relating locations with a furnace where TEs will initially release. Mathematical models are not enough, as they cannot fully connect the effects of the time-temperature dependent nature of coal combustion.

1.3. General Statement of the Problem

This research project undertakes modeling to predict TE partitioning by using computer programming in conjunction with *computational fluid dynamics* (CFD) software. The program developed describes TE liberation from the coal matrix during the combustion zone based on the initial form of the TE. The developed program also incorporates aspects found in various mathematical models previously developed by other researchers (Zeng, Sarofim, and Senior 2001; Yan 2000; Srinivasachar and Boni 1989; Srinivasachar, Helble, and Boni 1990; Bool III et al. 1997; Quann and Sarofim 1982; Krishnamoorthy and Veranth 2003; Ohno 1991; Bird, Stewart, and Lightfoot 2002; Wilke 1950; Richard 1996) while incorporating kinetic data relating to likely TE speciation that had previously been unavailable (Raeva 2011; Raeva et al. 2012; Raeva, Klykov, et al. 2011; Raeva, Pierce, et al. 2011). The program is also an enhancement of the mass transfer approach originally described by others (Zeng, Sarofim, and Senior 2001).

A semi-random distribution of mineral particles, which is based on *computer-controlled scanning electron microscopy* (CCSEM) data to generate statistically plausible coal particles with individualized composition, is developed. This methodology should provide better estimates

of mineral particle surface area, which is ultimately related to the flux of TEs from a coal particle during combustion.

The combination of particle track time-related temperature profiles from ANSYS Fluent and the developed program should help show users the regions within a furnace where TEs are released during pulverized coal combustion. By using the combined efforts of Fluent and the developed program, a means of understanding TE liberation from each of the TE modes of occurrence, “included,” “excluded,” and “organically bound” species, is undertaken.

To be applicable a model must incorporate (1) combustion system design characteristics, such as furnace design configuration, furnace size, burner arrangement, and combustion system thermal behavior, as well as (2) fuel properties, such as total ash content of the coal, ash constituents and properties, trace species thermodynamic properties, trace species’ modes of occurrence, distribution of mineral matter, and the distribution of trace species (Ratafia-Brown 1994).

Within the combustion zone, environmental properties vary as a function of time and space due to inherent temperature dependencies as well as the presence of both oxidative and reducing environments that are within and surrounding a particle. Mass and energy conservation as they relate to arsenic, antimony, and selenium represent the heart of this project.

The work described in this document is a part of a multi-task (DOE North Dakota Experimental Program to Stimulate Competitive Research Infrastructure Improvement Program) project (DOE contract # DE-FG01-05ER05-03 and DE-FG02-06ER46292) and may be useful for governmental, industrial, and academic entities that focus on TE partitioning within a

pulverized coal combustion process. This model incorporates details found in other mathematical models previously developed into a single computer program while incorporating kinetic data that has previously been unavailable.

Use of the kinetic data is one of the novel aspects of this research undertaking. However, the single most notable advance is the ability to treat TEs in each regime (inclusions, exclusions, and organically bound) separately and at conditions that more closely represent the actual conditions in these regimes. Previous efforts have exclusively used bulk conditions to predict TE behavior in coal combustion systems.

1.4. Scope of Dissertation

The current investigation utilizes advanced analytical characterization data plus thermodynamic and transport properties, including the velocity, composition, and temperature profile histories of particles within a pulverized-coal-combustion furnace. Physical transformations, such as fragmenting, melting, and coalescing of inorganic components during combustion are incorporated.

Computational fluid dynamic modeling of coal combustion within a furnace is first undertaken to determine the temperature histories possibly experienced by the individual coal particles during the combustion process. The modeling of coal is undertaken in a Lagrangian framework. These temperature histories then constitute a portion of the input into the TE partitioning model. It is important to note that TE modeling is undertaken in a post-processing manner with no feedback from the TE modeling program back to the CFD simulations. This

method is undertaken because the energy and mass source terms arising from the TE modeling will not significantly impact the global energy and mass balances within the furnace.

Text files formatted for the C⁺⁺ simulation environment form the backbone of the user interface. Data for the text files originates from CCSEM, proximate and ultimate coal analyses, furnace-specific geometrical and operational inputs, and data files from converged Fluent or other CFD software that portray the time-temperature profiles of coal combustion particles. The model developed is called TEPCC Jehoshaphat (**T**race **E**lement **P**artitioning during **C**oal **C**ombustion) and it includes subroutines to describe a semi-random mineral combination approach to determine the composition of coal particles, as well as initial TE partitioning from included pyritic family minerals, excluded pyritic family minerals, and TEs that originated as organically bound elements.

The remainder of this work is divided into the following chapters: *Chapter 2* provides a general literature review of trace element partitioning. Definitions related to the topic are also elaborated. *Chapter 3* provides foundational aspects of the developed model. The semi-random distribution of mineral groups is included. Attributes related to the coal used in this endeavor are also provided. *Chapter 4* reviews the use of CFD and related input parameters. Validation of the bulk temperature condition used in the particle tracks of the model is set forth. Next, *Chapter 5* examines results from the developed computer program and provides insights relating to observed trends. *Chapter 6* summarizes the discussion. Finally, a user manual for the developed computer program is provided in the appendices of this document.

2. LITERATURE REVIEW

Published literature reviews and research relating to the current state of understanding TE partitioning during coal combustion seem to increase after new governmental regulations are given. An expansion in research was particularly seen by the flux of papers presented on hazardous air pollutants after the Clean Air Act (Clean Air Act 1963) and its accompanied amendments were passed. Recent attention was regained in the field of clean coal technologies after the Endangerment finding was released in 2009 (U.S. Environmental Protection Agency 2009). Over the years a great deal of research on the topic of TE partitioning has been undertaken. Trace elements can act as catalyst poisons, which can in turn affect the remediation abilities of pollution control devices. The reviews and works of Werka et al., Rataia-Brown, Swaine, Davidson and Clarke, Xu et al., and Vejehati et al. vary in terms of expanse and focus but have been valuable to understanding some of the sciences related to coal technologies and utilization (Ratafia-Brown 1994; Xu et al. 2001; Xu et al. 2004; Wewerka et al. 1976; Vejehati, Xu, and Gupta 2010; Sen 2010; Davidson and Clarke 1996; Swaine 1994).

This literature review includes the following sections. *Section 1* provides general definitions that are required for a thorough discussion of the topic of TE partitioning. Though not a focus of this dissertation, a brief discussion of analytical techniques used in determining the modes of occurrence of TE species is also provided. *Section 2* elaborates on the role of pyrite in TE partitioning. *Section 3* discusses coal rank considerations. *Section 4* discusses three TE

species of interest and known relationships to them. Finally, *Section 5* details a brief synoptic history of modeling TE partitioning and some of the challenges that have been encountered in the past by other researchers.

2.1. Coal Definitions

Coal is a complex solid fossil fuel comprised of moisture, ash precursor materials, carbon, hydrogen, oxygen, nitrogen, and sulfur. Every piece of coal is unique in structure and composition. Nearly every, if not all, naturally occurring elements can be found within coal or coal-derived materials. For the purpose of this discussion, TEs are elements that are found in less than 0.1 weight % (1000 ppmw) of a coal's composition. Several of these elements are found on the scale of ppb and ppt.

Because of the multifarious nature of coal, illustrations depicting coal structure are simply well thought out drawings. There is no defined, rigid chemical configuration that can depict the composition of every piece and type of coal or even the chemical formula of two sections from the same coal seam. The result of the unique nature in which coal develops is illustrated by the wide distribution of maceral types (microscopically recognizable constituents in coal), dependent in the characteristics of initial plant material, the deposition environment, and the degree of coalification. Thus, different coals have independent distinctive properties.

Before the 1970's only limited attention was given to the chemistry of TEs in coal, and much of that was applied to coal wastes (Wewerka et al. 1976). However, techniques of detection, quantification and early modeling of TEs were beginning to be explored by early

pioneers within this field of study by the mid 1970's. These early researchers' works formed the foundation of the chemistry techniques used to analyze coal.

2.1.1. TE Partitioning Overview

Trace element partitioning during coal combustion depends upon its form of occurrence in the coal, the TEs volatility, and/or the solid-to-vapor-phase transformation mechanisms available to the TE within the combustor (Senior et al. 2001). Species that are partially or fully vaporized will undergo additional partitioning downstream as flue gas cools. According to Ratafia-Brown, this could include (1) heterogeneous condensation on entrained fly ash particles and heat transfer surfaces, (2) physical adsorption/chemisorption on fly ash particles, (3) homogeneous condensation and coalescences as submicron aerosols if super-saturation conditions exist, (4) homogeneous and heterogeneous chemical reaction among TEs, fly ash, and flue gas constituents, as well as (5) continuation in the vapor phase for species with high vapor pressures at typical exit temperatures (Ratafia-Brown 1994). It should be noted that only mechanism 2 is not volatility dependent. Some semi-volatile TEs are unlikely to experience mechanisms 1 and 4 in well-controlled environments. For example, the laminar behavior in small drop tube furnaces may inhibit interaction with the TEs on interior walls. More over regional super saturation conditions of a TE would be minimized by design characteristics.

Other researchers showed that during small scale testing at a combustion peak temperature of 1540 K, some TEs vaporize in the combustion zone, and then upon gas cooling partition back to the liquid and solid phases onto the surface or pores of super-micron-size particles in the post-combustion zone (Seames and Wendt 2000c; Seames 2000). Some coals favored reactive partitioning mechanisms while others favored a sorption mechanism. A

significant fraction of the original TEs present remained in the solid phase throughout the combustion system (Seames and Wendt 2001; Seames 2000). This behavior is likely due to the mode of occurrence of the TE (mineral, organic, or water associations) (Finkelman 1994; Raask 1985) as well as the specific conditions (temperature, oxygen concentration, residence time) to which the specific TE is exposed.

All methods describing partitioning have similar attributes. However, the differences are more related to the details of the combustion system studied rather than real discrepancies. The main difference observed within literature is the location in which the mechanisms are proposed to occur. It has been demonstrated that all the vaporization mechanisms occur in the near environment immediately surrounding the burning coal and not later in the post combustion environment (Seames and Wendt 2001). Interactions with sulfur, halogen containing gases, and aerosols downstream will also occur.

An illustration of typical equipment related to pulverized coal combustion technologies is found in Figure 2-1. Forms of occurrence of a TE species initiate within the system through the coal supply, and the TEs are released from a coal particle within the combustion zone. Based on the principles of the conservation of matter and energy, only a finite number of pathways exist in which trace materials can exit a typical pulverized coal combustion system. For the present illustration, TEs can exit with the fly ash or as a vapor within the flue gas of the stack, within the bottom ash, or through the exit streams of pollution control technologies that are present in a given system. Otherwise, accumulation of TEs within the system occurs. Many models developed have an inherent degree of uncertainty. Mass imbalances can occur as TEs can

condense and/or absorb on interior surfaces of equipment. Arsenic has shown a tendency of depositing on heating surfaces (Ratafia-Brown et al. 2002).

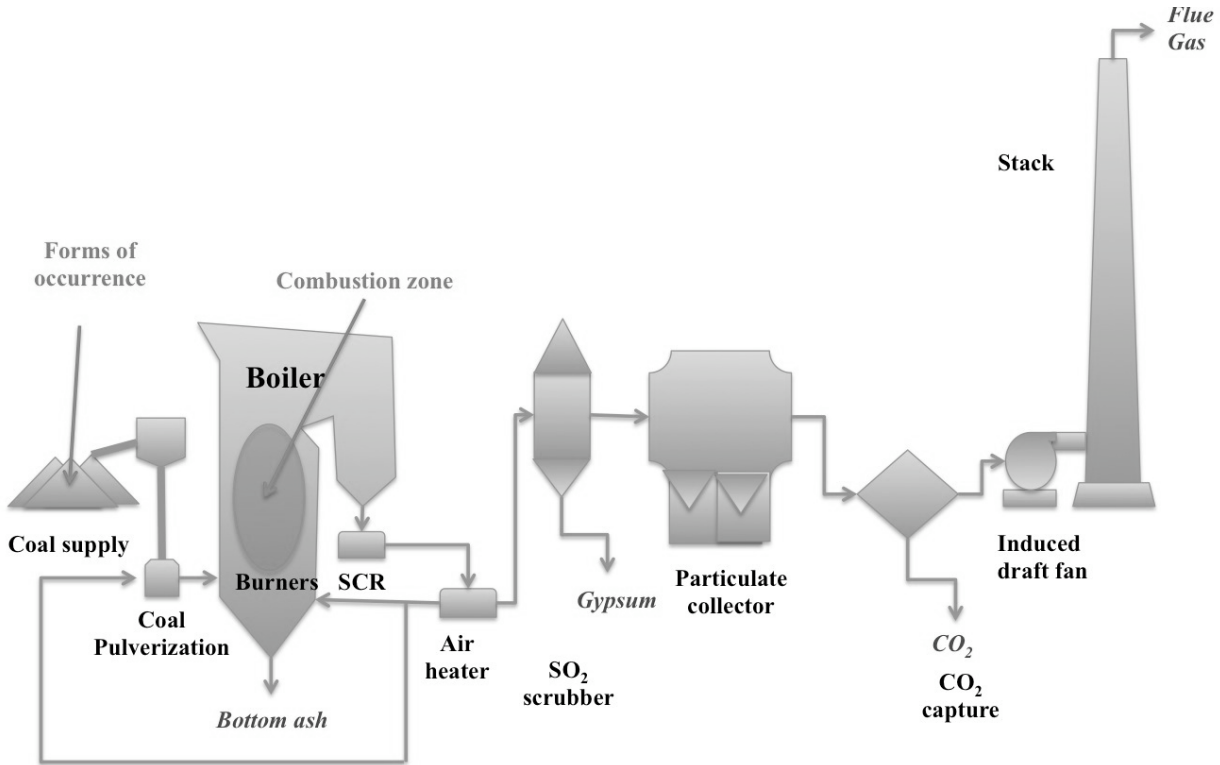


Figure 2-1 Illustration depicting a typical pulverized coal combustion system and related equipment

For the present discussion, fly ash is defined as the particulate matter that escapes the combustor with the flue gas. The impacts of a CO₂ capture technologies on the release of a TE is ambiguous at this time, as CO₂ capture technologies are still being developed.

2.1.2. TE Partitioning Pathways

During combustion, inorganic coal components may be found in vapor, liquid, and/or solid forms. Within the different physical phases, complex physical and chemical transformations produce intermediate ash species. An illustration of proposed physical transformation pathways of TE partitioning is found in Figure 2-2 (Benson 2011).

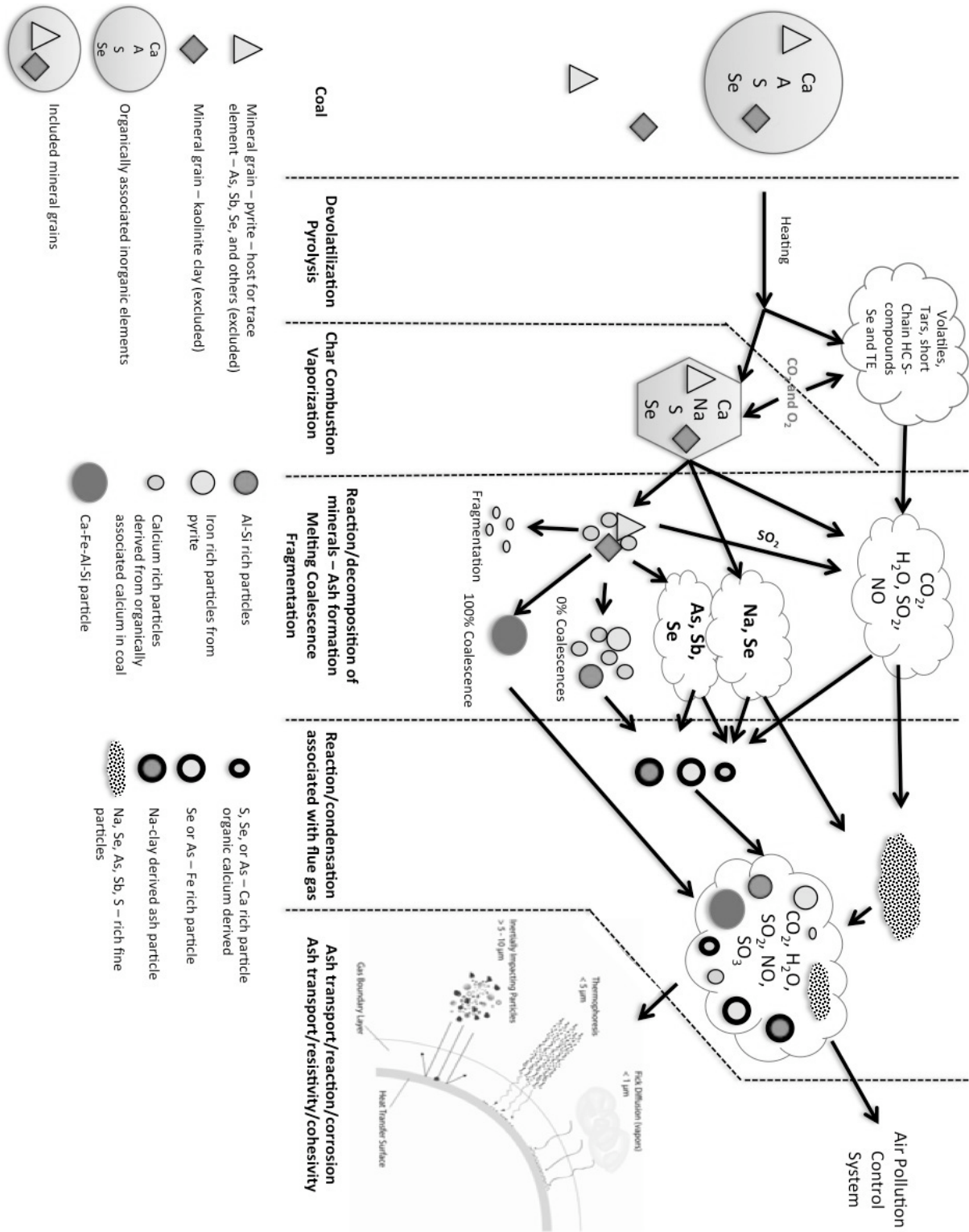


Figure 2-2 Behavior of impurities in coal (Benson 2011)

Figure 2-2 illustrates the types of transformations that are likely to occur during the coal combustion process for included TEs. A networked depiction of TE behavior was previously proposed by others (Senior 2000). The primary point of any given illustration has been to indicate that there are multiple pathways in which an element may travel until it reaches its final destination. The focus of this dissertation is restricted to the initial partitioning that occurs within the furnace combustion zone.

2.1.3. Included, Excluded, and Organically Associated TEs

As shown in Figure 2-2, a variety of partitioning pathways are present during coal combustion and must be understood in order to accurately describe TE partitioning behavior. Furthermore, this figure details that the origination sources of TEs found in coal are listed as portions of included minerals, portions of excluded minerals, and organically bound elements within the coal. A larger macro-scale illustration of this distinction is shown in Figure 2-3 (Raask 1985; Senior et al. 2001; Seames 2005, 2000).

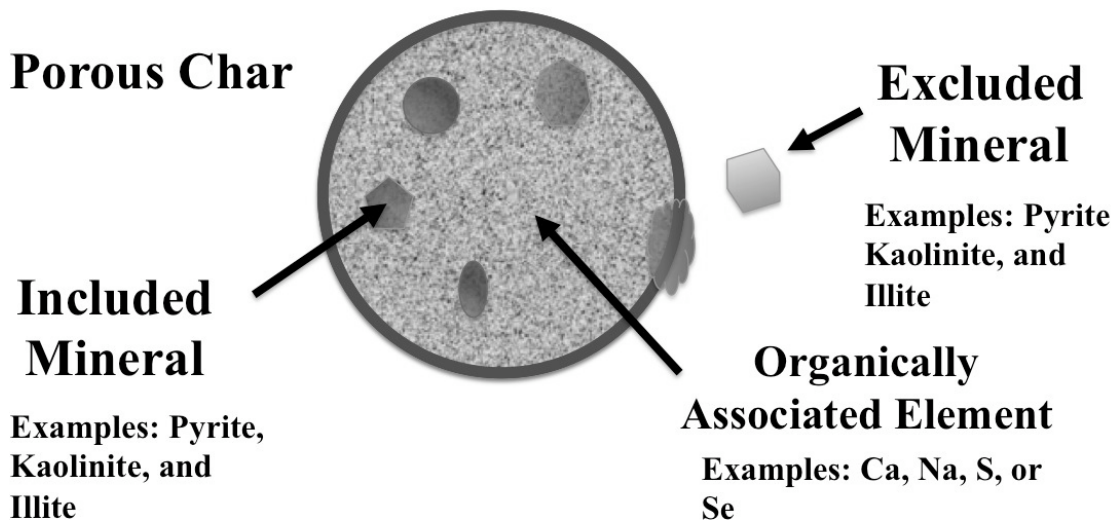


Figure 2-3 Illustration of modes of occurrence of inorganic constituents in coal: inclusions, exclusions, and organically bound materials in a porous char (Raask 1985)

After combustion takes place it is difficult to distinguish between elements that were initially included, excluded, or organically bound other than by where the species' collect (i.e., with the bottom ash, fly ash, or vapor). Included and excluded minerals are exposed to different combustion environments. This is a key factor for accurate modeling of TE partitioning. Understanding the definitions of each mineral type is important for the present discussion.

Milling can affect the mineral distribution in pulverized coals. Large original mineral grains and those that are weakly bonded with coal macerals tend to be liberated after milling (Yan 2000). Alternatively, finely grained minerals tend to not be affected as much by milling. High-density minerals grains and particles with higher mineral loading tend to be finer than organic-rich coals after milling because a mill classifier recycles heavier particles (Wigley, Williamson, and Gibb 1997). The implication of these statements is that although a mineral grain may start out included the minerals grains may be liberated from the organic matrix depending on the size of the parent mineral and the processing it receives.

The coal carbon matrix encapsulates *included minerals* during coalification. During combustion this type of particle encounters high temperatures, a reducing atmosphere. Inclusions have greater driving force towards liquefaction, diffusion, and vaporization compared to exclusions. Both included and excluded minerals are often hosts to volatile TE species of importance in pollution control technologies. Examples of TE-containing inclusions and exclusions include a wide variety of minerals such as pyrite, kaolinites, and illite.

Included minerals may be exposed to both reducing and oxidative environments during the temperature history of the particle. As the char is consumed, reactions near the surface of the particle consume most of the oxygen available. The center portion of the particle has reducing

conditions. Oxidation of included species will generally occur more readily closer to the surface rather than in the inner regions of the particle. Therefore, most oxygen is consumed by reaction with carbon before it can diffuse into the pores of the char in any great extent (Sarofim and Helble 1993). The liberation of the carbonaceous materials causes the weight fraction of the mineral derived ash components to increase. The center of the particle is exposed to greater oxygen contents after the carbon content is liberated. Exposed elements will be able to further react and change. The changes that occur are related to both the temperature, and the overall oxidative state of the species. Differences in time and position could yield great differences when it comes to the reactivity of the elements while they are released.

Trace elements in the larger inclusions and exclusions encounter an environment with temperatures from 1800 K to the burning char temperature depending on relative proximity to the char. The temperature of the char is such that many of the included-inorganic-based mineral particles will melt or soften (Seames 2005). Localized conditions determine the quantity of a TE that may be liberated from its parent structure. The quantity liberated is generally a function of the vapor pressure of the TE over the melt (Zeng, Sarofim, and Senior 2001).

Melted materials reorganize into structures with the lowest energy state. The lowest energy structure provides the characteristic spherical shape of the fly ash particles. Trace elements contained in these solid structures are less likely to volatilize (Seames 2005). However, the oxidation of pyritic family minerals is exothermic and may allow for additional vaporization of TEs.

Excluded minerals are inorganic constituents that may be mixed with the coal after coalification but are not intrinsic parts of the coal. This means that they tend to encounter lower

temperatures and neutral/oxidizing conditions, which have the potential to impact the release of the TEs by vaporization during combustion. Physical characteristics of the minerals influence melting behavior, relative position to other minerals, and transformations that may occur such as coalescence, fragmentation, and vaporization. The limited transport driving forces that may be seen for this type of particle are more important for modeling purposes than other phenomena.

Trace elements bound within the center core of included/excluded minerals are limited by diffusion, which likely contributes to the overall capture of trace materials. It is due to pore diffusion limitations that particle size has a great impact on the partitioning of materials within a given boiler. If the size is smaller the TEs can “escape” more easily to the bulk phase where they can interact with other elements.

Organically bound TEs include those elements that are bonded to carbon-based compounds within the coal (Vassilev and Tascón 2003). This type of element sees very high temperatures, a reducing atmosphere, and is released from the coal matrix as its carbon bonds break. After volatilization, the species must diffuse out of the surrounding structure, and past the boundary layer, to enter the bulk gas phase (Zeng, Sarofim, and Senior 2001). Some of these organically bound trace elements include Al, As, Ba, Ca, Cl, Fe, K, Mg, Na, S, Sb, Se, Si, Sr, and Ti.

2.1.4. Coal Mineral Types and Chemical Analysis

The associations of TEs prior to combustion will affect the phase, size and composition, distribution in the residual ash, and gas exit streams from a furnace. The three primary inorganic associations include cations dissolved in the pore water of coal, organically associated cations,

and discrete minerals (Benson et al. 1995). Water-associated constituents are generally in the form of sulfates or chlorides.

Organically associated TE species are generally found as salts of carboxylic acid groups bound within the carbon matrix and as coordination complexes (Benson et al. 1995). Associated TEs may include, among others, Hg, Se, Be, B, Sb, Ge, Co, Ni, and Cu. It is also suggested that TEs are associated with certain functional groups within the organic matter. These groups include carboxylic acid (-COOH), phenolic hydroxyl (-OH), mercapto (-SH), and imino (=NH) (Swaine and Goodarzi 1995). The presence of certain functional groups is related to the age of the coal. Some functional groups are no longer present as a coal changes during the coalification process.

For most coals, TEs: (1) are mainly associated with mineral matter, (2) are present as discrete minerals either free or embedded in the organic matter, (3) act as replacement interstitial species in minerals, and (4) are adsorbed on minerals (Swaine and Goodarzi 1995). The mineral matter of coal as part of the inorganic matter consists of various mineral species that belong to sulfides, sulfosalts, oxides-hydroxides, silicates, sulfates, carbonates, phosphates, chlorides, native elements, vanadates, and tungstates (Vassilev and Vassileva 1996; Vassilev and Tascón 2003). The amounts and kinds of minerals vary greatly and are undoubtedly related to the formation conditions of the coal (Valković 1983).

It is important to understand which minerals are present as they have the potential to behave differently while in the combustion zone. For example, the release of CO₂ from carbonates tends to increase the potential for fragmentation of the carbonate minerals. Clays with high levels of moisture may also fragment because of the release of H₂O from their porous

structures (Benson et al. 1995). Pyrite also tends to fragment during coal combustion (Jassim et al. 2010; Seames, Jassim, and Benson 2010; Srinivasachar and Boni 1989).

Coal combustion and its related TE partitioning behavior are dynamic in nature, and every subsequent step relies upon the previous step within the process. The particle size distribution of mineral grains strongly influences the kinetics and diffusion resistances involved in mineral reactions (Gupta et al. 2005). Fragmentation affects particle size, which affects temperature and, hence, the rate of TE evolution.

A list of common coal mineral groups and their related oxide ash species is found in Table 2-1 (Huggins 2002; Baxter 2010; Valković 1983). The list of minerals provided in Table 2-1 is not all-inclusive yet shows commonly present minerals in coal as well as TEs that may be associated with a given mineral grouping. The ash oxides show some of the paths whereby an inorganic constituent could have evolved from within the coal particle.

Chemical analyses provide valuable mineralogical data, such as the contents of carbonate CO₂, as well as pyritic, sulfate, or elemental sulfur. However, several issues exist with regard to chemical analysis for the calculation of original minerals present in coal by stoichiometric relationships: (1) elements have both organic and inorganic associations in coal; (2) some species are amorphous; (3) minerals can show significant variation in chemical composition; and (4) some elements can be volatilized during analysis (Vassilev and Tascón 2003).

Several options are available to determine the mineral matter composition, amount, and presence within coal. A thorough review of the subject is given by Vassilev (Vassilev and Tascón 2003). One of the primary methods used to determine the associations of inorganic

Table 2-1 Major minerals found in coal and some related inorganic oxides from ash analysis (Huggins 2002; Baxter 2010; Valković 1983)

Major Oxides in Ash	Common Minerals	Idealized Formula
	<u>Silicates</u> assoc with: B, Be, Ba, Co, Cr, Cu, Mn, Mo, Pb, Sb	
Al ₂ O ₃	Kaolinite	Al ₂ Si ₂ O ₅ (OH) ₄
	Illite	K _{0.75} (Al ₂)Al _{0.75} Si _{3.25} O ₁₀ (OH) ₂
K ₂ O	Muscovite	KAl ₂ (AlSi ₃ O ₁₀)(OH) ₂
	Chlorite**	Fe ₅ Al ₂ Si ₃ O ₁₀ (OH) ₈
Na ₂ O	Montmorillonite	Na _{0.75} Mg _{0.7} Al _{3.3} Si ₈ O ₂₀ (OH) ₂
	Plagioclase	(Na,Ca)Al(SiAl)Si ₂ O ₈
	<u>Carbonates</u> assoc with: Ba, Mn, Fe, Sr, Zn	
CaO	Calcite	CaCO ₃
	Aragonite	CaCO ₃
MgO	Dolomite	CaMg(CO ₃) ₂
	Ankerite	CaCO ₃ *(Mg, Fe, Mn)CO ₃
MnO	Rhodochrosite	MnCO ₃
	Siderite*	FeCO ₃
	<u>Oxides</u> assoc with: Cr, Ti	
SiO ₂	Quartz	SiO ₂
	Hematite	Fe ₂ O ₃
TiO ₂	Rutile	TiO ₂
	Alumina	Al ₂ O ₃
	Periclase	MgO
	<u>Sulfates</u>	
SO ₃	Gypsum	CaSO ₄ *2H ₂ O
	Jarosite**	(Na,K) Fe ₃ (SO ₄) ₂ (OH) ₆
BaO	Barite	BaSO ₄
	Thenardite	Na ₂ SO ₄
	Szomolnokite*	FeSO ₄ *H ₂ O
	<u>Sulfides</u> assoc with: As, Cd, Cu, Hg, Mn, Ni, Pb, Sb, Se, Zn	
Fe ₂ O ₃	Pyrite*	FeS ₂
	Pyrrhotite	Fe _{1-x} S (x=0 to 0.17)
	<u>Phosphates</u> assoc with: Rare Earth Elements	
P ₂ O ₅	Apatite	Ca ₅ (PO ₄) ₃ (OH)

—————> Defining contributors of what oxides seen from a normative analysis
 - - - - -> Subordinate contribution - other minerals are primary source of oxide

* Defined by forms of sulfur analysis

** Additional iron being components that could be defined by Mossbauer Analysis

components in coals is CCSEM, which has been in use and development for more than 30 years. CCSEM provides quantitative means to determine the abundance, shape and size of mineral grains, chemical form of minerals, and mode of occurrence of inorganic components of coal (Gupta 2007; Gupta et al. 2005; Huggins 2002).

Scanning electron microscopy is one of the best methods for mineral matter characterization of coal (Vassilev and Tascón 2003). The key components of a CCSEM system that make it possible to image and analyze inorganic particles are the automated scanning electron scanning electron microscope and related programs used to scan preselected areas of a polished sample to collect backscattered electron images (Gupta et al. 2005; Vassilev and Tascón 2003). Backscatter electron imaging can be used in CCSEM because the intensity of the backscattered electrons is a function of the average number of the features on or near the surface (Gardener 2009). The grains are classified into some known mineral, based on heuristics rules, using energy dispersive x-ray spectrums in conjunction with CCSEM. This, in turn, determines the elemental composition of each grain. The obtained images are used to determine the mineral type, mineral size, and if the mineral is included or excluded (Gupta et al. 2005; Vassilev and Tascón 2003).

High temperature ashing can be used concurrently to determine the abundance of TEs within coal. This technique involves the oxidation of the coal at 773 K to 1088 K followed by chemical analysis of the resultant ash. This method is not without error, and should be interpreted with caution. Volatilization of elements, and alteration, decomposition, transformation and recrystallization can occur that will lead to erroneous conclusions. Loss of water from clay minerals, sulfur from pyrite, and CO₂ from carbonates are just a few of the

issues that further complicate the analysis (Miller, Yarzab, and Given 1979; Vassilev and Tascón 2003).

Chemical fractionation is another method used to determine the abundance and type of organically associated inorganic elements within coal. Data obtained from chemical fractionation represent fuel specifications that are not obtainable from ASTM methods. Chemical fractionation represents a methodology whereby several modes of major inorganic species can be determined. Details on how this process works are independently discussed in the works of Benson and Gupta (Benson 1984; Gupta 2007). They indicate that chemical fractionation consists of three successive extractions: (1), the removal of water-soluble compounds such as alkali metal salts; (2), the residue of the extracted materials is next subjected to ammonium acetate aqueous solution to remove elements such as sodium, calcium, and other ion exchangeable elements like magnesium; and (3), the usage of hydrochloric acid to remove acid-soluble species such as iron and calcium that may be in the form of alkaline earth sulfates, oxides, carbonates, or hydroxides is undertaken. The residual matter after the three extractions are assumed to be insoluble mineral species, which are generally a mixture of silicates, oxides, and pyritic sulfides.

Determining origination of TEs is a multifaceted task wherein rank, mode of occurrence, size distribution, and other species present must be taken into account. It is noted that modes of occurrence between TEs and origination source are inferential at best.

2.1.5. Trace Element Volatility

Several researchers classified TEs based on their apparent volatility during combustion (Meij 1994; Clarke and Sloss 1992). Based on the classification given by Clarke and Sloss which

is illustrated in Figure 2-4 (Clarke and Sloss 1992), Class I elements are the least volatile and are generally partitioned between bottom ash and fly ash. These elements tend to not show significant enrichment or depletion in the ash. Class II elements have increased enrichment with a decreased particle size. These elements become concentrated in the fine-grained particles. Finally, Class III elements are the most volatile and contain elements that are not enriched in the solid phase.

The volatility of some species in relationship to one another can be found in Figure 2-4, which shows that elements such as arsenic, antimony, and selenium are all semi-volatile.

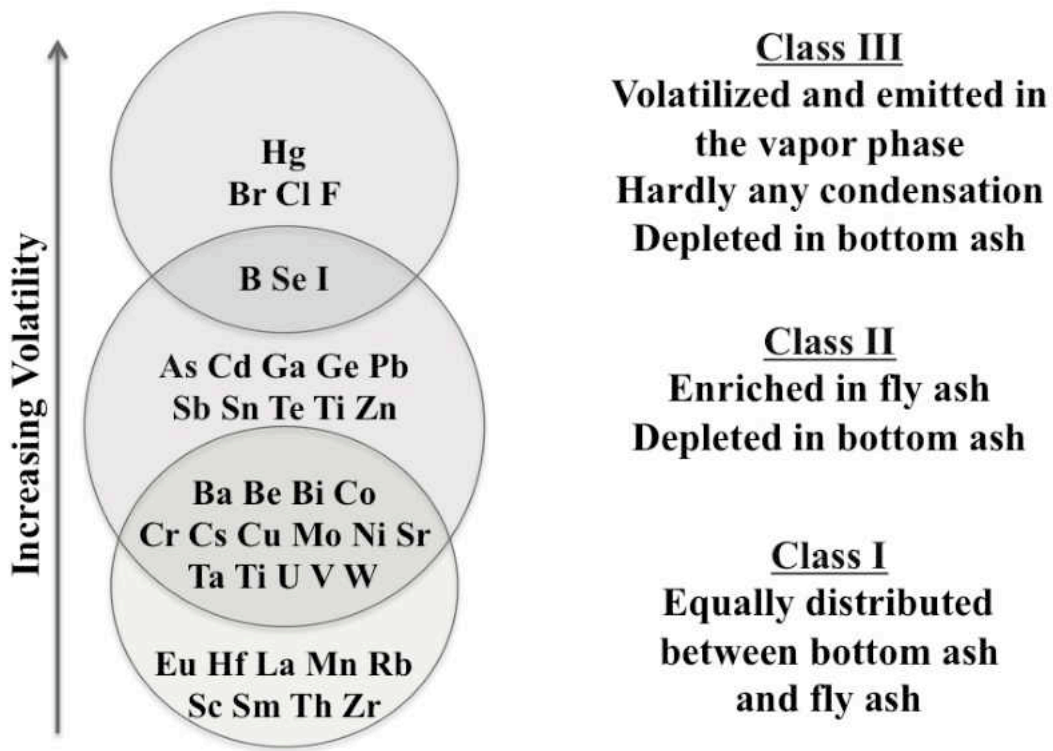


Figure 2-4 Relative enrichment and volatility of selected coal trace elements (Clarke and Sloss 1992; Meij 1994)

Trace elements that more readily volatilize during combustion represent a greater health and environmental concern than those that do not, as they are more likely to either be discharged into the atmosphere or partition preferentially on submicron-sized fly ash (Giere and Stille 2004). Organically bound ion exchangeable species also tend to sorb on fly ash (Boo III and Helble 1995). However, the ability of a TE to escape the particle is directly related to the associated minerals as well as the environment a mineral group encounters during combustion.

Class II elements that have a strong affinity for sulfur—chalcophilic elements—are claimed to be mostly volatilized during combustion because they occur as sulfides or sulfide minerals. Elevated temperatures as well as the reducing atmosphere directly surrounding a burning particle allow bonds between the sulfur and the class II elements to break. (Ratafia-Brown 1994).

Sarofim and co-workers undertook work demonstrating combustion zone transformations (Boo III et al. 1997). They found that in some experiments char particle temperature is a more important factor in determining vaporization for arsenic and selenium than is the mode of occurrence. They furthermore found that reducing conditions inhibited volatility for arsenic and selenium when they were associated with pyrite in coal. However, this is only the case for selenium with pyrite. Combustion stoichiometry showed little effect on vaporization of organically associated selenium. Zeng et al. proposed that, for some coals, arsenic, antimony, and selenium partition to the submicron particles via a vaporization condensation pathway even though the volatilities of the elements differ (Zeng, Sarofim, and Senior 2001). Condensation as it is used here actually means sorption, not physical vapor to liquid phase condensation.

2.2. The Importance of Pyrite

Pyrite has historically been shown to have several TE species associated within its mineral structure (Shah et al. 2007; Seames, Jassim, and Benson 2010; Spears and Booth 2002; Spears, Manzanares-Papayanopoulos, and Booth 1999; Srinivasachar and Boni 1989; Srinivasachar, Helble, and Boni 1990; Yudovich and Ketris 2005; Bool III and Helble 1995; Helble, Srinivasachar, and Boni 1990). Even though some subbituminous coals have shown a low pyrite content (Senior et al. 2000), the majority of lower-ranked coals have similar overall quantities of pyrite (Ilyushechkin et al. 2011; Linak and Wendt 1994).

Zeng et al.'s research (Zeng, Sarofim, and Senior 2001) presented the first quantitative physicochemical model for vaporization of arsenic, antimony, and selenium during coal pyrolysis and combustion from pyritic family minerals. The premise of their model is based on universally accepted mass transfer theories, and includes (1) the transport of atoms or molecules through the bulk pyrite liquid melt to the melt/gas interface, (2) vaporization of elements at the surface of the melt, and (3) transport through the pores to the atmosphere. Their presented model does not account for the time-temperature dependent nature of pyrite transformations, and thus availability of the pyrite melt needed for TE liberation to occur.

A kinetic model for pyrite transformations in a combustion environment has been developed by Srinivasachar and co-workers (Srinivasachar and Boni 1989). Their research also shows mineral behavior during coal combustion for pyrite transformations (Srinivasachar, Helble, and Boni 1990) as well as illite transformations (Srinivasachar et al. 1990). A conceptual model of pyrite exclusion transformations during coal combustion adapted from the description by Srinivasachar and Boni that has been confirmed by a variety of experimental studies is found

in Figure 2-5 (Srinivasachar and Boni 1989; Srinivasachar, Helble, and Boni 1990; Sheng and Li 2008; Sheng et al. 2010).

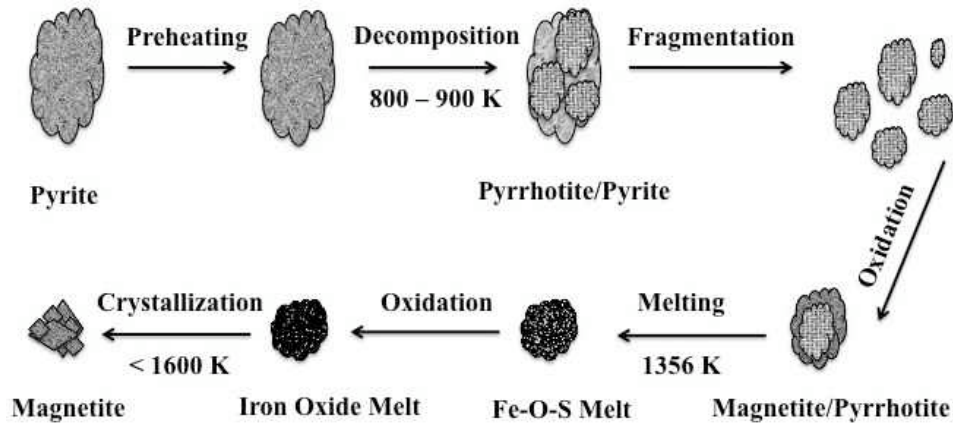
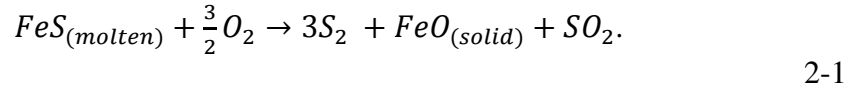


Figure 2-5 Pyrite transformation during combustion (Srinivasachar and Boni 1989)

Excluded pyrite behavior depends on the morphology of the mineral grain. Some pyrite may be present as roughly spherical aggregates of discrete equi-regular euhedral microcrystallites commonly called framboids. Framboidal-pyrite will fragment easier than massive pyrite particles. The pyrrhotite oxidizes to FeO, Fe₃O₄, and Fe₂O₃ during combustion (Srinivasachar and Boni 1989; Srinivasachar, Helble, and Boni 1990).

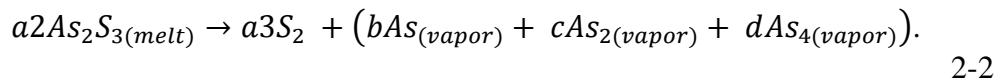
Included pyrite is held within the interior of the burning coal particle. The particle surface temperature increases during the devolatilization process of volatile matter and char combustion. However, when all the volatile matter is consumed, the pyrite is exposed to the high-temperature environment that allows for the liquefaction and at least partial vaporization of sulfur and the TEs encapsulated in the sulfide-rich portion of the pyrite particle.

The following reaction may occur after the initial liquid phase forms (Raask 1985):



Sulfur devolatilization during the decomposition of pyrrhotite is an exothermic reaction that will increase the particle surface temperature. This further impacts TE release from the pyrite mineral grains as particle temperature gradients induce various localized densities, which affect fragmentation (Jassim et al. 2010; Jassim et al. 2009). Fragmentation produces multiple smaller pyrite/pyrrhotite particles that will continue to heat up and release TEs that still remain. Pyrrhotite particles will fragment before they reach their melting point (Zeng 1998). The exothermic reaction described by the oxidation of pyrrhotite may allow for additional vaporization of TEs, as this reaction will cause the particle temperature to increase.

Before TEs can migrate out of a particle, the bonds that hold the elements must be broken, the evolution of products from sulfur oxidation reactions from the parent mineral gradually decay, and the surface of the pyrite melts. Therefore, the bonds containing the TEs are broken. According to Zeng et al., nearly all the arsenic in the coal they studied was associated in the form of As_2S_3 - FeS_2 . When the pyrite melts, some of the As_2S_3 may decompose, in a modified version from that given by Zeng et al (Zeng, Sarofim, and Senior 2001), as follows:



where a, b, c, d are balanced stoichiometric coefficients. This relationship is given with the caveat that only some of the arsenic may react in this manner. It does not imply that all the

arsenic will vaporize, as much of the excluded pyrite that exits the system with the bottom ash still has arsenic associations.

Arsenic vapor, from its pure solid modifications, consists of As_4 molecules up to 1073 K. After that point, As_2 begins to be seen; however, the change to As_2 is not complete below 1973 K (Sidgwick 1950). During coal combustion, it is highly improbable that the molecular As_4 will form in any significant amount due to its small relative abundance. The dimer As_2 is the more favorable of the two. It is more likely that some form of sulfide, oxide, or sulf-oxide species will occur.

Highly reducing conditions are present within the char. Char particle temperatures typically exceed gas temperatures by up to 200 – 300 K and may reach temperatures of up to 2000 K or higher for oxidizing combustion stoichiometry (Attalla et al. 2007). As indicated in Vejahati et al.'s review, which cites the work of Groves et al. (Groves, Williamson, and Sanyal 1987; Vejahati, Xu, and Gupta 2010), larger excluded mineral fragmentation, as compared to included minerals, is more apparent due to the severe temperature gradient of the particles. Excluded mineral fusion to form spherical molten ash droplets may occur if the particle temperature exceeds melting temperatures. Fusion is more mineral specific for excluded minerals (Vejahati, Xu, and Gupta 2010).

2.3. Coal Rank Considerations

Coal rank can also be correlated to TE behavior through the associations of mineral groups within the coal. Lower-rank coals have more distinguishable mineral groups than higher-rank coals that have further undergone the coalification process. Low-rank coals have mineral associations, organic associations, and water associations. Older higher-rank coals primarily

have mineral associations. This change is caused by the loss of water, COOH, and OH groups within the coal.

Lignite and subbituminous coals are considered non-caking while bituminous coals have more plastic properties. The caking and plasticity of a coal has the potential to affect the coalescence and fragmentation of particles, which in turn has the potential to affect TE partitioning.

Trace element associations are not a new field of study. Several researchers noted that the distribution of TEs differs between sources and seams (Swaine 1994; Raask 1985; Yan, Lu, and Zeng 1999; Ilyushechkin et al. 2011). Vassilev et al. showed the relationship between coal rank and chemical and mineral composition. They found that low-rank coal ash tended to have more abundant MgO and CaO than higher-ranked coals that demonstrated increased contents of SiO₂, Al₂O₃, Fe₂O₃, K₂O, Na₂O, and TiO₂. Furthermore, they found that coals enriched in illite, mica, chlorite, spinel, dolomite, siderite and hexahydrite, and partly in quartz, kaolinite, and iron oxyhydroxides, are of higher rank; while coals with increased contents of montmorillonite, feldspars, zeolite, aluminum oxyhydroxides, calcite, pyrite, gypsum, as well as Fe-, Al-, and Ba-sulfates are of lower rank (Vassilev, Kitano, and Vassileva 1996). Vejahati et al. discussed that there is a higher concentration of minerals in inertinite (Vejahati, Xu, and Gupta 2010). Inertinite burns comparatively slowly, which can cause retention of TEs in ash particles.

In order to successfully meet the demands of the variable nature of coal, as reported by Nelson (Nelson 2007), an initiative from the U.S. Geological Survey, the World Coal Quality Inventory, intends to establish an electronic database with information on most coal properties, including trace element contents (Quann and Sarofim 1986). Partners in some 40 countries are

reportedly involved. This initiative has the potential to further the understanding of TE abundances within coal and aid in developing remediation methods for their capture. As technology has continued to improve and develop, the understanding of the components, including TEs, in coal has and should increase.

Overall, the variation of TE concentration and affinity within the different ranks of coals has prevented general rules for TE associations from being developed. Although some trends are observable, researchers indicate different results to the quantity and association of TEs and coal rank. The vaporization rates of TEs from higher rank coals has been studied but the effects observed have been attributed to flame temperature rather than coal rank (Senior et al. 2006).

Trends outside of mineral association for coal rank, however, are also significant. For instance, during typical high temperature combustion, lower-rank coals burn in the diffusion-controlled regime (Boal III et al. 1997). They do not swell or shrink appreciably as the char is burned away, which means that a near-constant density can be assumed. Furthermore, lower-rank coals can burn faster than the bituminous coals. Finally, the combustion product at the surface of a lower-rank coal is considered to be CO.

Boal et al. describe four treatments of CO originating from surface oxidation of coal as follows:

‘(1) no oxidation, (2) infinitely thin flame so that no oxygen penetrates to the char surface, (3) CO oxidation is at the char particle, thus all the heat released by CO oxidation is imparted to the char particle, equivalent to having an oxidation product of CO₂, and finally (4) finite oxidation rate of CO with part of the heat released by CO imparted to the char particle.’ (Boal III et al. 1997)

These four treatments are significant in the way in which they could impact TE partitioning modeling. The heat absorbed by the particle is directly related to the calculated particle temperature. Bool et al. consider the fourth approach the most appropriate (Bool III et al. 1997).

2.4. Select TE Species

Several volumes of books have been written on the subject of TEs in coal (Valković 1983; Swaine 1990; Finkelman 1980; Swaine and Goodarzi 1995). An overly detailed synopsis of TE research is not the purpose of this section. Conversely, the purpose of this section is to briefly identify the modes of occurrence of a few select species; the modes will be important in understanding TE partitioning behavior.

Although the Clean Air Act Amendment of 1990 (101st Congress 1990) focused attention on 189 substances cited as potentially hazardous air pollutants, only 11 of the substances cited are inorganic elements. Each element cited is found related to coal and its use. Three such inorganic elements include arsenic, antimony, and selenium, which are semi-volatile and, therefore, have the potential to induce hazardous health effects on human, animal, and vegetative life.

Most of the arsenic, antimony, and selenium content in coal have been shown to be associated with three major mineral groups: pyrite, kaolinite, and illite (Davidson and Clarke 1996; Kolker et al. 1998). Distribution of minerals is not uniform among a single coal seam and varies greatly between origination sources. General rules cannot be used to obtain the relative amounts of TEs within coal based on coal rank. Lateral differences within the same coal seam are attributed to the coalification processes.

2.4.1. Arsenic

Finkelman reviewed the modes of occurrence of several TEs (Finkelman 1994). His work indicates that most of the arsenic in coal is associated with massive or late-stage pyrite yet does not exclude fine-grained pyrite and other sulfides. Arsenic does not occur as micron-sized accessory sulfide grains dispersed in an organic matrix; rather it occurs as a solid solution within pyrite (Finkelman 1980). Arsenic clustering in pyrites is also suggested (Huffman et al. 1994; Benson et al. 1994).

Finkelman provides some arsenic organic associations with a degree of skepticism. However, he indicates that the presence of *arsenopyrite* (FeAsS) within coal is doubtful at best. As cited in Valkovic, Swaine found associations with FeAsS in early research (Swaine 1977; Valković 1983). It is unclear if Swaine has since retracted this assertion or if that research is based on individual coal seams with different properties and mineral groups present than what Finkelman studied, which could have affected results. As disagreements are present, the mode of occurrence of arsenic, or any TE, must be identified through analysis of the coal bed. Caution must be maintained in coal characterization as ambient oxidation of a coal can change its chemical makeup and thus provide erroneous results. General consensus does not exist that could enable an empirical relationship to quantify arsenic concentration and mode for all coal seams.

2.4.2. Antimony

There are several ways in which antimony has shown to be associated within coal. Because of its strong chalcophilic tendencies, it may be part of a solid solution in pyrite (Finkelman 1980). Antimony can also occur as minute accessory sulfides, be dispersed through the organic matrix, or be organically bound (Finkelman 1994). Within the literature reviewed,

only one coal mineral directly contained antimony in its formula: ullmannite (NiSbS). This mineral was found in a carbonate vein in a British coal (Spencer 1910; Finkelman 1980).

2.4.3. Selenium

The majority of selenium has been found in organic constituents and a small part with pyrite and an even lesser portion with accessory minerals such as clausthalite and galena (Finkelman 1994, 1980). As cited by Valkovic, Miller lists correlations of selenium with calcite and quartz (Valković 1983). Micrometer-sized crystals of lead selenides are also a form that selenium can be found within coal (Finkelman 1994).

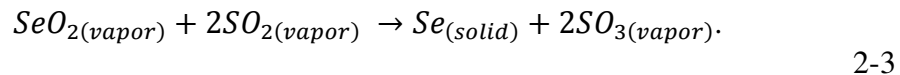
Selenium partitioning behavior was shown by Senior et al. to be greatly affected by the composition of the fly ash particles. They indicate that in a coal-fired boiler, gaseous selenium oxides are absorbed on the fly ash surface in the convective section by a chemical reaction (Senior et al. 2010). They further found that the temperature history of the parent coal particle, as well as the boiler temperature history profile, influence formation of selenium compounds on the surface of fly ash. More volatile elements such as arsenic and selenium have vaporization rates that are more highly char particle temperature dependent (Boal III et al. 1997).

2.4.4. Impact of Other Elements

Organically bound TEs have been shown to remain in the vapor phase during combustion. However iron, calcium and sulfur do not vaporize completely nor do they stay in the vapor phase. These species recombine/chemi-absorb with particles and form active sites of reaction for of the other elements.

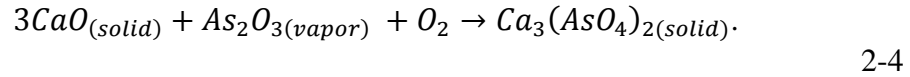
Elements interact in the combustion zone as well as the gas-cooling environment. This implies that the presence of certain elements or compounds could affect the partitioning behavior of arsenic, antimony, and selenium during combustion. The presence of sulfur, iron, or calcium can change partitioning behavior because they form or interact with active sites.

The presence of sulfur will inhibit the reaction of most volatilized TE oxy-anions with iron surface sites (Senior et al. 2001). This implies that the presence of excess sulfur could tie up active sites on fly ash surfaces, making them unavailable for further reactions. This is particularly pronounced for selenium, as it is classified within the same group on the periodic table as sulfur. Se(IV) is reduced by SO₂. This is also seen for SeO₂ in the flue gas, which is described by equation 2-3 (Dismukes 1994):



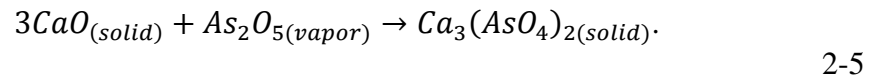
The addition of excess calcium and iron compounds also affects TEs behavior and partitioning. It has been found that arsenic and selenium associate with iron and calcium when active sites are available. Selenium reacts preferentially with iron over calcium when both are available, while arsenic reacts comparably with both iron and calcium. Sulfur can prevent the association of both arsenic and selenium by preferentially reacting with active sites (Seames and Wendt 2007). As indicated by Senior et al., for coals with sulfur contents greater than 1 wt%, volatilized TEs that form oxy-anions will partition by reaction with active calcium surface sites if they are available, whereas coals with lower sulfur content will partition by reaction with active iron and/or calcium sites depending upon their availability. (Senior et al. 2001; Senior et al. 2006). This can especially be seen with the reaction between diarsenic trioxide and calcium

oxide, which is described by equation 2-4 (Attalla, Chao, and Nelson 2003; Huffman et al. 1994).



One control method to prevent SCR catalyst poisoning by arsenic species used in industry is the injection of limestone to the fuel (Ake et al. 2003). The limestone provides a source for calcium when the coal has a lower content.

In the absence of sulfur, the reaction is slightly different for a TE species with the ash. A significant part of arsenic may be retained in the ash from the reaction of volatile As(V) with CaO to form calcium orthoarsenate, as described by equation 2-5 (Huffman et al. 1994).



Huffman further indicates that the arsenate in coarser ash fractions may represent AsO_4^{3-} incorporated as a network former in aluminosilicate glass phases through the reaction of arsenical pyrite with clays and quartz (Huffman et al. 1994).

Activation energy can be used to describe the preferential behavior of how TEs will liberate from the solid matrix. For some species, an increase in the activation energy required for atomization can be facilitated by the presence of other species (i.e., matrix effects). Attalla cites Cramer's work (Attalla, Chao, and Nelson 2003; Cramer 1986), which indicates that selenium is less volatile in the presence of $CaCO_3$. This is also seen in the increase in activation energy for antimony atomization, which is more pronounced than for selenium, due to retention by Fe_2O_3

(Raeva 2011; Raeva, Pierce, et al. 2011). This is significant in that increase in atomization/vaporization activation energies indicates increased TE retention in the solid phase.

Once the TEs have been liberated from the solid phase, the TEs can then be subject to additional reactions with active sites on the surfaces of the ash particles. For example, selenium is reactive in the presence of active calcium sites wherein calcium selenite can form (Attalla, Chao, and Nelson 2003).

General rules for reaction of vapor phase TE species with active sites, as described by Seames and others (Seames 2000; Seames and Wendt 2000b, 2000a, 2001) can be summarized as follows. Selenium will react with active sites from iron containing and then calcium-containing compounds that have been left behind after sulfur species react with As. Volatilized selenium is more reactive with iron and calcium sites than either arsenic or antimony (Senior et al. 2001). Next, arsenic species will follow a similar trend by reacting with remaining active iron-based and then calcium-based sites. Finally, antimony will react with iron and calcium sites unless not enough sites are available. Antimony can thus be emitted in the gaseous phase in greater quantities. Senior et al. also give similar rules of thumb. They indicate that almost all antimony present as volatilized antimony chloride will exit the system through the flue gas while the remaining antimony will partition as unreacted antimony to fly ash surfaces (Senior et al. 2001).

Environment, including temperature, pressure, and species concentrations, is directly related to the kinetic rates in which TEs can evolve. Historically, kinetic data that describe the behavioral interactions of TEs species during coal combustion has been unavailable. Research discussed in the dissertation and papers of Raeva and related colleagues at the University of

North Dakota (Raeva 2011; Raeva, Pierce, et al. 2011) have shown how kinetics can play a role in TE partitioning as the availability of some species, such as iron, calcium and aluminum, will affect the release and capture of TE species. Their work provides in-situ measurements of inorganic matrix effects on the partitioning of arsenic, antimony, and selenium. They sought to determine plausible mode of occurrence speciation during specific idealized combustion environments. Most importantly, they simulated conditions for each TE regime (inclusions, exclusions, and organically bound) separately.

2.5. Modeling

2.5.1. Swelling and Shrinking Behavior

Even before TE considerations can be taken into account within modeling, properties related to coal rank must be considered. Lower-rank coals tend to not have the same “plastic type” properties that higher-rank coals have. A shrinking core model is more effective at describing the behavior of lower-grade coals, while the swelling model is more effective for higher-rank coals. Gupta, Halder, Kang, and Sadhukhan show related research for this behavior (Gupta, Sadhukhan, and Saha 2007; Halder, Datta, and Chattopadhyay 1993; Kang et al. 1990; Sadhukhan, Gupta, and Saha 2008). Neither type of model describes trace element partitioning, yet both describe the means whereby the change in particle diameters can be viewed during combustion. The change in diameter directly relates to the retention of TEs from mineral inclusions contained with the parent coal particle. Fluent has sub-models to account for some of the differences between differing coal ranks.

2.5.2. Fragmentation

The fragmentation of char and minerals will have a substantial role on the final size distribution of ash particles as well as the surface area available for mass transfer release. Incorporating variables for surface area changes that will be incurred upon excluded particles during combustion has the potential to improve model predictions of TE release due to the fact that surface area to volume ratios are related to TE liberation.

It may be that fragmentation of excluded mineral particles is more important than for included mineral particles. According to Kang, fragmentation of included mineral grains may be negligible due to the fact that the surrounding carbon matrix may hold resultant pieces together (Kang 1991). The number of fragments relates to the number of active sites available for TE interaction.

The approach described by Srinivasachar and Boni (Srinivasachar and Boni 1989; Srinivasachar, Helble, and Boni 1990) indicates that an average 4 offspring particles are generated from parent excluded pyrite particles during the transformation of pyrite into pyrrhotite (Yan 2000). Similarly, calcite and dolomite particles appear to break into 3 offspring particles while other major mineral species are not expected to fragment significantly (Yan 2000). However, generalized rules for coal tend to be broken in practice. Models may benefit from having a flexible fragmentation input value rather than an arbitrarily set number of offspring particles that does not take into account differences between rank or coal blends.

Rank plays a role in char fragmentation. Those ranks with higher rates of fragmentation, such as some bituminous coals, result in finer ash particle formation. Lignite fragmentation was found to be less extensive, did not show the same size dependence as bituminous coal, and

resulted in a broader distribution of sizes. Size is important in modeling TE species behavior because fine ash particles tend to be enriched with TEs.

Numerical modeling of a coalescence and fragmentation approach using CCSEM data has been undertaken by Wang et al and has shown some success with modeling the PM10 size fraction of drop-tube furnace fly ash samples (Wang et al. 2007, 2008, 2009). Their approach uses the methods described by Yan, in which a Poisson distribution is utilized to describe the random nature of coalescence and fragmentation of particles (Yan 2000). Their approach does not give the individual composition of coal particles that are time and spatially tracked but does provide a random combination of particles that may interact with one another. It is noted that these data must be used with caution, as drop tube furnaces do not have sufficient particle-particle interactions to fully replicate commercially relevant fine-fragment-sized particles.

2.5.3. Partitioning Approaches

Where a TE resides will affect its behavior during combustion. Partitioning is affected by the mode of occurrence and the association of a TE species as well as its concentration (Huggins 2002). Due to the complexity of coal, researchers agree that the different modes of occurrence for TEs are paramount to modeling. Elemental modes of occurrence—whether organically bound, included, or excluded—affect thermodynamic calculations used to describe partitioning of TE materials.

Some previous models focused only on TE fly ash concentration (Murarks, Mattigod, and Keefer 1993). However, this type of model neglects TE partitioning within the combustion zone. Alternatively, Senior and Lignell model partitioning of arsenic between the vapor phase

from volatilization and arsenic on the ash particles due to surface reactions and/or condensation (Senior et al. 2006). This approach seems more appropriate as the interaction of TEs and other elements in coal was shown by Yinghui (Yinghui, Chuguang, and Quanhai 2003) as well as Diaz-Somoano and colleagues (Diaz-Somoano and Martinez-Tarazona 2003) to play a role in partitioning. Any models developed that describe the ultimate form of the TE should take into account the concentration of other species present as well as the transformations of the particle on a time-temperature dependent manner. This will be distinctive for each coal, based on the rank and petrographical maceral groups present.

The modeling of coal combustion behavior and ash characteristics is not a new field. However, most TE studies are empirically derived or based on simple gas-phased bulk thermodynamic estimates. Early-stage models of TE partitioning were based primarily on concentration and thermodynamic equilibrium-based calculations (Diaz-Somoano and Martinez-Tarazona 2003; Thompson and Argent 2002). However, concentration-based calculations are not enough to understand how TEs will behave. Nelson indicates that thermodynamic equilibrium-based calculations were used because kinetic data were not available (Nelson 2007). The methodologies described, and data obtained, within Raeva and colleague's work (Raeva, Pierce, et al. 2011) may make a first principles-based model more easily attainable and may begin to fill the void.

2.5.4. Transition from Microscopic Environment to Flue Gas Environment

As a TE leaves the vicinity of the char, the change to the bulk conditions is quite drastic. Temperatures can go from that of the burning char (near flame temperature) to the bulk gas (near 1000 K). Coal particle temperatures during pyrolysis have been modeled by Maloney et al.

(Maloney, Sampath, and Zondlo 1999). Fluent includes subroutines to describe particle heat absorption during combustion, which relates to particle temperature.

2.5.5. Modeling History

The review for the Australian government's cooperative research centers program details some of the history of TE partitioning modeling (Attalla, Chao, and Nelson 2003). They indicate that integrated modeling approaches have been seen at least as early as 1993. Early models combined the use of thermodynamic data, mass balance calculations, and other relevant models to the combustion system being studied.

Released in 1994, Linak and Wendt's mathematical model emphasized size-segregation of trace metals in pulverized-coal systems, while modeling trace metal transformation mechanisms during coal combustion. They note that the vapor pressures of pure compounds do not predict which species are favored and cannot alone be used to predict under what conditions condensation will occur (Linak and Wendt 1994).

Bool and Helbe's mathematical model, published in 1995, incorporates vaporization and subsequent condensation of many TEs during coal combustion (Bool III and Helble 1995). Within their model they showed how TE associated forms dictate partitioning behavior.

By 1995, the UND EERC TraceTran program (not available publicly) was developed (McCullor et al. 2003; Benson et al. 2002; Benson et al. 2007). Their empirical model describes the transformation of minerals during coal combustion and gas cooling. This model is based on the ATRAN model (Hurley et al. 1992; Benson et al. 2002; Ma 2007) and is written as a C++ computer code (Sarofim and Helble 1993). The model is intended to predict the evolution of

major species, minor species, and TEs during coal combustion and gasification while predicting the size, composition, and phase of inorganic species at a given temperature and pressure. Thermochemical data from FACT are incorporated within their program (Attalla, Chao, and Nelson 2003).

In 2000, Lockwood and Yousif released a mathematical model for the predicting the fate of hazardous metals during combustion by accounting for the formation of new particles through nucleation and growth of existing particles through the pathways of condensation and coagulation (Lockwood and Yousif 2000). In their model it was assumed that complete vaporization of the metal occurred near the injection point of the coal into the furnace, which means that quantities of TEs were taken from the Ultimate analysis of the coal rather than from mineralogical data sets. Their model suggests that the subdivision of particles into just two modes, coarse and fine, would be sufficient. Partitioning of the semi-volatile metals lead and cadmium was predicted. A lack of chemical kinetic data was mentioned as well as the fact that their proposed model did not account for vaporization rates based on particle size, chemical state of the metal or the distribution of the metallic species within the particle.

The *Toxic Partitioning Engineering Model* was a collaborative effort by a number of institutions, universities, and governmental agencies to develop sub-models for an existing engineering model for ash formation. Actual coding was reportedly never performed. Quarterly reports detailing the findings from a range of topics were released from 1995 to 2001 (United States Geological Survey 1998; Bool III et al. 1997; Bool III, Senior, Huggins, Huffman, Shah, Wendt, Peterson, et al. 1996; Bool III, Senior, Huggins, Huffman, Shah, Wendt, Sarofim, et al. 1996; Bool III, Senior, Huggins, Huffman, and Shah 1996; Crowley et al. 1996; Kolker et al.

2002; Kolker, Mroczkowski, et al. 1999; Kolker et al. 1998; Kolker, Sarofim, et al. 1999; Senior et al. 1996; Bool III, Senior, Sarofim, et al. 1996; Senior et al. 1998; Senior et al. 2001).

2.6. Summary

Bulk gas-phase conditions and empirically derived predictors are the basis of many current models. Although empirical models can replicate current systems, they can be insufficient when new equipment configurations, modes of operation, or TE remediation practices are implemented (Seames 2005). Accurate models are one way in which the behavior of TE species can be explored prior to significant capital investments.

The goal of this review is to show the state of TE partitioning research and identify areas where improvements could be added. This is accomplished through the discussion of TE partitioning for arsenic, antimony, and selenium.

Care must be given in development of models as the properties and tendencies of lower-ranked coals are different than those of higher-ranked seams. Trace element partitioning modeling for lower-grade as well as higher-grade coals represents an area in which improvements can be made. In order to accurately describe TE partitioning, a model must incorporate combustion system design characteristics as well as fuel properties (Ratafia-Brown 1994).

3. MODEL FUNDAMENTALS

Modeling TE partitioning involves simultaneous tracking of heat and mass transfer, momentum transfer, and phase changes that occur in and around a particle subjected to intense temperature gradients and diversified oxidative and reductive conditions. In this investigation, a transient-lumped-capacity model is developed that predicts the transformations of a select three TE species (arsenic, antimony, and selenium) as a function of time/position of a particle within the combustion chamber environment. This, in turn, relates to particle temperature, composition, system pressure, system chemistry, and thermodynamics of species within their various phases within a pulverized coal combustion environment. This research undertaking is an enhancement of the mathematical approach presented by Zeng et al (Zeng, Sarofim, and Senior 2001), yet is unique in that it combines the approach presented by Yan (Yan 2000) to determine a unique mineral distribution within the coal particles while taking into account kinetic data speciation provided through the research of Raeva and colleagues (Raeva 2011; Raeva, Pierce, et al. 2011). The computer program developed to describe this modeling approach was constructed in a modular fashion to more easily account for additional TE species or variations in combustion environments.

The objectives of the project relating to this dissertation are to provide a simulation model that involves macroscopic level simulation structures that specifically handle: (1) volatilization of the three TEs (arsenic, antimony, and selenium) associated within the

combustion system as a portion of pyritic family mineral inclusions; (2) volatilization of these three TEs associated within the combustion system as a portion of pyritic family exclusions; and (3) volatilization of organically associated trace elements. In order to accomplish initial TE partitioning from these original associations, a mass balance is undertaken. Time-temperature-dependent aspects of coal particles in a combustor are simulated and incorporated into the model. Generated text files from Fluent in conjunction with the developed C++ program provide a convenient user interface for the computational engine.

This chapter includes the following sections. *Section 1* provides assumptions and limitations of this model. *Section 2* describes the boundary conditions of this modeling approach. *Section 3* details the model design and sub-relations inherent within, including a broad overview of related necessary input data. Next, *Section 4* discusses ANSYS Fluent and its usage in connection with the proposed model. After that, *Section 5* details C++ programming benefits as they relate to the discussion. Finally, in *Section 6*, details incorporating mathematical relationships utilized within the code are provided and expounded upon.

3.1. Assumptions/Limitations

The following assumptions allow tractable mathematical model development:

- All properties are assumed to be transient and one-dimensional in space.
- Local thermal equilibrium exists between the solid/liquid melt and vapor phase at the interface.
- The environment is a pulverized dry bottom coal combustion system.

- Rank of the coal currently modeled in this system includes a Southern *Powder River Basin* (PRB) subbituminous coal species.
- All TEs originating within a pyritic-family-mineral melt are uniformly dispersed.
- Internal resistance is rate controlling for the mass transfer rates.
- Data provided from previous steps (such as from ANSYS Fluent) are valid for use within the model.

3.2. Boundary Conditions

Although this modeling approach is identified as a transient problem it is only transient in the way in which calculations are performed. The model treats each particle the same way, regardless of direction of flow around it. Thus, even though a particle is tracked based on radial and axial coordinates as they relate to their time dependencies in the furnace, the particles are treated as a function of the composition of that position and area directly adjacent to that position.

For a transient model in spherical coordinates, the radial direction, r , cannot capture the effect of bulk flue gas flow around the particle except by changing the film thickness, which is the distance from the particle surface to the bulk conditions (Bird, Stewart, and Lightfoot 2002; Roberts 2006). A transient model can only accurately predict the boundary layer characteristics when the bulk gas is stagnant or when the bulk conditions include a thick film. By placing the bulk conditions closer to the particle, the heat and the mass transfer rates accurately describe overall particle conditions even if axial flow is ignored and variations in the second dimension are ignored (Roberts 2006).

3.3. Model Design

The C⁺⁺ program is designed to predict the state of inorganic constituents in coal during pulverized coal combustion. This includes the location and composition in which a TE species may be liberated from its related mineral or organically bound state. An overview of the model is illustrated in Figure 3-1. The algorithm shows the ways in which the program input datum interact with one another to give the final predicted results.

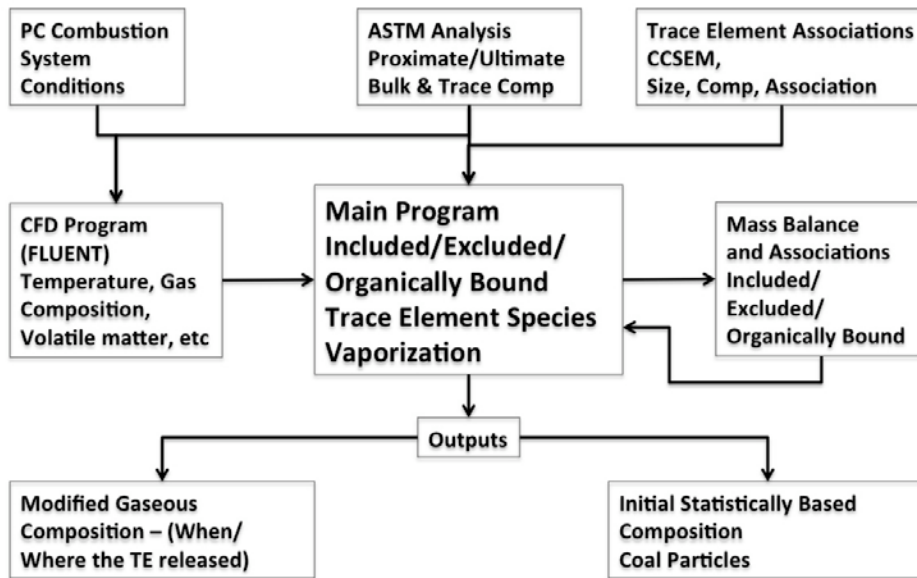


Figure 3-1 Developed C⁺⁺ program model algorithm

The overall model is designed around fundamental mechanistic attributes identified in the literature review included in Chapter 2, as well as that outlined in the work of Zeng et al, which is summarized in Section 3.6.2 (Zeng, Sarofim, and Senior 2001). Several of the blocks shown in Figure 3-1 will be discussed in detail. A portion of the program user guide is included in Appendix A.

3.3.1. ASTM Analysis

ASTM analysis results are reported on an as-received dry basis. This analysis details the weight percent of carbon, hydrogen, nitrogen, sulfur, oxygen (by difference), and percent ash related to a coal sample. This information is necessary for calculations within the model as well as within the computational fluid dynamics package used during preliminary calculations. An example input file that describes details of the coal particle and related chemistry information is included in Appendix B.

3.3.1.1. Analysis of Ash

The composition of TEs from the ash analysis is also necessary due to the fact that the TE composition is used in calculations. Many methods exist to obtain these data, and no method is preeminent for all situations. The ASTM method provides information on the bulk chemical composition and combustion characteristics (such as the higher and lower heating values) of the coal.

The chemical composition of the coal ash is given on a wt% basis. Information regarding SiO_2 , Al_2O_3 , TiO_2 , Fe_2O_3 , CaO , MgO , K_2O , Na_2O , SO_3 , P_2O_5 , BaO , SrO and MnO_2 is provided. Calculations are made on a sulfur-free basis. An example input file that describes details of the coal particle and related chemistry information is included in Appendix B.

3.3.1.2. Ash TE Bulk Analysis

The ash bulk element analysis includes additional species required for coding. Specifically, Na, Mg, Al, Si, P, S, Cl, K, Ca, Fe, and Ba are provided.

Arsenic and antimony are chalcophilic elements meaning that they have a strong affinity for sulfur. The concentrations of these TEs within pyritic-family-mineral samples are the most significant for partitioning purposes. Information regarding the arsenic, antimony, or selenium concentration in pyrite can be obtained through any valid method. Early analytical methods as well as their limitations are described by Babu (Babu 1975). For coding purposes, the relative quantity of the TE species is specified in a text file, and the specified quantity is used for calculations. An example input file that describes details of the coal particle and related chemistry information is included in Appendix B.

3.3.2. CCSEM Mineral Associations

Before computations can begin, the model requires fundamental information such as the associations of major, minor, and TEs within coal. Associations affect phase, size, and composition of the gas and ash. This information is obtained through CCSEM, which is also used to determine the size and composition of minerals within the coal. The CCSEM method provides quantitative information on the distribution of elements among mineral constituents of the coal studied.

A CCSEM mineralogical analysis provides information of either two or three different magnification files. These include 50x, 250x, and the highest, 800x. Each of the raw files (as provided by Microbeam Technologies) has 25 columns of data for each mineral particle and a varying number of rows. One mineral particle of the coal is identified for each row. The columns are arranged according to particle number, chemical type, x-ray count, Si, Al, Fe, Ti, P, Ca, Mg, Na, K, S, Ba, Cl, Particle centroid (x-coordinate and y-coordinate), average diameter, maximum

diameter, area, perimeter, shape factor, frame number, and excluded/included. An example input file relating CCSEM data is included in Appendix B.

3.3.3. Mass Balance and Associations

Elemental species must be conserved in any process. The usage of data obtained from CCSEM and the ASTM proximate and ultimate analyses allows understanding of which minerals are present and how they are associated through a general mass balance of TEs in the solid, liquid, and gaseous phases. The Chemical fractionation could also be used in conjunction with the CCSEM and ASTM analyses but is unnecessary, as a mass balance will provide the same information, detailing the abundance of water-soluble, acid soluble, and ion-exchange mineral groups.

3.3.4. Coal PSD

A particle size distribution of a pulverized coal can be obtained using a Malvern Mastersizer. A Mastersizer generally uses laser diffraction to determine the relative size and distribution on a cumulative percent passing-volumetric basis. This method is good for measuring particle sizes between 0.1 and 3000 μm . Malvern technology is different than that obtained on the mass basis from sieve tray analysis. Sieve analysis has the disadvantage in that it cannot practically account for very fine particles. An example input file for the Coal PSD is included in Appendix B.

3.4. ANSYS Fluent

Computational fluid dynamics programs are valuable tools available for use throughout industry. However, their abilities to accurately predict combustion characteristics are only as

good as the accuracy of the models used within them. Thus far, only limited CFD modeling of TE partitioning is available, and generally it is for a specific elemental species rather than several broad species types (Jassim 2009; Jassim et al. 2010; Jassim et al. 2009; Seames, Jassim, and Benson 2010).

Calculating TE partitioning using solely CFD would be computationally expensive if all plausible reaction mechanisms were considered. Even simpler carbon-based combustion processes such as modeling methane combustion with air can be described by 279 reactions with over 49 species (Turns 2000). When thinking of coal, one must realize that reactions occurring during combustion are far broader than a simplified methane combustion model; multiple pathways in which reactions can proceed are present. Many potential pathways are heavily influenced by fuel properties and combustion environment, as well as particle size distributions.

Fluent provides an environment wherein the evolution of gaseous species may be determined. The drawback to this approach is that the model can only include those species and relationships included in the set-up of the model. Results and reactions involving minor combustion species are not always included in a model, and a simple mechanism cannot describe information on any species not previously identified. Even elaborate thermodynamics-based TE partitioning models, which include TEs, have shown flaws.

3.4.1. Other CFD Package Options

ANSYS Fluent 14.0 is used as the CFD user interface in this study. It was chosen based on familiarity, accessibility, and widespread usage within industry. However, the developed C⁺⁺ program was established to read tab-delimited text files and not function exclusively with Fluent.

Any appropriate CFD software may be employed, including later versions of Fluent, as long as the particle tracks taken from the CFD program are formatted to match those presented in Appendix B. The C⁺⁺ program developed for this research project could be modified to allow communication with the Fluent platform, but that is outside of the intended reach of this study and may prove too computationally expensive for practical purposes. For information on programming user-defined functions, see the user-defined function manual (ANSYS 2006, 2009).

This dissertation is written with the expectation that the reader has some familiarity with Fluent, Gambit, their related software packages, and their basic purpose/function. The intention is to provide details regarding the developed TE partitioning computer program, not to provide details of the modeling practices that may be undertaken through ANSYS Fluent. Particulars are only briefly highlighted, as numerous tutorials are also readily available for the interested reader. For information on specific details, the appropriate user manual should be consulted (ANSYS 2012). Information regarding specific usage of models relating to the validation of modeling experimentally determined gaseous temperature profiles is shown in Chapter 4, in which an experimental system is discussed.

3.4.2. Gaseous Species

The reactions involving TE species are neglected within Fluent because they are on the scale of ppm to ppt, and their inclusion would be computationally expensive. Simple rate expressions describing their release and subsequent reactions are unavailable. The research performed and subsequently reported in this dissertation is a direct result of the desire to acquire this mission information.

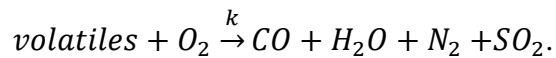
Primary and minor gaseous species programmed into Fluent include CO₂, CO, O₂, N₂, H₂O, H₂, SO₂, and volatiles. This list is not all-inclusive and can be modified based on the end users' needs. Compounds related to the formation of SO_x are included because they play a role in TE partitioning.

Species included in the CFD software must include those species listed above (CO₂, CO, O₂, N₂, H₂O, H₂, SO₂, and volatiles), unless modification to the program is undertaken. Null values are acceptable. Additional species may also be included as needed. Information important to the user should govern the decisions regarding modeling.

3.4.3. Primary Pyrolysis

To take material from a coal analysis and glean information regarding a particle track using Fluent, accurate kinetic data describing the bulk major gaseous species are needed. It was felt that the two-step chemistry provided in Fluent did not provide enough detail for the current study. Therefore, other reactions were also employed.

For a simplified approximation of coal combustion, the following volumetric reaction is used.



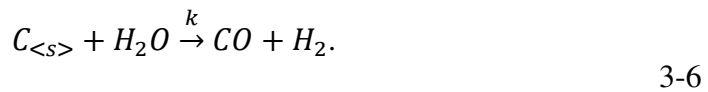
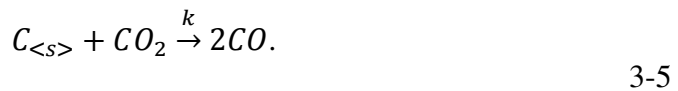
3-1

The volatile matter is released during primary pyrolysis. Gases released are considered to react following the simplified kinetic mechanisms identified by Jones and Lindstedt (Jones and Lindstedt 1988).



3.4.4. Char Burnout

After volatile matter is completely released during primary pyrolysis, the char remaining in the coal particle reacts with the surrounding gas phase. The heterogeneous reactions of char with O₂, CO₂, and H₂O are described in reactions 3-4 to 3-6. A frozen flame approach is employed, which means that the oxygen that penetrates the particle is consumed during char oxidation.



For air combustion, reaction 3-4 is the most relevant. Reaction 3-5 plays more of a role during oxy-combustion due to the high partial pressure of CO₂. Reaction 3-6 is most relevant for gasification conditions.

Reaction rates are limited by the diffusion of the oxidant species from the bulk gas phase to the particle surface. Rate constants for reactions 3-4 to 3-6 are provided in Table 3-1.

Table 3-1 Heterogeneous surface reaction kinetic rate data

Reaction	A, kg/s m² Pa	E, J/kmol	Order n	Reference
3-4	0.005	7.4E+07	1	(Field 1969)
3-5	6.351E-03	16.2E+07	1	(Smoot 1997)
3-6	1.921E-03	14.7E+07	1	(Smoot 1997)

As scientists verify models and kinetic data, updated information is released and different parameters may be accessible. Updating kinetic data used in Fluent with the advent of new techniques is not an issue within this project, since the purpose of using this CFD package is to obtain a dataset that can be used with the C⁺⁺ program. The gas phase kinetic reactions are not programmed in the developed software. The variable nature of parameters is mentioned as this may account for irregularities between the results of data obtained from Fluent and experimentally obtained results reported in literature. The purpose of this dissertation is to demonstrate aspects of the developed program. The program was written under the assumption that input data are correct.

3.4.5. Devolatilization

Sub-models activated within ANSYS Fluent have a great effect upon the predicted results. One sub-model that has repeatedly been shown within literature to have an affect on temperature conditions is the devolatilization model. Options such as using a constant rate, multiple kinetic-devolatilization rate expressions (Kobayashi, Howard, and Sarofim 1977), or more advanced modeling techniques—the *chemical percolation model* (CPD) (Fletcher et al.

1990; Grant et al. 1989)—are generally made based on the computational expense and the level of accuracy required.

3.4.6. Particle Temperature Profile

A spherical particle with no internal circulation or volume change transfers heat in distinct regions. These include the liquid region composed of the melt, the solid region composed of any exterior residual char or inorganic shell, and the gaseous region composed of the species present during combustion. For the purpose of this model, because the ratio of bulk gas to solid is large and internal circulation is likely within a melted particle, the temperature of the particle is considered the same as the surface of the particle.

3.4.7. Particle Tracks

Once the user has determined that convergence has been achieved for the CFD mode, the user exports the particle track datasets from Fluent and then must format them appropriately. Microsoft Excel provides a user-friendly environment in which the data may be maneuvered and then exported as a tab-delineated txt file that can be read by the C⁺⁺ program.

Particle track information extracted from ANSYS Fluent includes time (s), particle temperature (K), particle diameter (m), particle mass (kg), particle char mass fraction, particle volatile mass fraction, particle time step (s), particle x positioning (m), particle radial positioning (m), particle theta positioning, static temperature (K), static pressure (Pa), and gas mole fractions. An example input file is included in Appendix B.

3.5. Object Oriented C⁺⁺

The complexity of TE partitioning and the vast arrays of both existing and new data that has and would be generated required a modular structure to be implemented for this model. The C⁺⁺ programming language allows for more dynamic ability while reducing mistakes and excess coding that would be required by C or Fortran. C⁺⁺ is object oriented by design.

The object-oriented approach encourages the programmer to place data where they are not directly accessible by the rest of the program. Instead, data are accessible by calling specially written functions, which are inherited from “class objects.” This method wraps datum within a certain area to ensure it is used appropriately, rather than having all information accessible at the same time. By the object-oriented approach, data are generated and called from functions only when needed. This form of programming also allows implementation of different types of objects that correspond to the managed use of a particular kind of complex datum.

The C⁺⁺ code developed in this research separates information into various classes based on the information contained therein. This includes classes for reference data, particle track information, CCSEM related information, excluded fragmentation information, coal PSD information, and coal particle information. Reference data include information derived from the periodic table of elements, thermodynamic database sets, and other necessary sources which are related to solving relationships described within the works of Quann et al. (Quann, Neville, and Sarofim 1990), Yan (Yan 2000), and Zeng et al (Zeng, Sarofim, and Senior 2001). By using the object-oriented approach, the three elements listed (arsenic, antimony, and selenium) have been programmed. Additional TEs can be added in the future if/when the need arises.

3.6. Data Solver – The Black Box Explained

The information manipulated within the data solver works together to give the final outputs. The information contained therein can be subdivided into subsections: mineral distribution, organically bound distribution and vaporization, vaporization from inclusions, and vaporization from exclusions. Details needed for Fluent injections are provided as a check for the user to determine that the input data matches that described using Fluent.

The mass transfer approach described by Zeng et al (Zeng, Sarofim, and Senior 2001) applies mainly to the inclusion and exclusion subsections, whereas the organically bound portion of the program assumes that organically bound TEs are released proportionally with the char combustion. Aspects from the kinetic data provided by Raeva and co-workers are used in all vaporization subsections (Raeva 2011; Raeva et al. 2012; Raeva, Klykov, et al. 2011; Raeva, Pierce, et al. 2011).

3.6.1. Particle Size Distribution Development

Particle size is directly related to many facets related to TE liberation. CCSEM data is used to provide the size and distribution of mineral grains within coal particles. Mineral grain CCSEM data are divided between included or excluded mineral grains using a Monte Carlo method to “randomly” redistribute mineral grains among simulated coal particles (Yan 2000).

A modified approach to that suggested by Yan provides a means whereby the *particle size distribution* (PSD) of residual matter could be approximated from CCSEM data using the concepts of a Poisson distribution (Yan 2000). In this modified approach, an original particle size distribution of the raw coal is determined (generally through the usage of a Malvern Mastersizer)

and divided into a number of discrete size ranges or bins. All particles within the same bin have the same nominal particle size when entered in calculations.

For the purpose of the developed C⁺⁺ program, included and excluded mineral grain data were preprocessed by Microbeam Technologies into six discrete size bins. These include sizes: (bin 1) 1.0~2.2 μm , (bin 2) 2.2~4.6 μm , (bin 3) 4.6~10.0 μm , (bin 4) 10.0~22.0 μm , (bin 5) 22.0~46.0 μm , and (bin 6) 46.0~400.0 μm . These bins provide the basis of separation of mineral grains within parent raw coal particles.

Details of a few select mineral groups for a Southern PRB subbituminous coal, their weight percent (on a total mass basis of all mineral groups), and their relative sizes can be found in Figure 3-2. The total mineral mass is 6.4 weight percent of the total coal mass. As can be seen in this figure, not all mineral groups are found in every mineral size bin. Furthermore, the mineral groups will not necessarily have the same relative abundances.

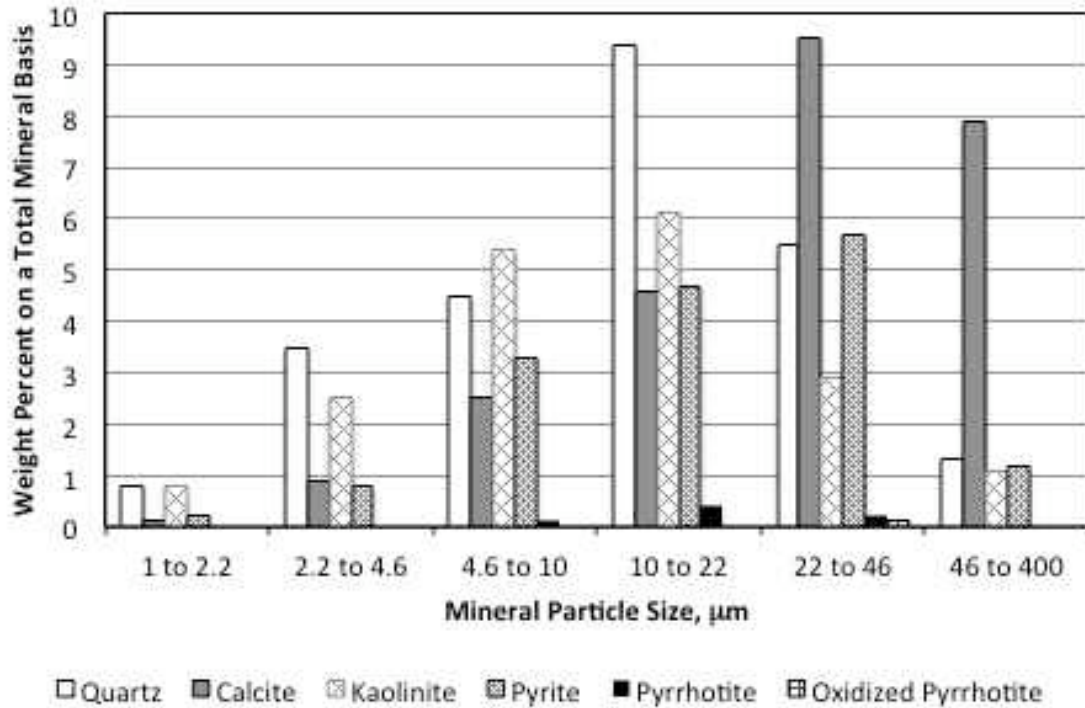


Figure 3-2 Weight percent on a mineral basis of select mineral groups, by mineral particle size, detected by CCSEM for the Southern PRB subbituminous coal

Once the raw coal is divided into bins, data from the approximate and ultimate analyses of the coal as well as the CCSEM analysis are used to determine the volumetric fraction of the mineral content of the coal per particle. At this point the volumetric fraction of the coal is available but still considered a *mineral-free volume* (V_{mfree}), meaning that a corresponding mineral grain has not been assigned to fill the fraction of the coal particle.

Data from the CCSEM analysis then permits the distribution of mineral grains, one by one, into selected coal particles. The V_{mfree} of all particles is tracked. A *mineral grain volume* (V_{m}) can be dispersed into a V_{mfree} of a selected coal particle only if $V_{\text{m}} < V_{\text{mfree}}$. Once a volume is added to a particle, the V_{mfree} is reduced by the volume of the mineral grain added. An inventory is kept to record mineral inclusions (types and size) accumulated into each particle. Segregation of mineral groups into mineral-free volumes starts with the largest available V_{mfree}

this ensures that mineral grains are distributed to several particles rather than only a few particles within a given size fraction. The location of one mineral grain is assumed to be independent of any other mineral grains. An illustrated graph showing the coal particle size distribution and the calculated (based on CCSEM data) initial V_{mfree} equivalent PSD is found in Figure 3-3. The data will have similar trends to one another as is shown in the figure.

Although the organically bound portion of the coal is considered uniformly distributed, through the use of the semi-random mineral distribution methodology, each coal particle potentially has a distinctive inorganic-based material composition. The developed model accounts for arsenic, antimony, and selenium bound within pyritic family minerals. Other minerals, such as illite, can be incorporated into the model once mass transfer coefficients

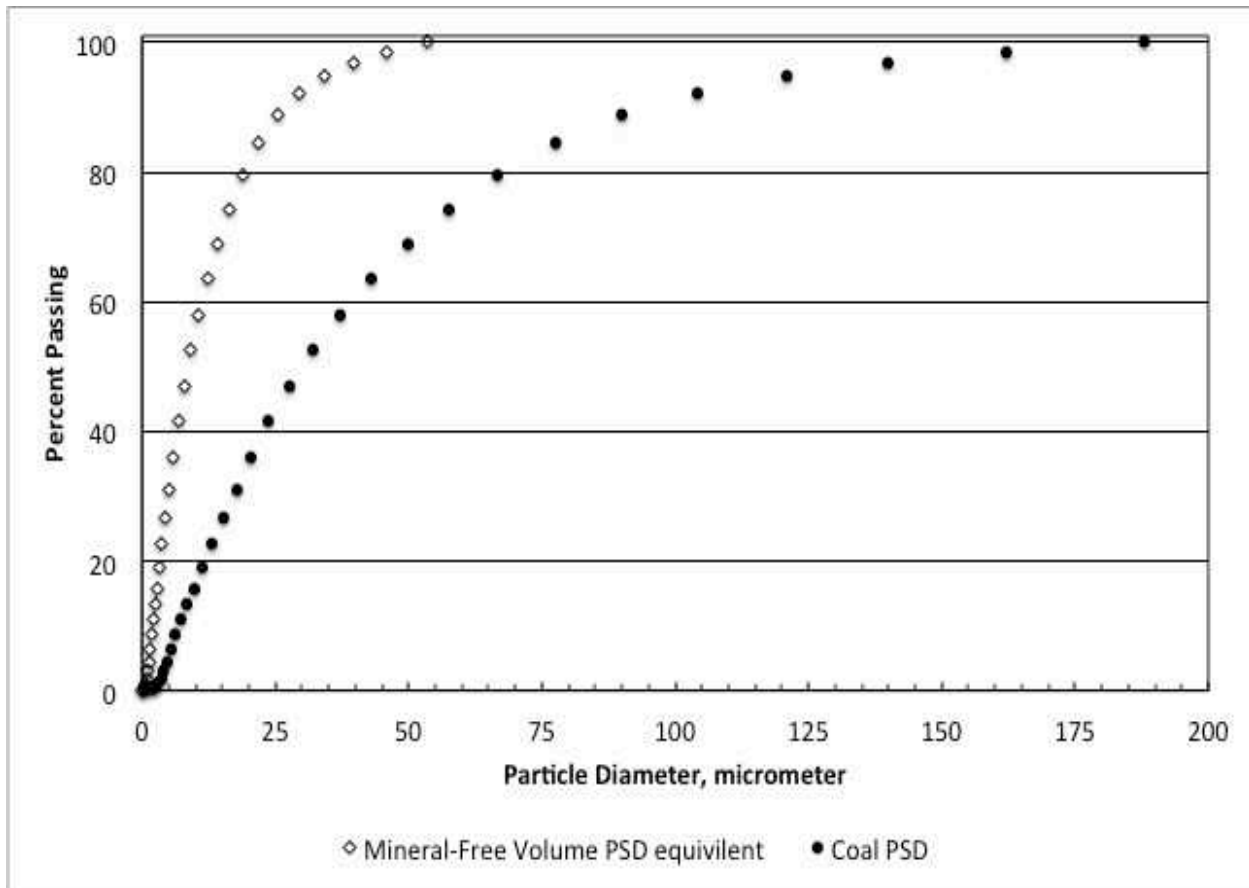


Figure 3-3 Example Southern PRB subbituminous coal particle size distribution and calculated mineral-free volume particle size distribution equivalent

through the melt are determined. Minerals accounted for in the developed model include pyrite, pyrrhotite, and oxidized pyrrhotite and the changes these minerals undertake during coal combustion. The semi-random nature of mineral distribution may produce coal particle bins that do not have included pyritic family minerals as can be seen in Figure 3-4 the example bin sizes are found in the coal PSD listed in Appendix B.5. Both bin number and size range grouping of the coal particles are shown in the figure.

Figure 3-4 compares the calculated number of coal particles and the calculated number of coal particles of that bin that have one of more pyritic family minerals included therein for a given pulse duration.

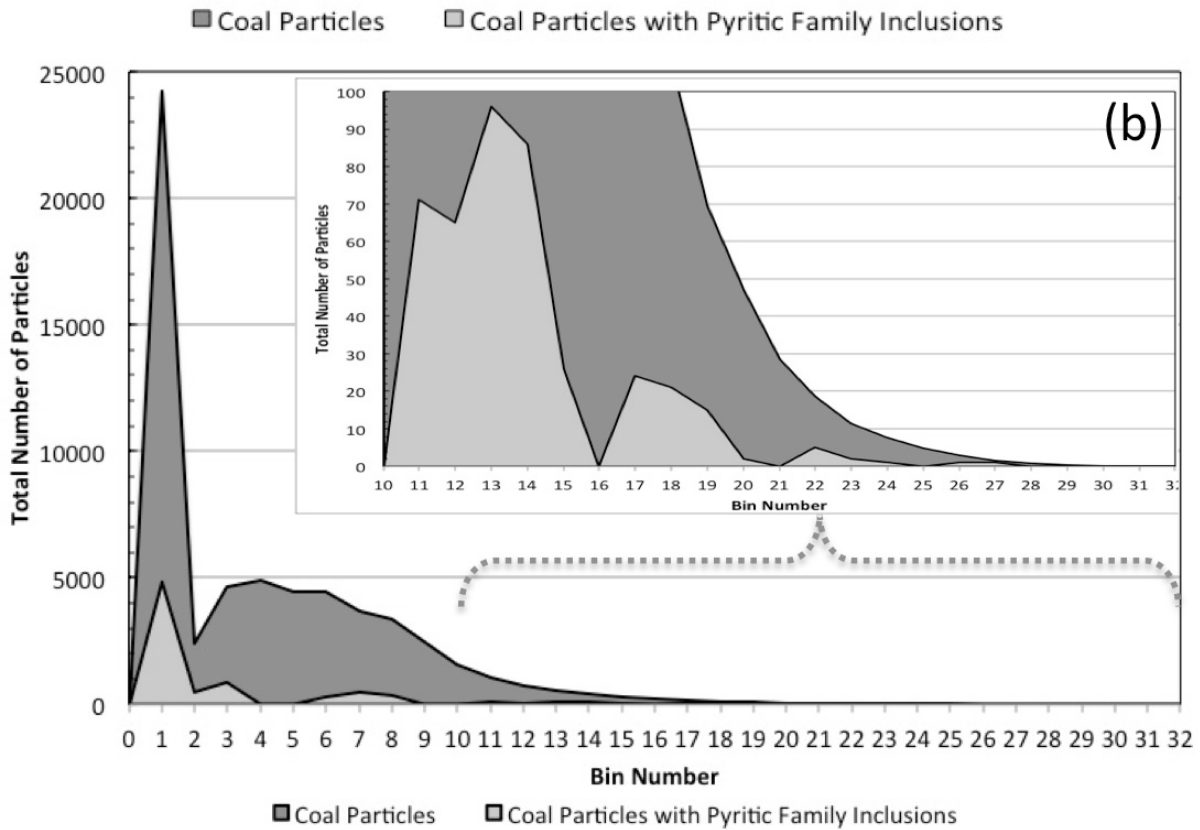
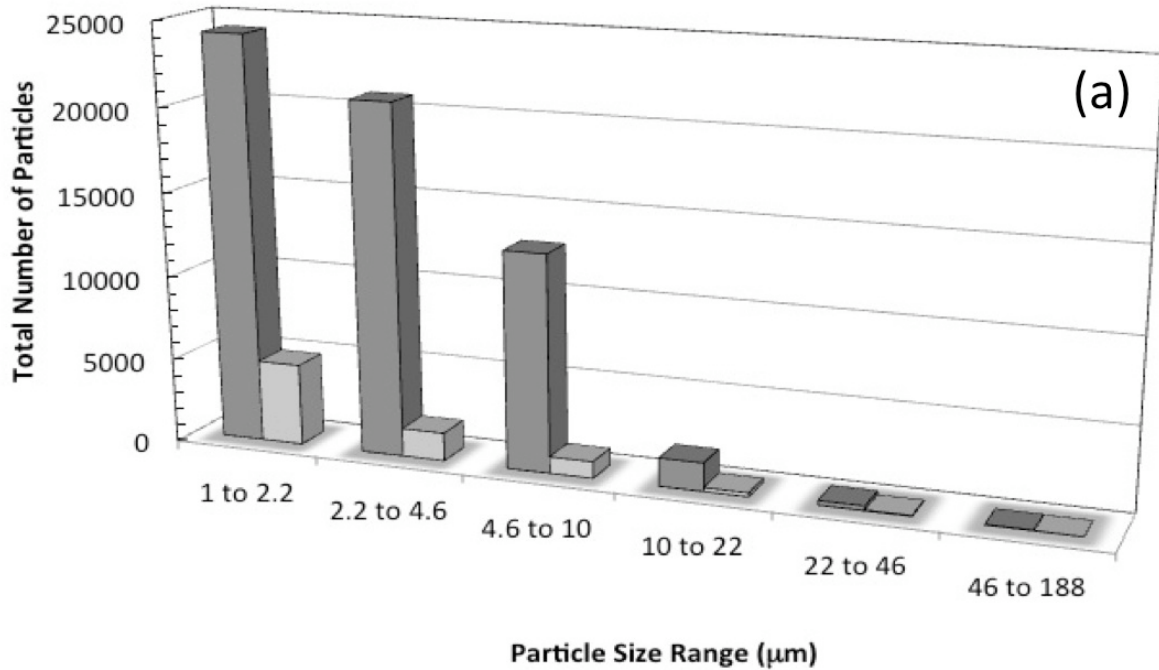


Figure 3-4 Example of calculated results of the number of coal particles generated during the program as well as the number of those particles that actually have any combination of pyrite, pyrrhotite, or oxidized pyrrhotite minerals within those coal particles for a given pulse duration

The pulse duration is the time basis for which coal particles are released into the combustion environment. Each coal particle could have multiple distinctive inclusions. A small subsection of the higher bin numbered coal particles (larger diameter particles) is also shown in the Figure 3-4-b for visualization purposes due to the vast differences in y-axis scale. The programming feature of a semi-random mineral composition for each coal particle helps contribute to the simulation of TE partitioning from coal particles with more realistic compositions than would be seen from a uniform distribution. As coal is not uniformly distributed, particles will be more realistically modeled in that they have unique compositions based on the CCSEM analysis rather than a uniform overall composition based on the proximate and ultimate analyses.

Excluded mineral particles are also treated differently than could be given in a uniform distribution approach in that their size distribution is taken directly from the CCSEM data. Their behavior within the combustion zone is related to the temperature differences the excluded mineral grain will likely encounter within the furnace environment. The distribution of organically bound inorganic elements is determined from the mass balance of those elements present in an ash analysis to the required quantities that would be taken up in the included and excluded fractions.

During combustion, given enough time and under appropriate conditions, mineral grains can eventually transform into their corresponding oxide residue. These include carbon dioxide for carbonates, sulfur dioxide from sulfates/sulfides, and/or moisture from hydrates.

Ash formation is related to the fragmentation of particles during combustion and the coalescence of mineral residues on the char surface (Yan 2000). When the bulk gas temperature falls below the coalescence temperature of the oxides, the nuclei coagulate and grow. The final

particle size distribution of the submicron ash is determined by the oxidant-temperature-mixing histories encountered by the particles. After the molten stage, in the course of transformation, ash particles are assumed to be spherical. Aerosol dynamics can be employed to describe the evolution of the particle size distribution beyond the formation of the first nuclei (Neville and Sarofim 1982). Ash cenospheres are neglected in the present work.

3.6.2. Mass Transfer

The details of the mass transfer approach described by Zeng et al., originally based on bituminous coal, are used in this model for TEs associated with included or excluded pyritic family minerals (Zeng, Sarofim, and Senior 2001). Arsenic, antimony, and selenium are specifically mentioned. Further elaboration for the details used within the vaporization model can be found in the works of Bool et al. and Zeng et al. (Zeng, Sarofim, and Senior 2001; Bool III et al. 1997). Aspects of the related calculations as taken from Zeng et al., and Quann et al. are given in this section and subsections of the document (Quann et al. 1982; Zeng, Sarofim, and Senior 2001). A portion of the model presented is based on the work of Ohno (Ohno 1991). Other calculations/derivations and useful relationships can be found in Appendix E.

The modeling theory discusses the vaporization of TEs from a liquid melt. The objective for using this approach is to determine the overall mass transport rates of the species from within a burning coal particle to the bulk gas phase. Diffusion through the melt is the rate-limiting step of TE liberation from pyrite.

3.6.2.1. Melting Points

Before a TE species can be released from inclusions and exclusions, the bonds holding it in the crystalline lattice must have enough energy to break and rearrange to more thermodynamically favorable configurations. As discussed in Section 2.2, during combustion, pyrite grains (FeS_2) become pyrrhotite (FeS) melts. Within the melt, the associated TE species are assumed atomically dispersed. Coalescence and sintering of iron and aluminum silicates during combustion creates a glassy layer where TEs can diffuse. Diffusion through the glassy layer is neglected within the developed vaporization model. The glassy layer would dilute the overall concentration of the TEs but its impact is minimal.

Melting points of select pure idealized mineral groups typically found in coal are shown in Table 3-2.

Table 3-2 Melting points of idealized pure components of several minerals typically found in coals (Yan 2000; Green and Perry 2008)

Common Minerals	Idealized Formula	Melting Point (K)
Kaolinite	$\text{Al}_2\text{Si}_2\text{O}_5(\text{OH})_4$	2086
Montmorillonite	$\text{Na}_{0.75}\text{Mg}_{0.7}\text{Al}_{3.3}\text{Si}_8\text{O}_{20}(\text{OH})_2$	2500
Calcite	CaCO_3	1612
Dolomite	$\text{CaMg}(\text{CO}_3)_2$	d 1003 - 1033
Ankerite	$\text{CaCO}_3^*(\text{Mg}, \text{Fe}, \text{Mn})\text{CO}_3$	1000
Quartz	SiO_2	tr < 1698
Rutile	TiO_2	1913 d
Gypsum	$\text{CaSO}_4 \cdot 2\text{H}_2\text{O}$	1723
Barite	BaSO_4	1853
Pyrite	FeS_2	tr 723
Pyrrhotite	Fe_{1-x}S (x=0 to 0.17)	d > 973*

* 1461 K from Lide (Lide 2002), 1296 K from Yan (Yan 2000)

d = decomposes; tr = transition

These values are only provided as reference values for determining behavior of some components. The mineral grains found in coal are not perfect, single crystals and should not be thought of in that manner. However, the melting points presented show temperature ranges in which included and excluded mineral groups may have some of their initial TE species more easily devolatilized. Several species such as quartz, calcite, montmorillonite, and kaolinite have relatively high melting temperatures in comparison to pyritic family minerals.

3.6.2.2. Mass Transfer Coefficient

As illustrated in Figure 3-5, the vaporization processes for arsenic, antimony, and selenium, can be described by three distinct transitions.

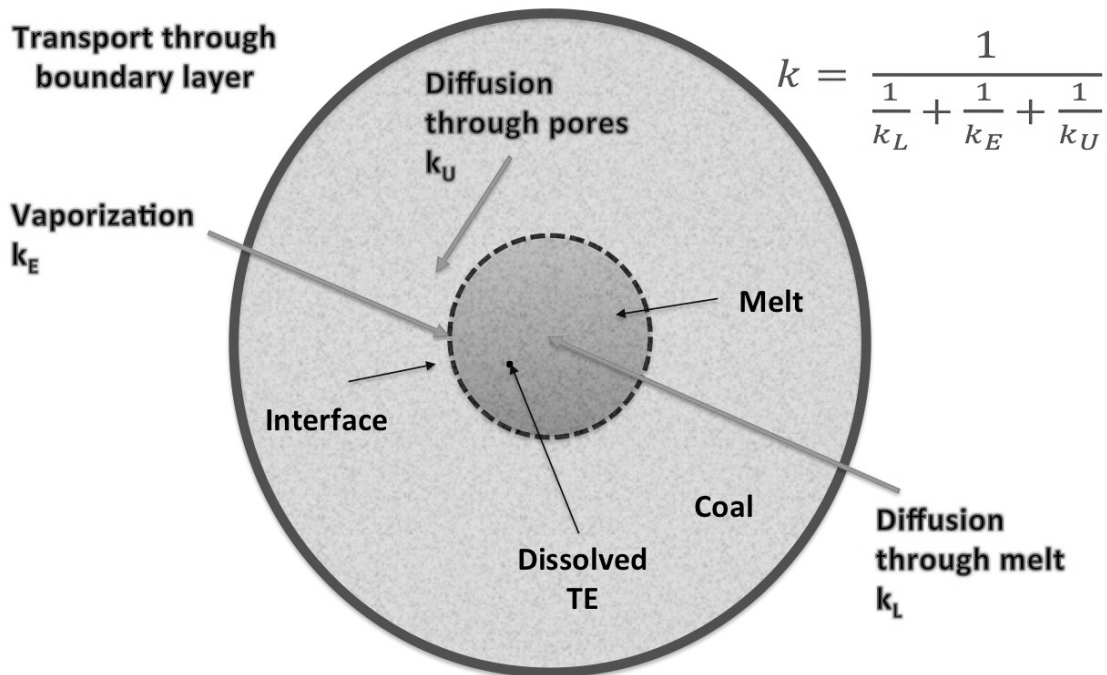


Figure 3-5 Vaporization processes for TEs (Zeng, Sarofim, and Senior 2001)

The overall mass transfer coefficient, k , is a function of the following transitions: (1) diffusion of TEs through the pyrite melt to the melt/gas interphase, k_L ; (2) vaporization of the elements once they reach the surface, k_E ; and finally, (3) transport of molecules/atoms through the pores of any remaining char/pyrrhotite shell that may be present, k_U (Zeng, Sarofim, and Senior 2001). The overall mass transfer relationship is described by:

$$k = \frac{1}{\frac{1}{k_L} + \frac{1}{k_E} + \frac{1}{k_U}}.$$

3-7

Transport through the boundary layer surrounding the particle is neglected when internal resistance is controlling, as is the case during pulverized coal combustion (Bool III et al. 1997).

Bool et al. suggest that the fate of copper and nickel could also be explained and predicted in a similar manner, dependent upon parent grain type (Bool III et al. 1997). However, this is not included within this program.

Within the works of Zeng et al. as well as Bool et al., the complete derivation of k_L , k_U , k_E , and k are provided (Bool III et al. 1997; Zeng, Sarofim, and Senior 2001). Only the concluding relationships of the derivations are provided herein. Their developed mathematical model does not account for the time-temperature dependent nature of pyrite transformations and thus the availability of the pyrite melt needed for TE liberation to occur. Nor does their mathematical model account for multiple particles of differing composition. The current program does take these attributes into account.

First, the overall vaporization process of a TE species is controlled by its diffusion through the melt. This implies that aspects of the relationships described are valid for inclusions

as well as exclusions. Even though arsenic, antimony, and selenium have varied physical properties, the diffusion rate in the pyrite melt for these TEs are of the same order of magnitude (Zeng, Sarofim, and Senior 2001). A first-order approximation, derived by Lynch, is used instead of the Machlin ridged body melt model to express k_L in the following form:

$$k_L = \frac{1}{r_i} D_o e^{\left(\frac{-E_D}{RT}\right)}, \quad 3-8$$

where, D_o (m^2/s) and E_D (J/mole K) are constants calculated from k_U , k_E , and k . R is the universal gas constant, T is the temperature of the melt, and r_i is the inclusion radius.

Next, k_U (m/s) is defined as:

$$k_U = \frac{P_i^0 \gamma_i M_{FeS} \eta D_i}{\rho_{FeS} r_i RT}, \quad 3-9$$

where P_i^0 is the vapor pressure of the pure element, γ_i is the Raoultian activity coefficient of solute i in the infinitely dilute solution, D_i is the effective Knudsen diffusivity, M_{FeS} is the molar mass of FeS (~ 87.9107 gm/mol), and ρ_{FeS} is the density of FeS (held constant at ~ 5000 kg/m³).

The effectiveness factor η is described as (Quann and Sarofim 1982):

$$\eta = \frac{3}{\phi} \left(\frac{1}{\tanh \phi} - \frac{1}{\phi} \right) \left[1 + \frac{D_i}{\beta D_{oxy}} \left(\frac{\phi}{\tanh \phi} - 1 \right) \right]^{-1}, \quad 3-10$$

where the Thiele modulus, ϕ , is:

$$\phi = \sqrt{30} \frac{r_p}{r_i} \quad 3-11$$

and

$$\beta = \frac{\ln(1+x_{oxy,b})}{1-\exp\left(-\frac{D_{oxy}}{D_m} \ln(1+x_{oxy,b})\right)}. \quad 3-12$$

D_{oxy} is the diffusivity of oxygen in the bulk gas, D_m is the diffusivity of element i in the bulk gas, $x_{oxy,b}$ is the mole fraction of O_2 in the bulk gas, and r_p is the char radius.

The main components of the reacting gases surrounding the particle accounted for in the present model are CO_2 , CO , O_2 , H_2O , and N_2 . Although N_2 and O_2 are by far the most prevalent species in air combustion, the more rigorous calculations for multicomponent diffusion are undertaken in an effort to make the model more applicable for other technologies such as oxy-fuel combustion environments. A listing of related equations is found in Appendix E. For binary diffusion the following relationship is useful:

$$D_{oxy} = 0.0018583 * \sqrt{T^3 \left(\frac{1}{M_A} + \frac{1}{M_B} \right) \frac{101325}{p\sigma^2\Omega_{DAB}}}, \quad 3-13$$

where D_{ab} has units of cm^2/s , σ_{ab} is 3.5785 Angstrom, \AA , T is in Kelvins, p is has units of Pa, (Bird, Stewart, and Lightfoot 2002). Finally, k_E (m/s) is described by:

$$k_E = \frac{\alpha' P_i^0 \gamma_i M_{FeS}}{\rho_{FeS} \sqrt{2\pi R T M_i}}, \quad 3-14$$

where α' is re-condensation coefficient, which is generally taken as unity for liquids.

3.6.2.3. Vapor Pressure

Due to the fact that there is little to no data for the vapor pressure of elements above their dilute solutions in liquid pyrrhotite or iron glass, the mass transfer approach uses the vapor pressure of pure elements to determine the mass transfer coefficient of a TE (Zeng, Sarofim, and Senior 2001). The equilibrium partial pressure of the TE in the pyrite melt, FeS, is described by:

$$P_{i,e} = P_i^{\circ} \gamma_i Y_i ,$$

3-15

where, $P_{i,e}$, is the equilibrium vapor pressure of the solute i ; P_i° is the vapor pressure of the pure element; and, Y_i is the mole fraction of solute i in melt.

Vapor pressure data are not available for all temperatures likely to be encountered during combustion. For instance, at temperatures greater than 973 K pyrrhotite decomposes (Green and Perry 2008). The method of extrapolation, as utilized by Zeng et al., is continued in this undertaking for species where coefficients for Antoine and Clausius-Clapeyron relationships were not available (Boal III et al. 1997; Zeng, Sarofim, and Senior 2001). When coefficients were unavailable, the nonlinear regression statistical program 'R' was used to determine parameters. Speciation suggested in the works of Raeva et al. was considered in the current model.

3.6.2.4. Relative Volatility

The modeling program developed requires vapor pressure data to calculate the separation of the TE species from the multicomponent-melt mixture. Binary-solution data are not enough to adequately represent the evolution of TEs. Another parameter is needed. This includes the relative volatility, α (Zeng, Sarofim, and Senior 2001), which is described by:

$$\alpha = \gamma_i \left(\frac{P_i^o}{P_{FeS}^o} \right).$$

3-16

The described relationship for α neglects solute-solute interactions.

Values of the relative volatility of arsenic, antimony, and selenium can be calculated using tabulated thermodynamic data. If the relative volatility is much greater than one, or much less than one, separation is possible. Relative volatility near unity implies no preferential separation is possible (Senior et al. 2001). Indirectly, estimated values of γ_i of the various species are provided in Table 3-3 (Boo III et al. 1997; Zeng, Sarofim, and Senior 2001).

Table 3-3 Raoultian activity coefficient of various species (Zeng, Sarofim, and Senior 2001; Hino et al. 1994)

Species	γ_i
As	0.0065
Sb	0.1500
Se	0.0080
FeS	1.0000

3.6.2.5. Overall Mass Transport Rate

The rate of TE vaporization is proportional to the trace element's concentration in the coal and in the parent minerals. The overall mass transport rate is described as (Boo III et al. 1997; Zeng, Sarofim, and Senior 2001):

$$J_i = k \frac{SA}{V} [C_{i,b}],$$

3-17

where: J_i has units of mole/m³s; k (m/s) is the overall rate constant; SA (m²) is the total surface area of the melt; V (m³) is the total volume of the melt; and, $C_{i,b}$ (mole/m³) is the bulk concentration of solute i in the melt.

The molar flux of species i described by the transfer of the solute atoms through the liquid melt is expressed as:

$$J_i = k_L(C_i - C_i^*) . \quad 3-18$$

C_i^* is the surface mole concentration of the solute i ; and C_i is the concentration of the gases.

Predicted sink and source terms of gas-phase and melt-phase species, in a computational iteration, respectively balance. Reactions are not allowed to reduce the calculated matter to less than zero during computations. Mass is conserved by maintaining the balance between the melt and gas phases.

4. TEMPERATURE VALIDATION

Measurements made by previous graduate students from the operation of the 19 kW lab-scale down-fired furnace maintained by the Department of Chemical Engineering at the University of North Dakota was used for the temperature validation study. Details relating to the furnace are briefly expounded in this chapter.

4.1. UND Furnace Specifications

Only a brief description of the UND furnace is provided. The UND furnace is a 19 kW down-fired furnace. Details of operation and specification of the furnace can be found in related presentations (Seames et al. 2006; Seshadri et al. 2011; Sisk 2011b, 2011a). The original specifications provided have had at least four major modifications. These modifications include changes to: (1) the injection system, (2) the feed system, (3) the ash collection system, and (4) changes which allow both air-combustion as well as oxy-combustion environments to be simulated (Lentz et al. 2012). A diagram of the furnace is shown in Appendix D.

4.1.1. Furnace Geometry

Information relevant to the operating conditions of the simulated pulverized coal combustion environment is included within the model through Fluent and Gambit. Figure 4-1

provides the geometric bounds of the UND furnace shown along the axis of symmetry with gravity in the x-direction. The figure is not to scale.

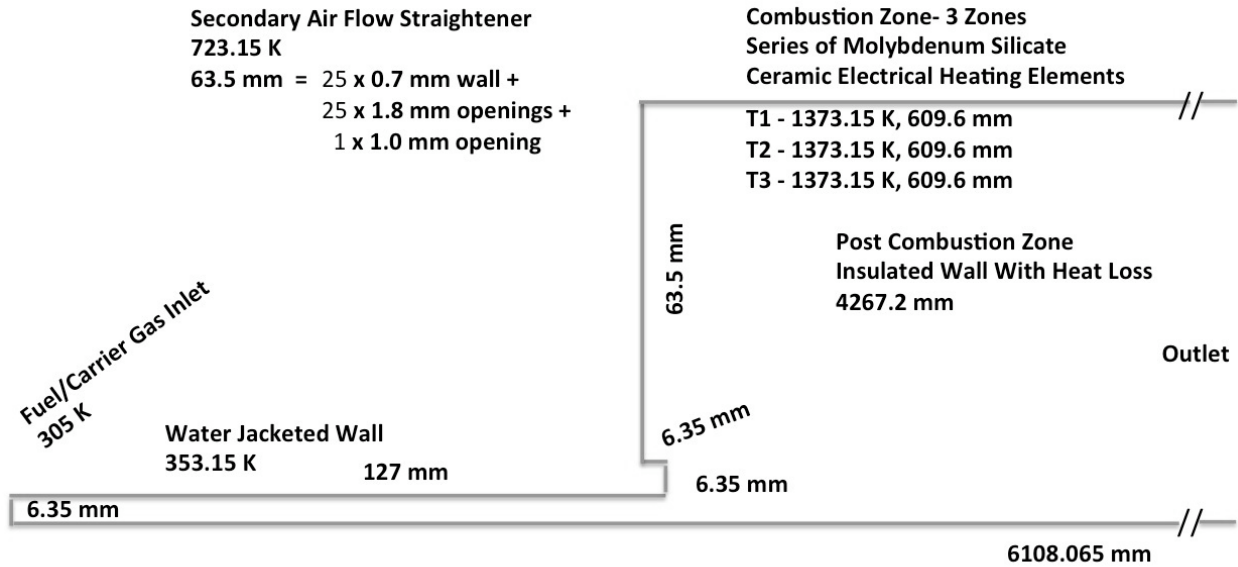


Figure 4-1 UND 19kw down-fired furnace configuration

As shown in Figure 4-1, the combustor is 6.1 m tall with an 0.15 m ID (Seames et al. 2006). Sample ports are placed to obtain in-situ ash samples and determine the centerline temperature profile of the combustion zone and post combustion zone at 0.57 m, 0.88 m, 1.18 m, 2.10 m, 2.71 m, 3.31 m, 3.92 m, 4.53 m, and 5.75 m from the bottom edge of the flowstraightener. A burner cap helps form the interfacial area in which the primary fuel carrier gas stream enters the furnace through a water-cooled jacket (Seshadri et al. 2011). A secondary oxidizer stream travels through a honeycomb flow straightener before being introduced within the furnace. The temperature profile was set up to mimic a full-scale boiler maximum-peak temperature and gas-cooling rates (Wibberley and Wall 1982). However, the temperature profile is strictly controlled due to the materials of construction and is limited to prevent damage. A full

scale PRB fired boiler would likely have higher localized temperatures, which would affect TE vaporization.

After initial warm up, the furnace is meant to be self-sustaining. However, temperature is maintained at 1377 K by embedded heater coils through a feedback control loop control system. Higher-grade coals power draw to keep this set temperature is quite small. Alternatively, for lower-grade coals such as lignite coals, the power draw is more substantial. For Fluent modeling purposes, heat is lost from the lower walls of the post combustion zone to the surrounding environment.

4.1.2. Boundary Conditions/Fluent Specifications

Information relevant to the boundary conditions entered into Fluent to model the combustion chamber is discussed in this section. Details of a Southern PRB subbituminous coal are also shown.

The water jacket nozzle temperature is maintained at 353 K. Parameters of the fuel/carrier gas inlet and secondary air inlets are found in Table 4-1 and Table 4-2, respectively.

Table 4-1 Fuel/carrier gas inlet parameters

Parameter	Value
Overall fuel mass flow rate (kg/s)	3.15×10^{-4}
Carrier gas velocity magnitude (m/s)	1.55
Carrier gas temperature (K)	305
Specific Mass Fraction of Oxygen	0.23

Table 4-2 Secondary air inlet parameters

Parameter	Value
Carrier gas velocity magnitude (m/s)	0.37
Carrier gas temperature (K)	723
Specific Mass Fraction of Oxygen	0.23

4.1.3. Coal Details

The proximate and ultimate analyses of the coal are shown in in Table 4-3 and Table 4-4, respectively.

Table 4-3 Proximate analysis of Southern PRB subbituminous coal

Proximate analysis (wt%)	
Moisture	26.36
Ash	4.10
Volatile Matter	31.47
Fix Carbon	38.07

Table 4-4 Ultimate analysis of Southern PRB subbituminous coal

Ultimate Analysis (wt% daf basis)	
C	79.32
H	5.29
O	13.66
N	0.81
S	0.92

The ash composition determined by the coal analysis is listed in Table 4-5. Organically bound materials are determined from a mass balance between that suggested using the CCSEM analysis and that obtained using the ash analysis. The example CCSEM data set is found in Appendix B.1. For the purpose of the developed program, organically bound TEs are evenly distributed within the organic portion of the coal. This helps contribute to the unique composition of the coal particles determined by the program.

Table 4-5 Ash composition of the Southern PRB subbituminous coal

Oxide	wt%
SiO ₂	34.88
Al ₂ O ₃	15.51
TiO ₂	0.65
Fe ₂ O ₃	4.34
CaO	20.65
MgO	4.06
K ₂ O	0.40
Na ₂ O	2.33
SO ₃	13.68
P ₂ O ₅	0.54
BaO	0.32
MnO ₂	0.10
Unknown	2.54

4.2. UND Furnace Temperature Profiles

Sub-models activated within ANSYS Fluent have a great effect upon the predicted temperature and compositional profile results. One sub-model that has repeatedly been shown within literature to have an effect on temperature conditions is the devolatilization model. For the current study, the experimentally obtained temperature profile of the UND furnace is compared to the predicted temperature profiles obtained using Fluent's devolatilization models in Figure 4-2. In this figure the centerline temperature profiles as a function of distance from the top of the furnace are shown. To provide valid TE release data, the developed model requires temperature profiles comparable to the actual furnace being modeled. As can be seen in Figure 4-2, the devolatilization models have similar bulk-gas-temperature trends. However, the location where the furnace reaches its maximum temperature value varies between models.

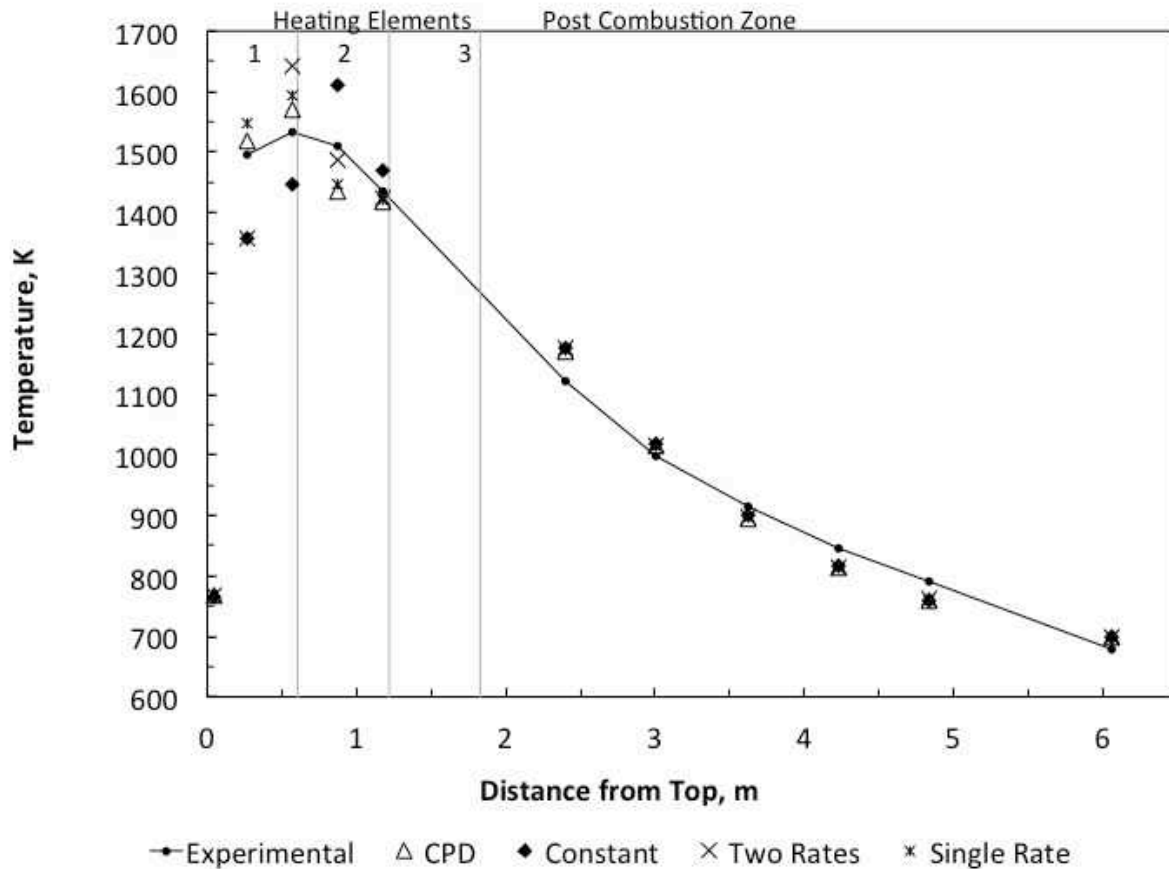


Figure 4-2 Illustration of the differences between devolatilization models predicted temperature profiles and the 19kw down-fired UND furnace burning a Southern PRB subbituminous coal

The CPD model data set was chosen for continued use within this study due to the similar trend of the experimentally obtained temperature values. Figure 4-3 shows a portion of the temperature contour plot of the UND furnace combustion zone using the CPD model. Regions of highest temperature have lighter colored contours. The region with the highest temperature profile is found between 0.1 and 0.7 meters from the top of the furnace. The majority of the reactions involving TE liberation occur in the combustion zone (top 2 meters of the furnace); therefore, matching this profile is felt to be the most important. The length from the top of the furnace before the initial bulk gaseous temperature rapid increase is directly related to the devolatilization model employed.

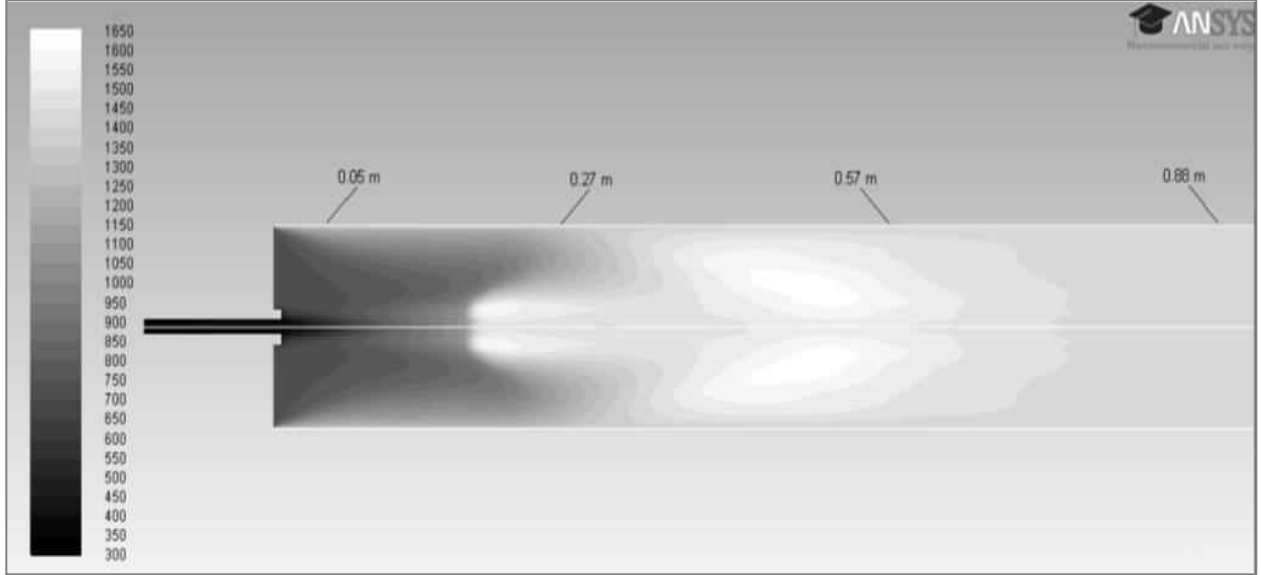


Figure 4-3 Illustration of the ANSYS Fluent modeled static temperature profile described as part of the current investigation for the CPD model

In the current investigation, particle temperature profiles and the bulk gaseous temperatures differ from one another. The degree of variance depends on the particle track. However, in general, the expected combusting particle temperature should be significantly higher than the temperature profile of the bulk gas. The discrete phase model in Fluent contains parameters for performing coupled calculations of the continuous and discrete phase flows. Reaction heat fraction, f_h , absorbed by solid is a parameter, which controls the distribution of heat of reaction between the particle and the continuous phase. As described in the ANSYS Fluent user's guide the particle heat balance during surface reaction is (ANSYS 2012):

$$m_p C_p \frac{dT_p}{dt} = h A_p (T_\infty - T_p) - f_h \frac{dm_p}{dt} H_{reac} + A_p \varepsilon_p \sigma (\theta_R^4 - T_p^4). \quad 4-1$$

where m_p is the mass of the particle, C_p is the specific heat, T_p is the particle temperature, t is time, h is the Fourier heat transfer coefficient, A_p is the area of the particle exposed to convection, T_∞ is the bulk temperature, H_{reac} is the heat released by the surface reaction, ε_p is the

particle emissivity, σ is the Boltzmann constant, and θ_R is the temperature of the surroundings. If the char burnout product is CO during coal combustion then $f_h = 1.0$ is appropriate. If the primary char burnout product is CO₂ then a value $f_h = 0.3$ is more appropriate.

Differences in particle temperature and bulk gas temperatures are accounted for by the use of this sub-model. Figure 4-4 shows plots of ΔT of particle temperature and bulk gas temperature versus path length for several coal PSD bins using the CPD devolatilization model. Bin numbers correspond to the coal PSD shown in Figure 3-3 and Appendix B.5 with larger bin numbers corresponding to larger particle sizes.

As shown in Figure 4-4, the difference between the particle temperature and the bulk gas temperature varies based on particle bin. Smaller particles have a smaller char fraction to combust and therefore the significant differences in temperature over shorter path lengths. Larger particle bins, those with higher bin numbers, tend to have particles that contribute more to the combustion environmental conditions over greater path lengths. Particle bins in the middle exhibit the greatest temperature difference between the particle surface and bulk gas phase.

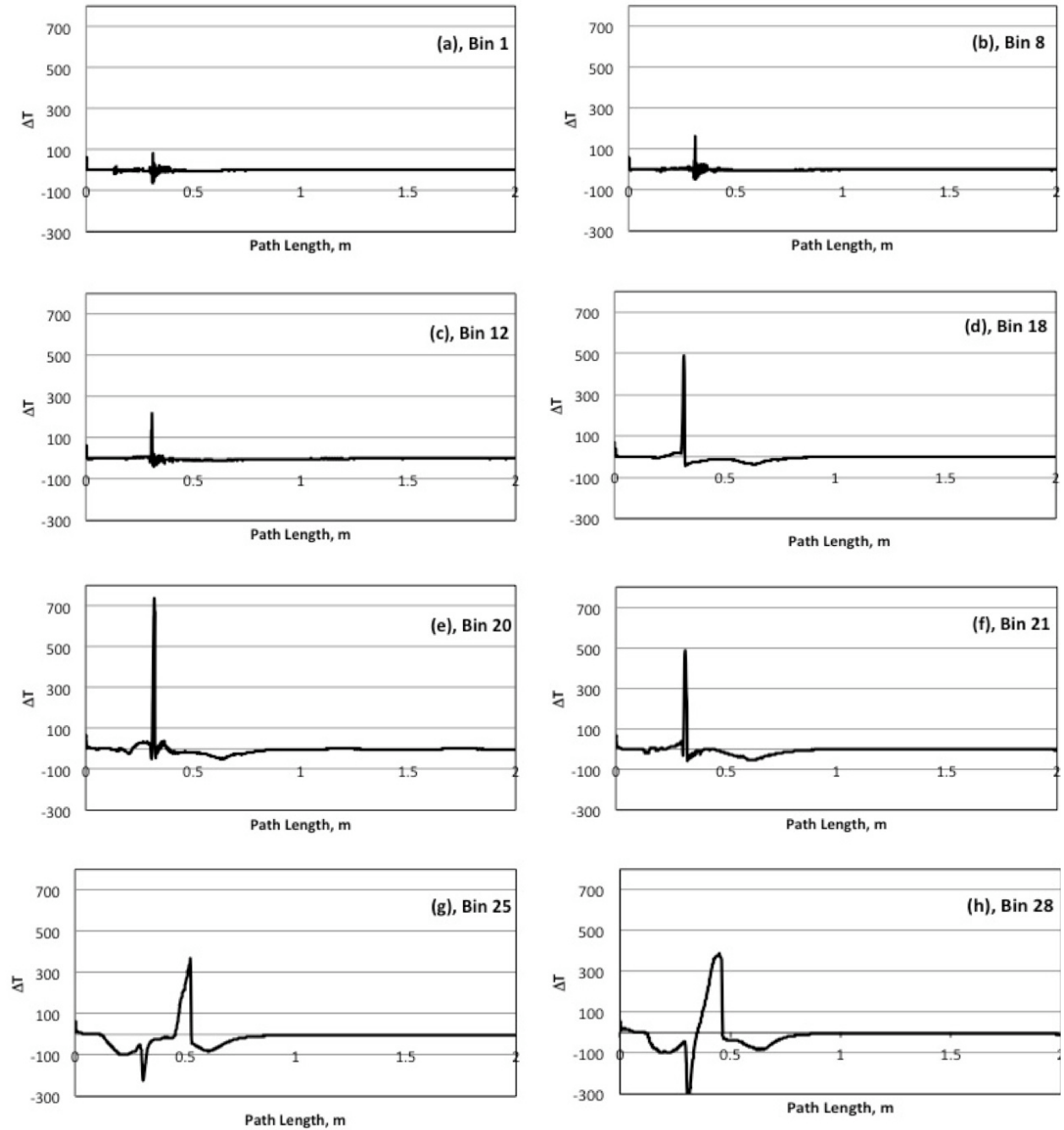


Figure 4-4 Plots (a) through (h) of the difference in particle and static temperatures versus particle path length using the CPD model as part of the current investigation

4.3. UND Furnace Volatile and Char Mass Fractions

The moisture and volatile mass fractions of the coal for all particle tracks is released within the first 0.45 seconds of being introduced into the furnace. This contributes to the temperature profile of the CPD model. A plot of the volatile mass fraction as a function of time for each coal particle bin separated by size is shown in Figure 4-5. Actual bounds of the coal particle size distribution bins can be found in Appendix B.5. Larger particles have higher bin numbers.

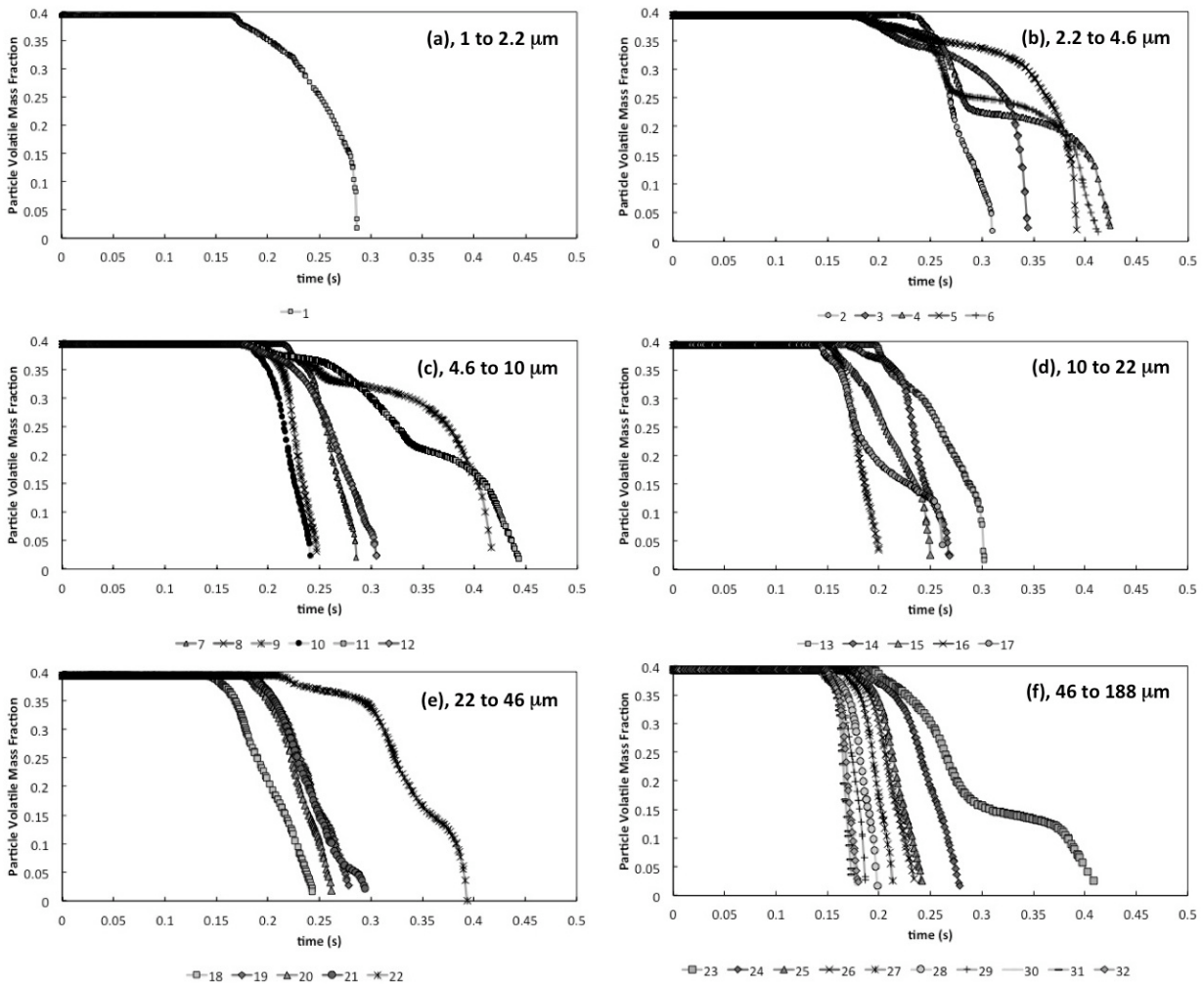


Figure 4-5 Modeled UND down-fired furnace volatile mass fractions as a function of time and bin number for all the particle tracks of a Southern PRB subbituminous coal

Figure 4-6 shows the average calculated time taken for coal particles of the size ranges and bins listed to release moisture and volatile content.

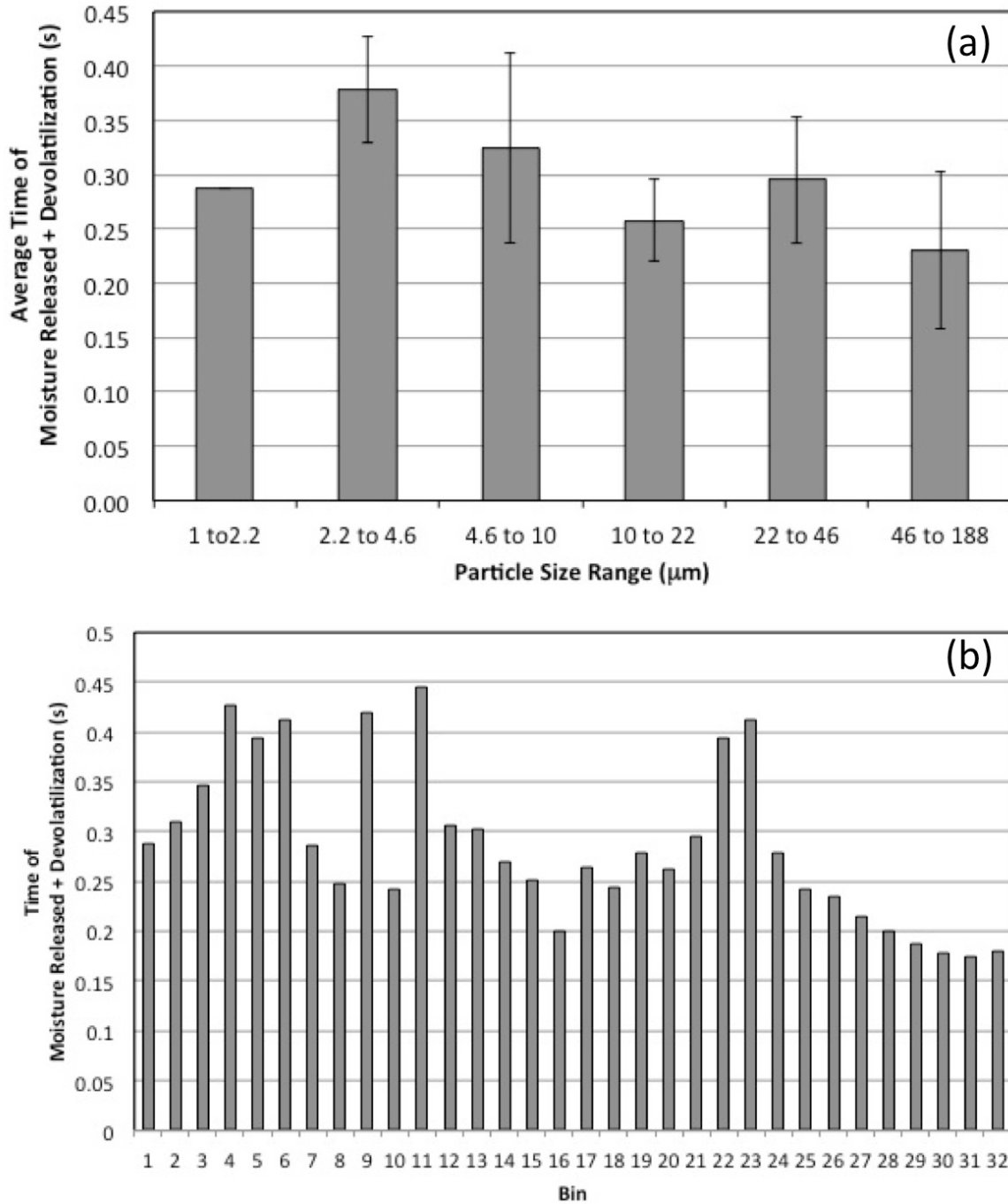


Figure 4-6 Modeled UND down-fired furnace time of moisture + devolatilization release as a function of time coal particle size range and bin number for all the particle tracks of a Southern PRB subbituminous coal

Figure 4-7 shows the calculated duration in which devolatilization of the coal particles of the size ranges and bins listed occurred.

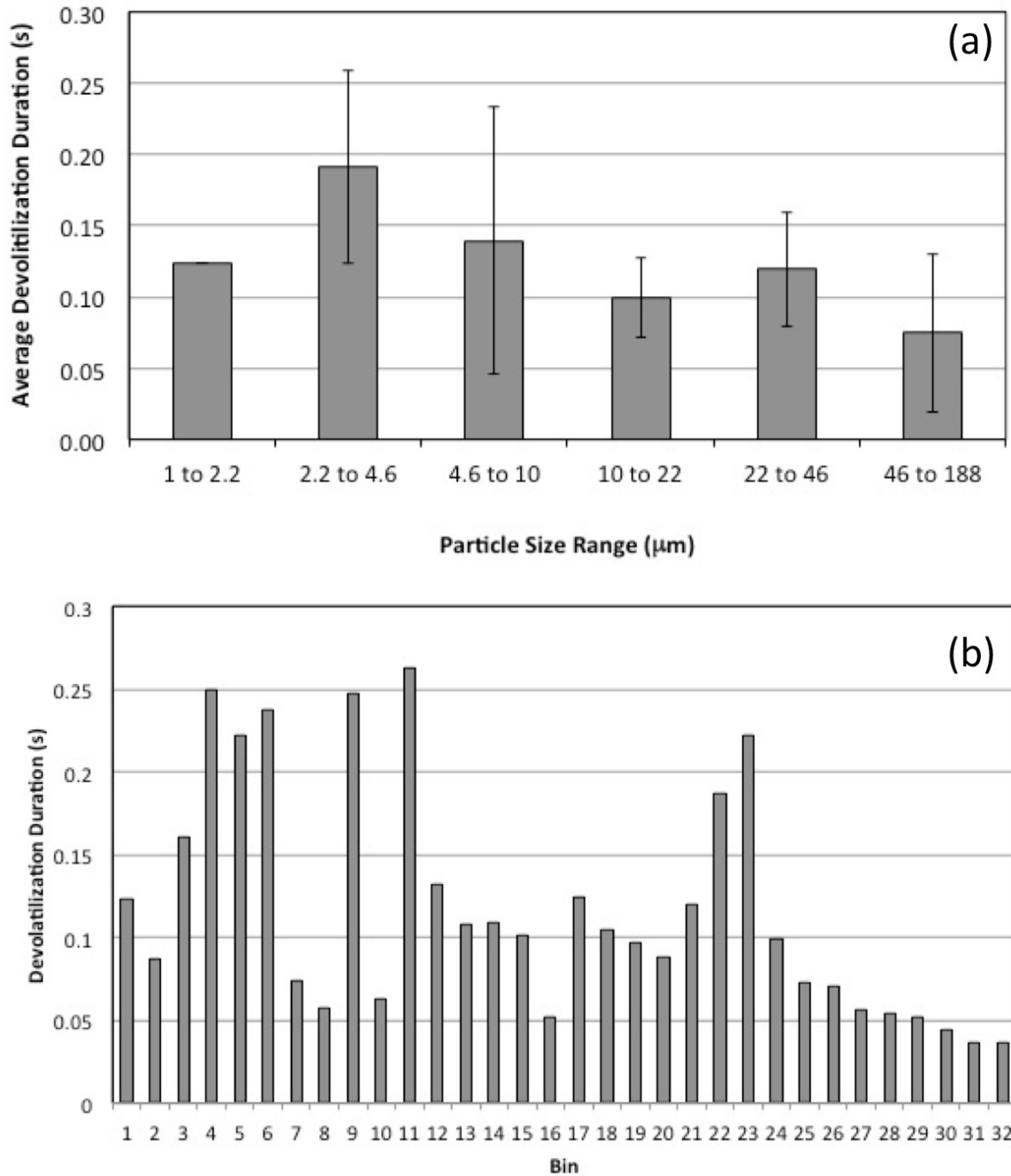


Figure 4-7 Modeled UND down-fired furnace duration of devolatilization as a function of coal particle size range and bin number for all the particle tracks of a Southern PRB subbituminous coal

As shown in Figure 4-5 to Figure 4-7 larger diameter particles' moisture mass fraction and volatile mass fraction tended to release more quickly than smaller particles. This attribute is likely due to the fact that larger particles will reach the high temperature zone faster than their smaller counterparts. Once these particles are in the high temperature zone they will further help the process continue its self-sustaining nature.

A plot of the particle char mass fraction versus path length for each bin size is shown in Figure 4-8, for the various particle track bins separated by size range.

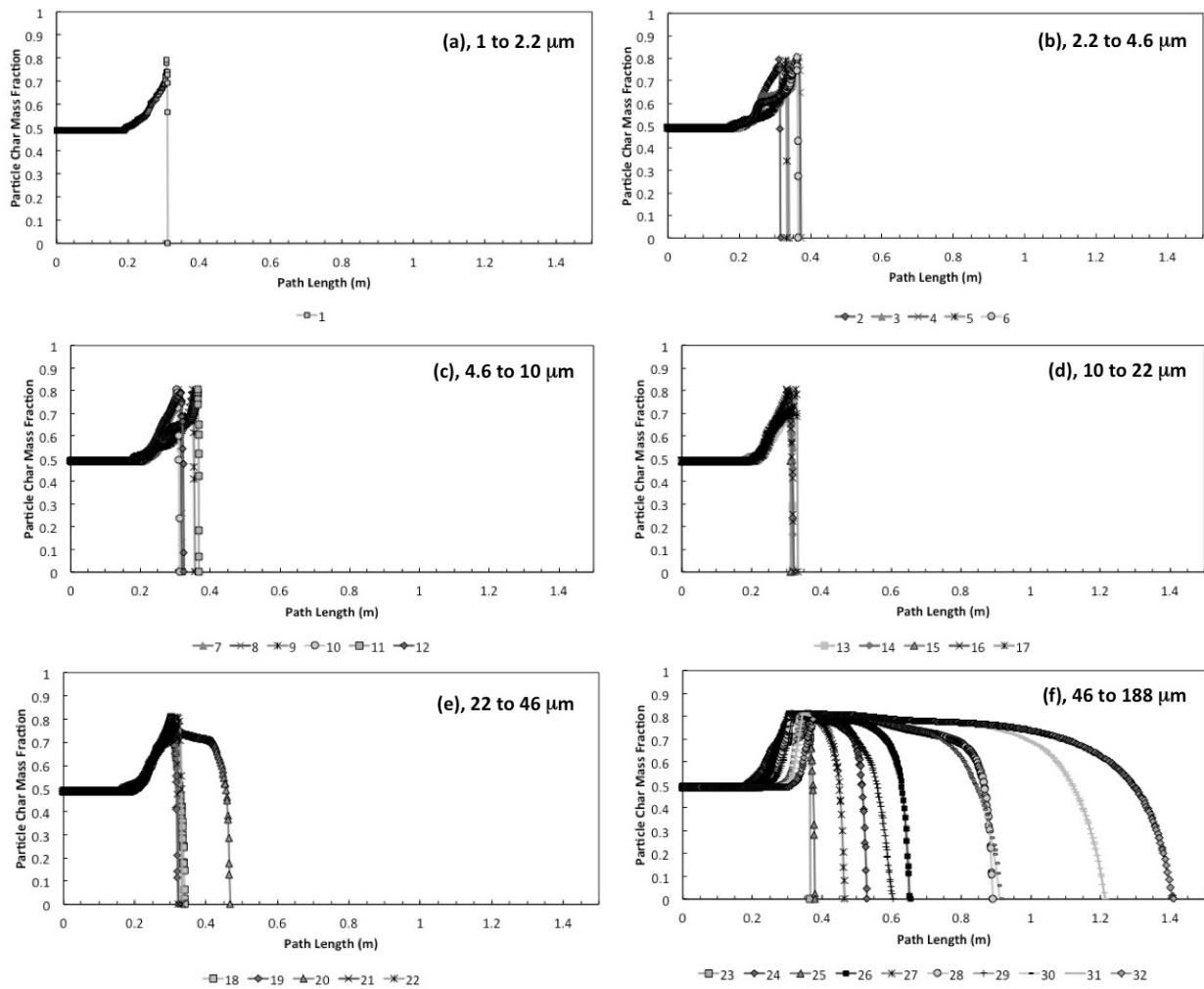


Figure 4-8 Modeled UND down-fired furnace particle char mass fractions as a function of path length for all the particle tracks for a Southern PRB subbituminous coal

Based on the particle char mass fraction, it can be seen that devolatilization of the subbituminous coal for all particle tracks is complete within a path length of ~1.4 meters from initial release. Devolatilization of the smaller-bins particle tracks of the subbituminous coal is complete within a path length of ~0.4 meters from initial release. The shorter distance traveled by smaller particles until completion of devolatilization occurs is likely a function of the relative quantities of volatiles present in comparison to larger coal particles.

Details regarding the char mass fraction are important, since they directly relate to the release of organically bound TEs. The initial increase in char mass fraction at path length ~0.2 to ~0.4 m is related to the devolatilization of the particles. Devolatilization is dependent on particle temperature and until coal-particle temperature is great enough, devolatilization will not occur. The steep incline of the particle-char mass fraction relates directly to devolatilization. As the volatile fraction is released, the remaining char-mass-fraction portion increases.

5. MODEL RESULTS AND DISCUSSION

Example data sets based on a Southern PRB subbituminous coal used in the UND furnace are discussed for (1) TEs that originated from inclusions, (2) TEs that originated from exclusions, and (3) organically bound TEs. The TE concentrations are based on arsenic, antimony, and selenium relationship data found in literature (Finkelman 1994) and not necessarily that given for the PRB coal.

Details relating to TEs originally associated with mineral inclusions and exclusions, as well as organically bound TEs, are also examined. Select model parameter sensitivities are further discussed within the following sections.

5.1. Select Parameter Sensitivities

5.1.1. Particle Temperature

Particle temperature has an effect on the overall quantities of the TE retained within the mineral particles. The particle temperature is the temperature inclusions will encounter during combustion, which is the reason it is used in modeling. When comparisons between the total fractions of the TEs released as a function of coal particle initial size bin using the gas temperature versus the particle temperature were made, a variance of less than 1.5% was observed for all three TE species across all bins in the present study.

The relatively small difference is likely a function of the furnace specifications. Comparisons with a temperature profile of a furnace less limited by materials of construction may show greater differences in the fractions of TEs released from pyritic family mineral inclusions during coal combustion. Arsenic and antimony were more affected by temperature difference than selenium. As selenium is more volatile than arsenic or antimony the increased temperatures should have less of an effect in this case. Overall, the small fractional differences observed for TE release are likely related to the relatively short path lengths wherein the particle temperatures exceed the bulk gas temperature in the present examples, which is illustrated in Figure 4-4. Differences between TE release of function of bulk temperature or particle temperature are potentially a function of the size of the combustion zone as well as the duration and intensity of the delta T between the surface of the particle and the bulk gas conditions.

Particle temperature relates directly to TE release for the given model. It is for this reason that the particle temperatures are used and are recommended. In all further portions of the study the particle temperature is solely used. Any additional increase in TE release during combustion because of elevated particle temperatures will help model the total quantities of the TEs released.

5.1.2. Pulse Duration

Although, the combustion environment is modeled using a steady state Lagrangian framework, some means of normalizing the mass distribution of the particles was needed for the developed model. As multiple injections files are used, the user must choose one time step to have coal flow rates based upon in order to have a basis of comparison. This value is referred to in the present discussion as the '*pulse duration.*' The pulse duration relates directly to the

number of particles that can enter the furnace at a given mass flow-rate. It is the basis of mass-balance calculations.

A similar fraction of the combined total number of coal particles containing pyritic family minerals for different pulse durations, as shown in Figure 5-1, is seen for differing pulse durations. The use of only the fraction of the coal particles that contain a pyritic family mineral group does not provide an adequate means of displaying pulse sensitivity as the different pulse durations listed as short ($\sim 3.69 \times 10^{-5}$ s), mid ($\sim 4.69 \times 10^{-5}$ s), and longer ($\sim 7.69 \times 10^{-5}$ s) all have the similar relative fractions throughout the bins as is observable by the fact that the plots overlap one another.

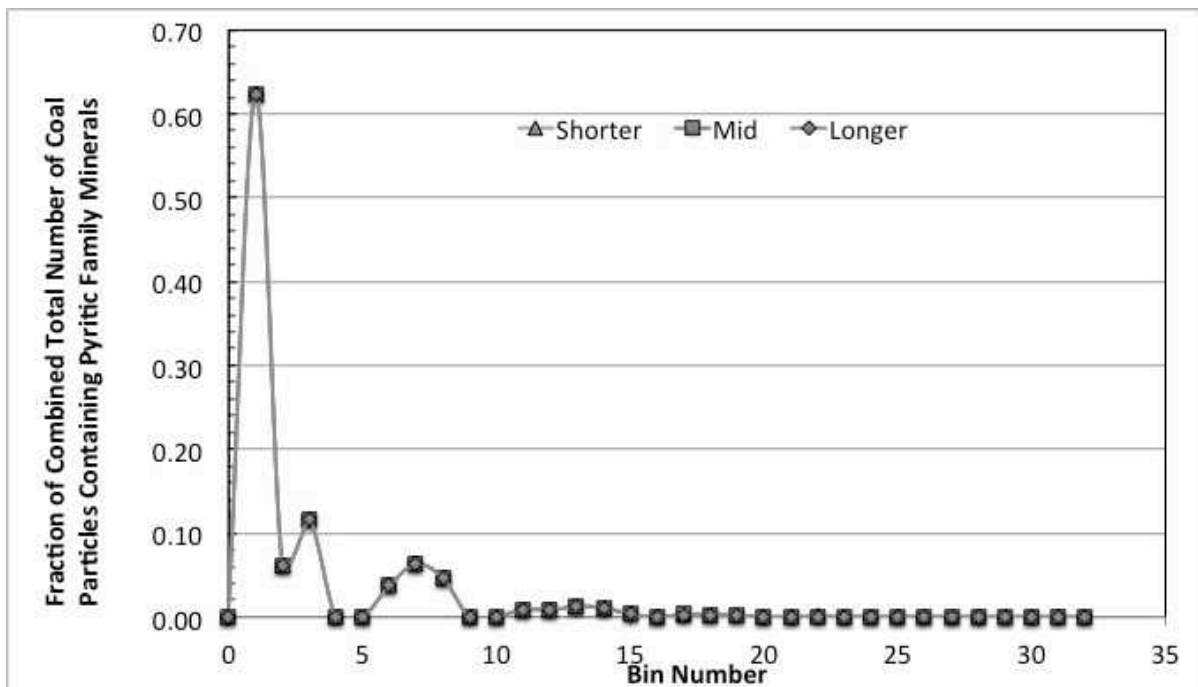


Figure 5-1 Plot depicting the fraction of combined total number of coal particles containing pyritic family minerals by particle track bin number

The fact that the plots overlap one another suggests only slight pulse-duration parameter dependence for the development of the mineral distribution. However, the fraction of the total

pyritic surface area shows more evidence of the pulse duration sensitivity, as can be seen in Figure 5-2.

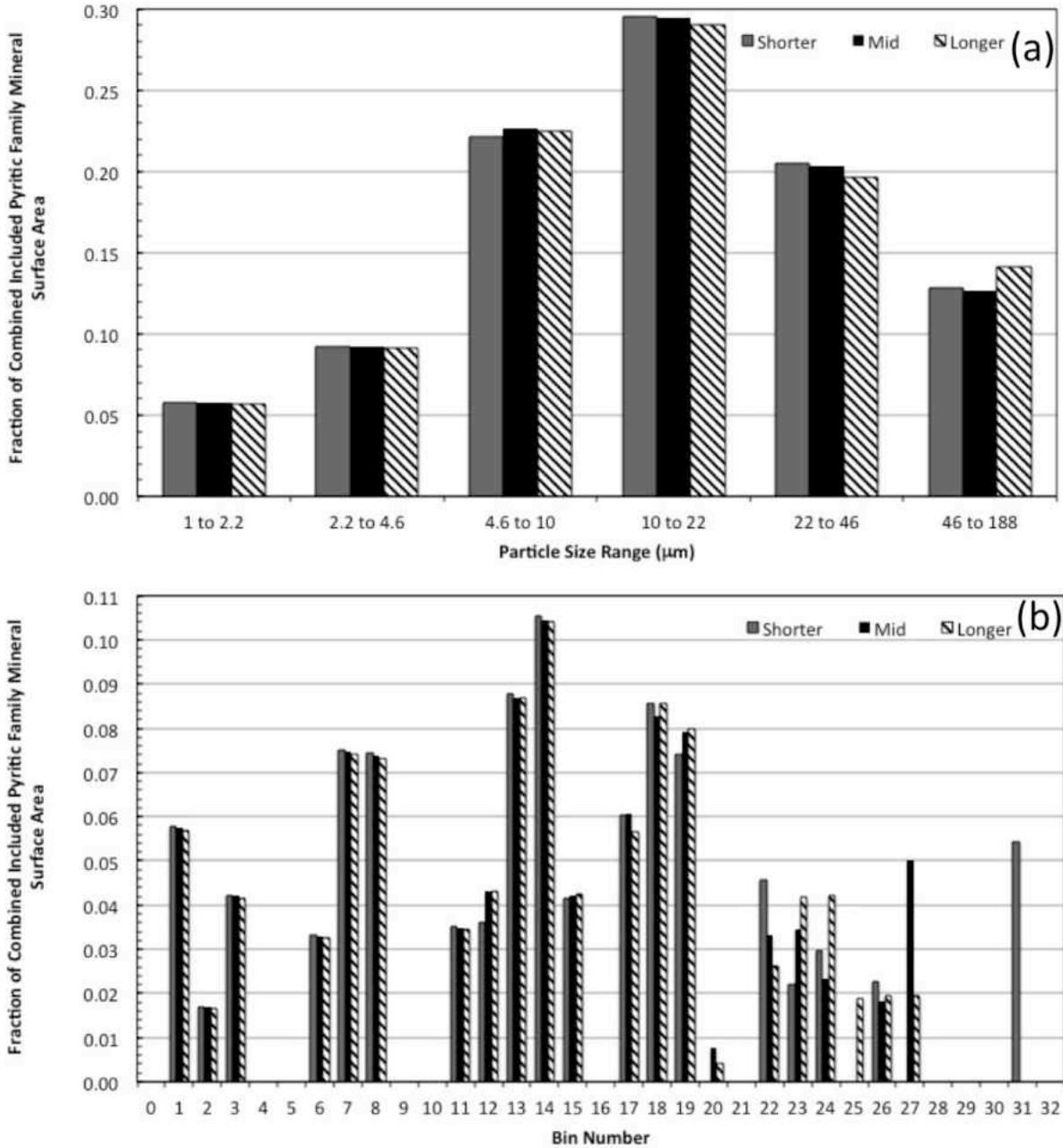


Figure 5-2 Plot depicting the fraction of combined included pyritic family mineral surface area by particle track size range and bin number

In this figure the fraction of the combined included pyritic family mineral surface area as a function of coal particle size range and bin number are shown for the shorter, mid, and longer durations. Overall, the size ranges of the various pulse durations shows a normal Gaussian distribution of pyritic family minerals.

Variations seen in the larger bin sizes are attributed to the small number of particles actually accounted for of that diameter. Because larger bin particles are a smaller fraction of the total coal content, small changes to their numbers have less effect on overall calculated outcomes. The fraction of the pyritic surface area shows how changes can be seen when larger bins have larger mineral inclusions.

There is a fine balance that must be considered when dictating the pulse time step used in the developed program. If the time step is too short, the combined total V_{mfree} may not actually be great enough to be able to contain the volume required to accurately model the larger mineral particles. The program will stop and indicate an error message for the user to ensure this is not continued. Alternatively if the pulse is too great, then the computer memory may not be sufficient to perform the calculations. As advancements in technology continue, this will likely only be a short-term issue. The limits of the pulse duration should come from the Fluent particle tracks. Calculations used in the developed program, for the current study, are based on an initial pulse duration of $\sim 4.69 \times 10^{-5}$ s, unless otherwise specified. This value was chosen from the initial time steps of the particle tracks taken from Fluent and for the fore mentioned reasons.

5.2. Inclusions

After combustion takes place, there is no real way to distinguish between initially included, excluded, or organically bound elements other than in what form a species exits the

system (i.e. with the bottom ash, fly ash, or vapor). The real difference between included and excluded minerals exists in the environment seen during combustion. This is a key factor for accurate modeling of TE partitioning.

Output data showing the relative intensities of the furnace region where the initially included TEs are released is visualized for the southern PRB subbituminous coal for the given boundary conditions and specifications in Figure 5-3 to Figure 5-5. The figures show the intensities of the TEs after they are released from the mineral inclusions. Darker regions on the figure indicate higher localized TE concentrations.

Arsenic and antimony have similar trends to one another, which is observed by the continued release of the TEs throughout the combustion zone. Alternatively, selenium seemingly has a much more localized initial release followed by a slower continued release throughout the combustion zone.

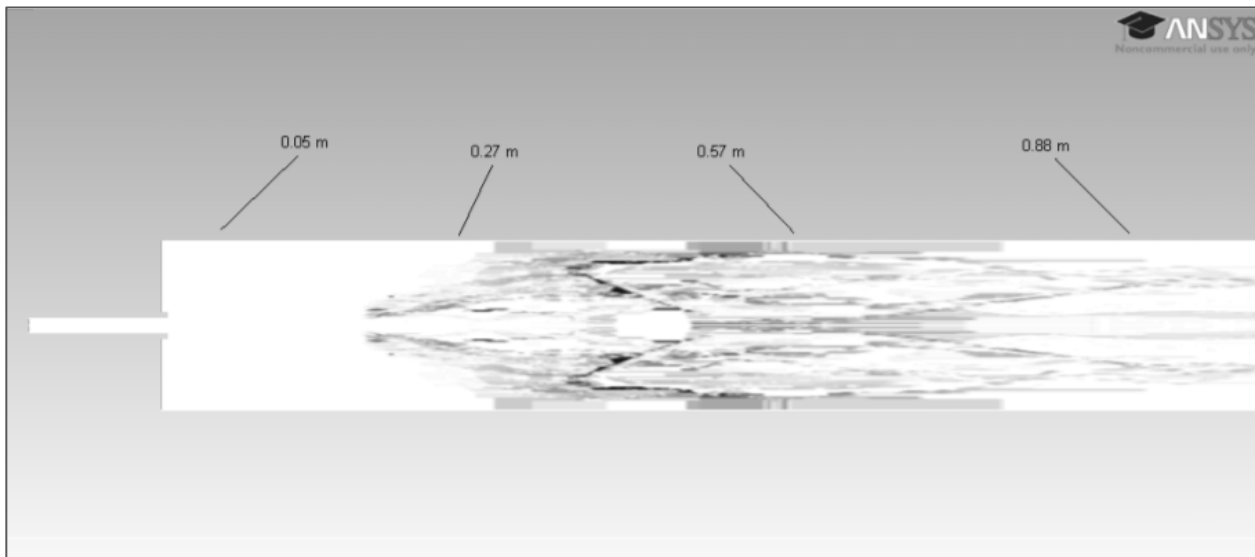


Figure 5-3 Contour plot of predicted arsenic released from pyritic family mineral inclusions for UND furnace; darker colors represent higher localized concentrations

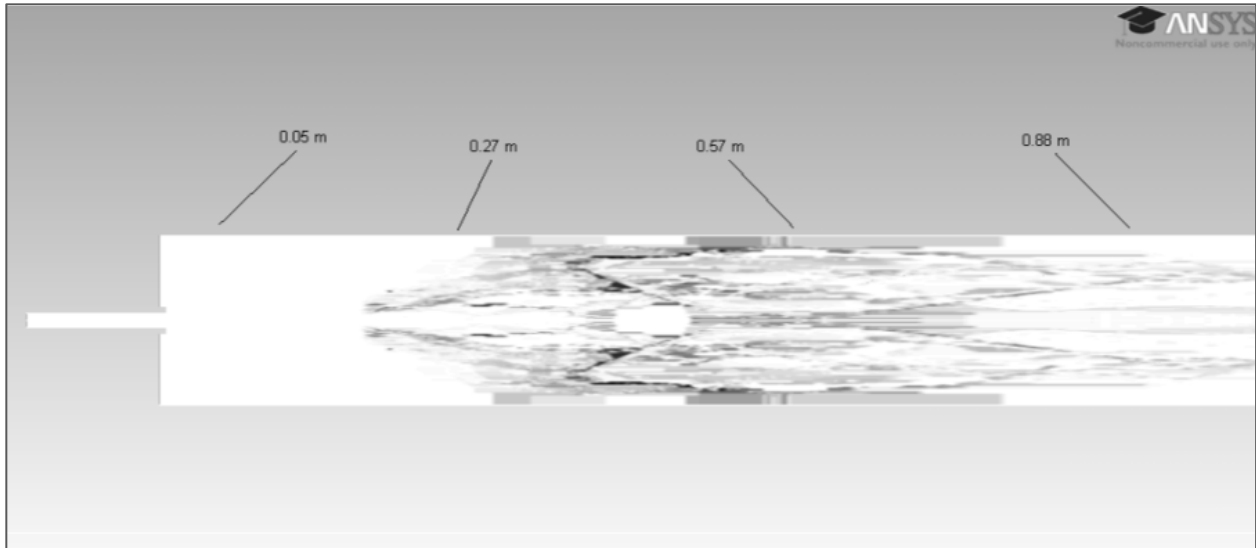


Figure 5-4 Contour plot of predicted antimony released from pyritic family mineral inclusions for UND furnace; darker colors represent higher localized concentrations

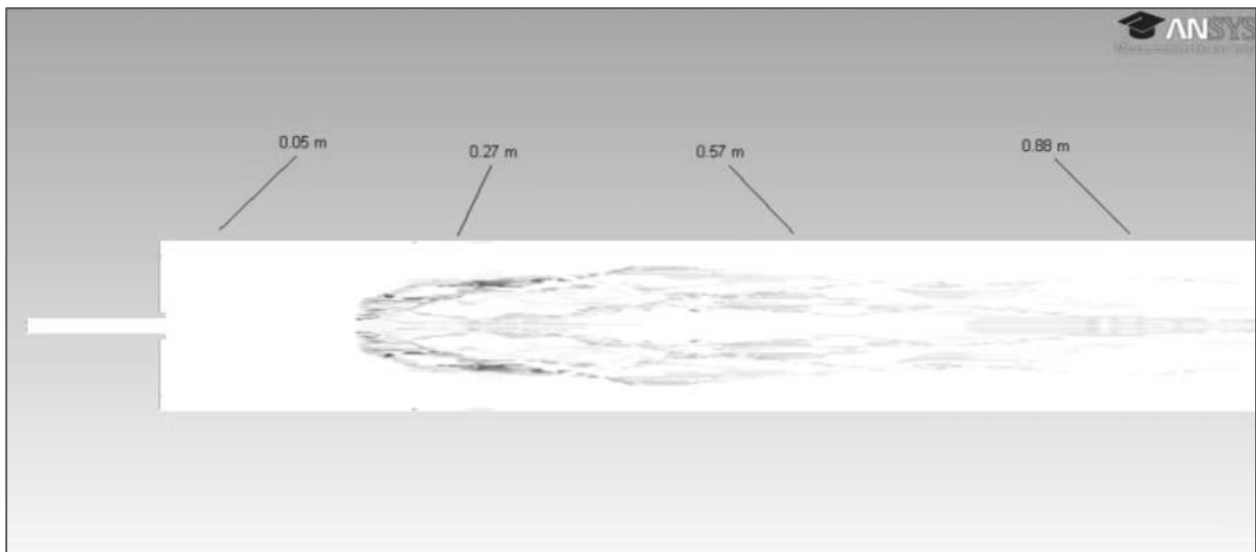


Figure 5-5 Contour plot of predicted selenium released from pyritic family mineral inclusions for UND furnace; darker colors represent higher localized concentrations

Knowing the way in which the TEs will behave during combustion can help in setting up pollution control technologies. Understanding where TEs are released may show combustion environments wherein additives help change the chemistry and physics of coal particles during

combustion. The use of additives in coal technologies to minimize elemental deposits within a system is already in use.

For the particle tracks, that have calculated pyritic family mineral inclusions distributed within, the overall fraction of the released TE as compared to the TE moles initially available in the inclusion melt, is shown in Figure 5-6 for the various size ranges as well as bin numbers. Figure 5-6 shows that the various original coal particle size bins can have dramatic differences in the total fraction of TE found in included pyritic family member minerals. Larger particles (those with larger bin numbers) tend to retain more of their initial arsenic, antimony, and selenium TEs during combustion than do smaller particles. It is noted that the current simulation is limited by the operating conditions of the furnace.

The similar trends of the arsenic and the antimony match the relative enrichment classification shown in Figure 2-4 in which both of these elements are in the same class. Selenium is listed in a higher volatility class (Meij 1994), which also matches the greater fraction of the trace element released from coal particle inclusions as shown in Figure 5-6.

Differences between particle bins could be related to the original inclusion size. However, it is more likely due to the temperature differences that each particle track undergoes during combustion. As is shown in Figure 4-5 to Figure 4-7 in which the time required for the release of the moisture content and the volatile content of the coal particles is illustrated, larger particles tend to travel through the furnace, as well as combustion zone, with shorter residence times than smaller particles. The surface area to volume ratios of mineral inclusions in the larger coal particles is likely smaller. Thus for the shorter time, based on the mass transfer rates of the TEs, only smaller portion of the larger particles' TEs may be released. As is shown in Figure 4-4

the point along the path length of the particle in which the greatest difference between the bulk-gas phase and the particle-surface temperature is greatest, does vary between coal particle bins.

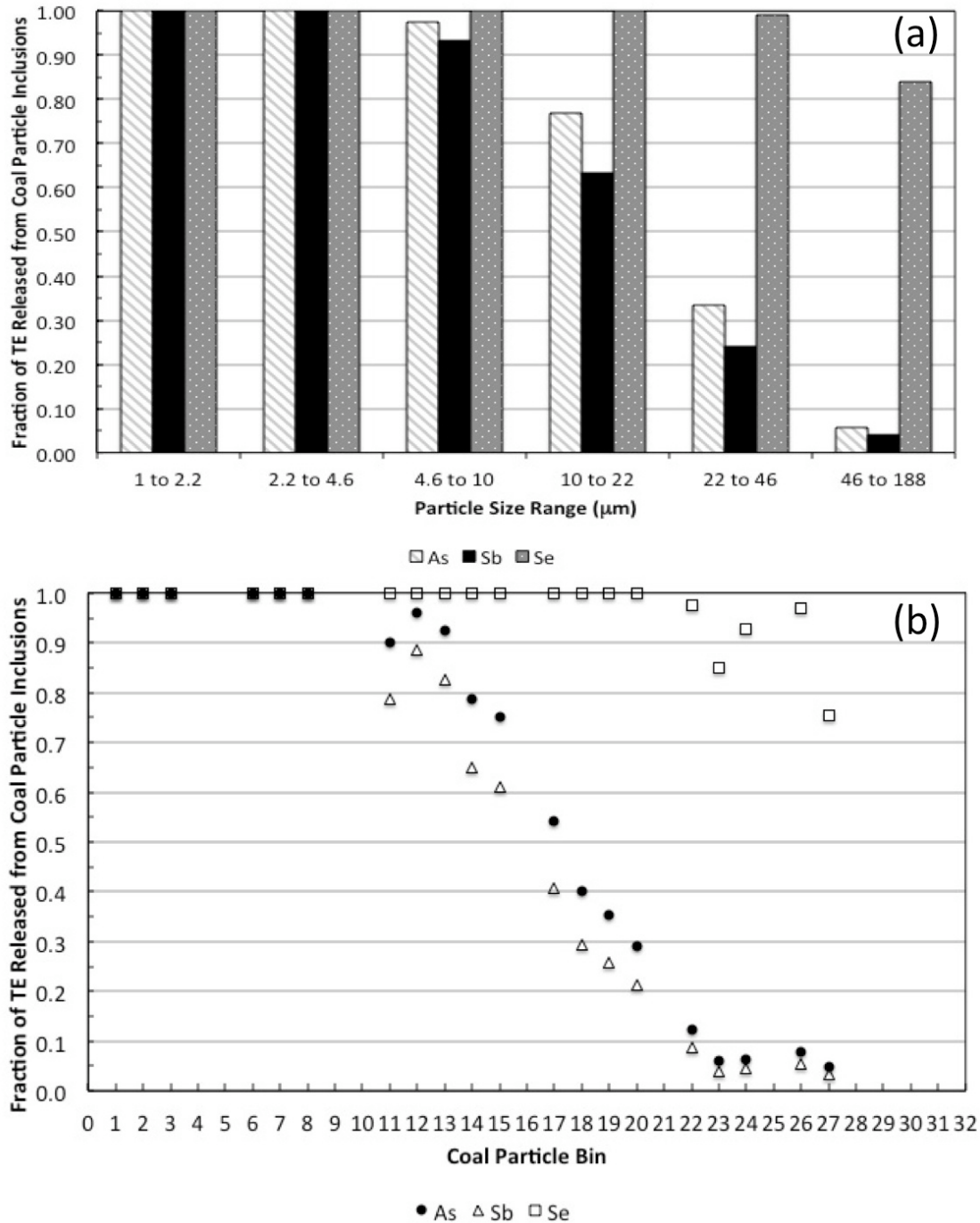


Figure 5-6 Plot depicting the overall arsenic, antimony, and selenium fractions released from pyritic family mineral inclusions found within each of the coal particle bins and size ranges indicated

Data sets given by Zeng et al. also provide a reference point for the developed model (Zeng, Sarofim, and Senior 2001). However, the values provided by Zeng et al. are not truly comparable in that the current developed model describes the fraction released for all pyritic family mineral inclusions (pyrite, pyrrhotite, and oxidized pyrrhotite) of each mineral size. Their experimental works suggests ~58% of arsenic was retained in the coarse ash fraction example; and for selenium, ~6% was retained in the coarse ash fraction. The experimental results are for a single pyrite inclusion of 4 μm in a coal particle of diameter 49 μm . If all the moles of original arsenic, antimony, or selenium from pyritic family mineral inclusions were combined in the current study and compared to the calculated moles released during combustion then 38%, 32% and 94% of the original arsenic, antimony, and selenium, respectively, was released.

Calculations in the developed computer program are performed for all particles within a bin. This means that if 25,000 coal particles from a single bin are released within the pulse duration, then the rates of reaction are calculated for each position along the particle track for all 25,000-coal particles. The overall combined amounts are reported.

5.3. Exclusions

Excluded TEs will most likely be retained more within the parent minerals than their included counterparts due to the fact that they tend to encounter lower temperatures during combustion. Figure 5-7 shows the fraction of the TEs released from the pyritic family minerals during combustion as a function of the original mineral size bin.

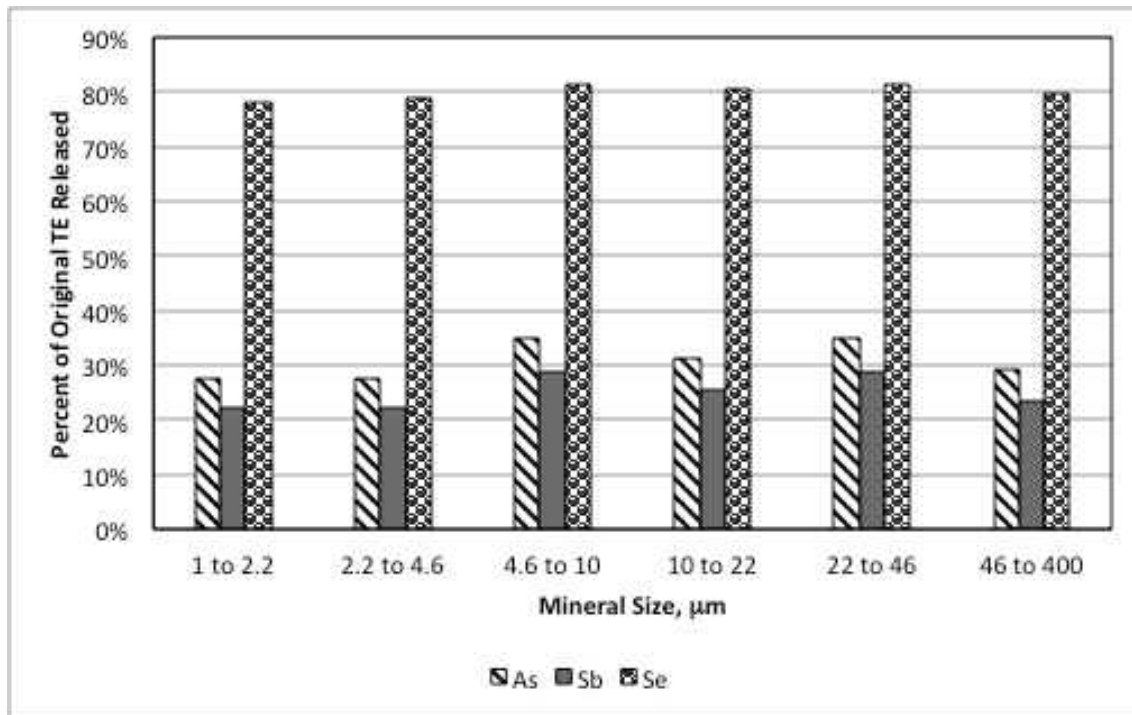


Figure 5-7 Plot depicting the overall arsenic, antimony, and selenium fractions released from pyritic family mineral exclusions found within the mineral particle size ranges indicated

Relative to the initial level of the trace elements in the excluded mineral bins, the fraction of selenium released for all size bins is greater than arsenic or antimony. Though the arsenic fraction released is found to be similar antimony, the plot indicates that more of the initial arsenic contained in the pyritic-family-mineral inclusions will be released than that of the antimony. Calculations suggest that selenium will be more readily release than either arsenic or antimony. However, the degree of TE release is still less than that observed for inclusions.

Fragmentation of excluded particles should increase the release of some of the TEs due to the fact that excluded mineral surface area will also increase. Fragmentation is likely one of the sources of the fairly level quantities of TEs released based on mineral bin size. In the developed model, the degree of fragmentation is a user input and should be adjusted based on an ash size analysis due to the fact that the degree of fragmentation is coal and mineral specific. Figure 5-8

and Figure 5-9 depict the cumulative total percent of the released excluded arsenic and selenium from the various indicates size bins as a function of distance from the top of the furnace. Mineral sizes are given in μm . Arsenic and antimony had similar trends; therefore antimony's plot is not shown.

The sharper edge shown Figure 5-8 for the largest exclusions, in the bin 46 to 400 μm , at ~ 0.6 m from the furnace top is likely a function of the point in which the particle temperature met the requirements for particle fragmentation of that bin to occur. As indicated by the steep climb in the curve of Figure 5-9, selenium originating from exclusions tends to have a more rapid initial release than arsenic for all mineral bins sizes.

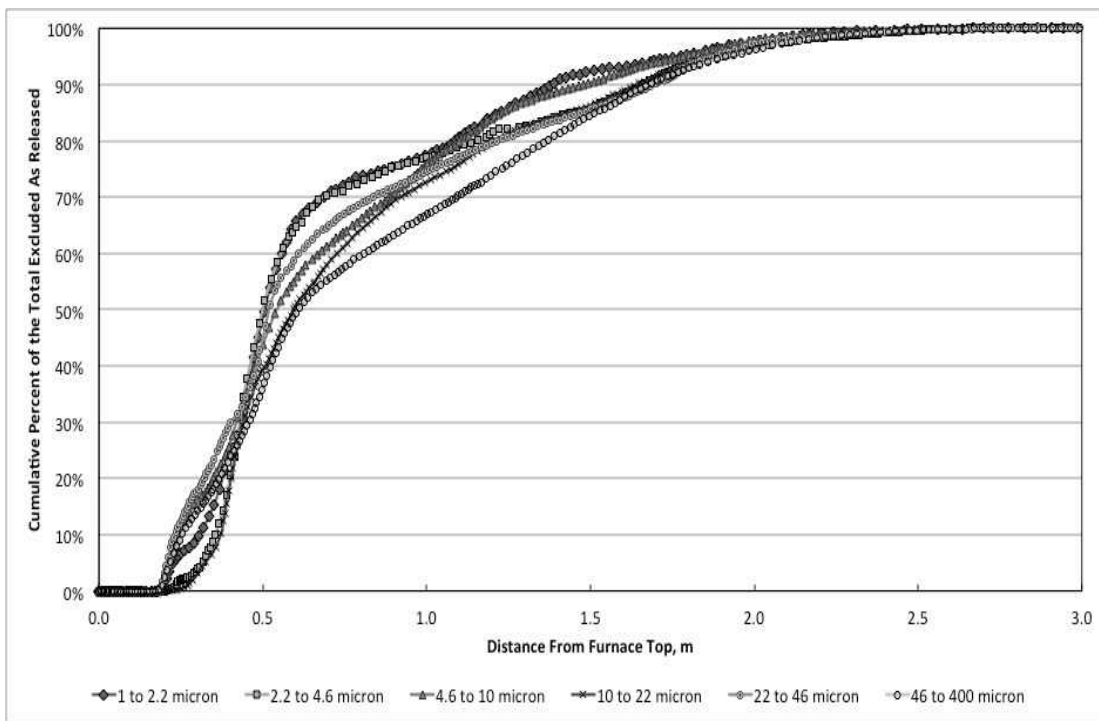


Figure 5-8 Plot depicting the cumulative percent of the total arsenic released from exclusions based on initial mineral size, μm , and distance from the top of the furnace

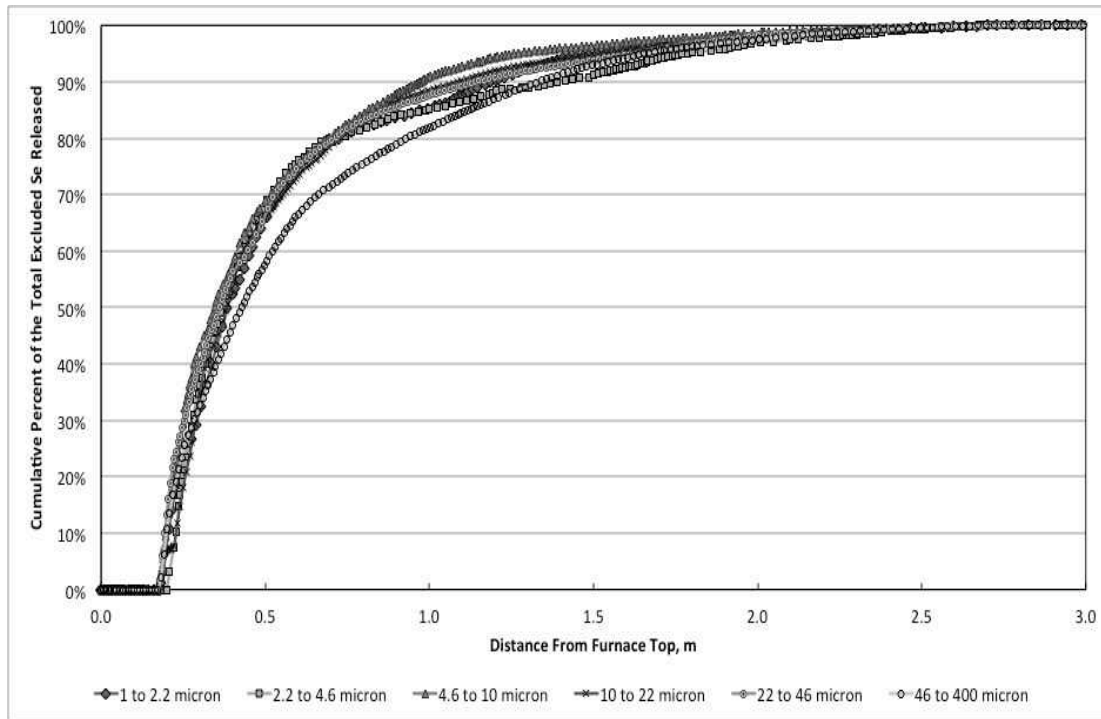


Figure 5-9 Plot depicting the cumulative percent of the total selenium released from exclusions based on initial mineral size, μm , and distance from the top of the furnace

The initial rapid release of selenium shown in Figure 5-9 is likely a function of its volatility as compared to lower volatility of arsenic. The larger bin tends to have the slowest rate of release. The slower rates of release are likely functions of the surface area to volume ratios of the excluded minerals. Based on the acceleration of the particles as functions of gravity alone larger particles have shorter residence times within the combustion zone. Thus larger particles have shorter durations wherein mass transfer through the bounds of the particle interface can occur.

5.4. Inclusion/Exclusion Comparisons

Comparatively, exclusions and inclusions release different proportions of the original TE present during combustion. For example, calculations indicate that approximately 80% of original moles of selenium from pyritic family mineral exclusions was released during

combustion in the current study. This is roughly 14% lower than that released for the combined percentage of selenium from pyritic family mineral inclusions.

If all the moles of original arsenic or antimony pyritic family mineral inclusions were, respectively, lumped together and compared to the calculated moles released during combustion then 31% and 25% of the original arsenic and antimony was released from inclusions in the current study. This is roughly 7% less than either released from the combined quantity released from inclusions. Similarities are likely related to the volatilities of the elements. For more details of the relative enrichment classifications of arsenic and antimony as well as differences in volatilities see Figure 2-4. The calculated differences noted between inclusions and exclusions release of TEs during combustion further demonstrates the need for individual treatment based on type of TE initial association.

5.5. Organically Bound

Due to the fact that Raeva et al. used an idealized coal combustion environment, in which interactions between differing coal mineral matrices were only beginning to be explored, parameter estimates provided within their work cannot simply be put into the model and run (Raeva, Pierce, et al. 2011). This would cause erroneous results, which would underestimate the overall amounts of the TEs species released. Their work is more important in that it describes possible speciation of the TEs during combustion.

The majority of organically bound TE species will be initially released during the char oxidation. Regions where this occurs more readily for arsenic are shown in Figure 5-10. Darker regions on the figure indicate higher localized TE intensity. Similar trends were observed for

antimony and selenium. The similarity between species correlates to the fact that they are released with the char oxidation in the model.

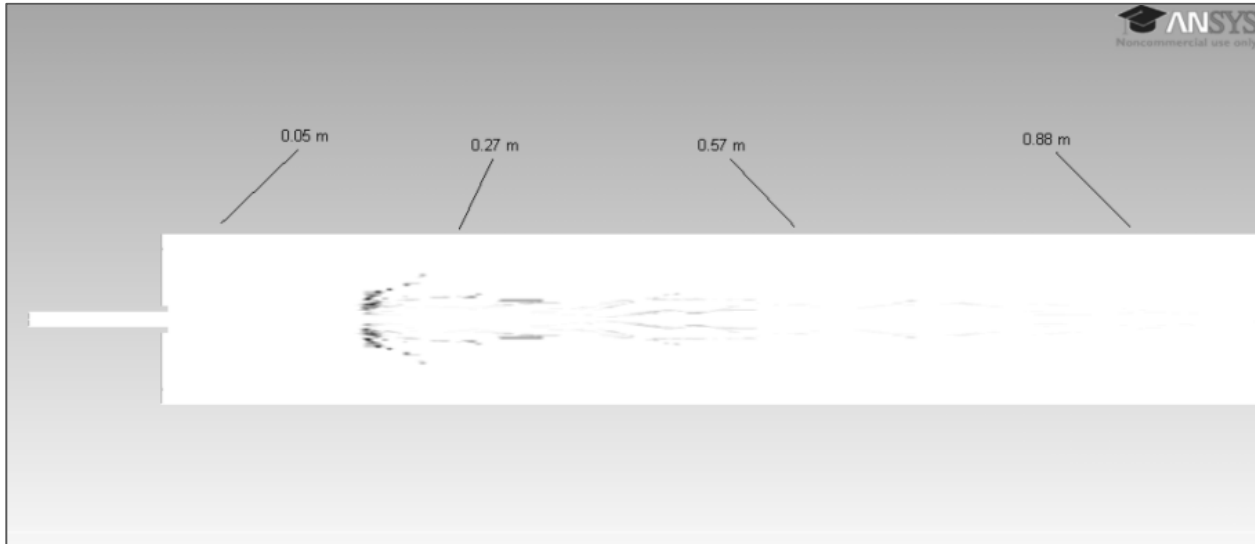


Figure 5-10 Contour plot of predicted initially organically bound arsenic released for UND furnace; darker colors represent higher localized concentrations

5.6. (PM10) Fraction

Several options are available to describe particle behavior during combustion as well as after combustion occurs. These include a lumped assimilation of the inorganic materials, no assimilation of the inorganic materials, and combination approaches that incorporate various degrees of fragmentation and coalescence of the particles (Wang et al. 2007, 2008, 2009). The current investigation is in the preliminary stages of outlet particle size development. The PM10 fraction for the different methodologies is given in Figure 5-11 for comparison purposes only.

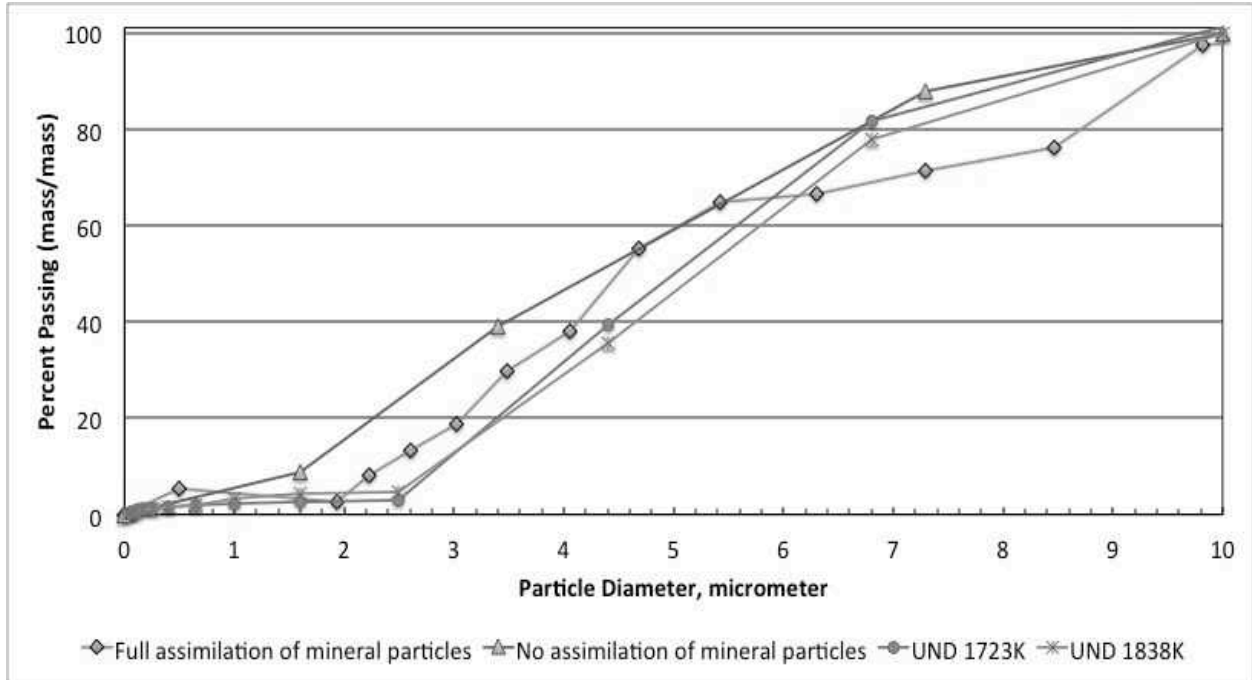


Figure 5-11 Graph of PM10 for full assimilation of mineral inclusions, no assimilation of inclusions, and experimentally determined outlet fly ash sizes (as taken by other graduate students) for the UND furnace with the localized-measured-high temperatures shown.

The plot found in Figure 5-11 shows that no assimilation of mineral particles matches the experimentally determined particle size distribution of the PM10 fraction better for the particles in the range of 6 to 10 micrometer particles than the complete assimilation of particles. The complete assimilation of the particles shows similar trends for particles smaller than 6 micrometers than does the no assimilation method.

Because both of methods of modeling show merit, a combined approach will likely describe the post combustion ash PSD better than either a simple lumped assimilation or no assimilation approach of the parent minerals. In the current study, the assimilation methodologies lack ash vaporization as well as the deposition of species back onto the surface of the particles

after they are initially released. Ash vaporization and coagulation of particles could shift the plots to match the experimental data within a better tolerance.

6. RECOMMENDATIONS AND CONCLUSIONS

The intention of the developed program is to provide a means whereby academia and industry can look for trends depicting when and where TEs are released during pulverized coal combustion. By understanding TE behavior, pollution control methodologies can be developed. The computer model described shows an approach whereby initial TE partitioning from pyritic family minerals can be calculated. Results of the program can be visualized through ANSYS Fluent. Recommendations for the program, cautionary considerations regarding the program, as well as concluding remarks are provided in this section.

6.1. Recommendations

The developed program is able to generate a semi-random distribution of mineral particles in an effort to simulate real coal to describe initial TE partitioning. However, there are still several places in which improvements to the program can be made. Some of these identified shortcomings are provided within this subsection. These shortcomings include both user-friendly aspects as well as modeling aspects.

User-friendly aspects of the program could include:

- Development of a GUID interface for the user, which would allow the pausing of the program.

- Implementation of additional flexibility in input/output file naming.
- Developments of check boxes to mark sub-functions that should be initialized prior to the programs' execution.

Modeling aspects of the program could include:

- Develop coalescence and fragmentation model subroutines, which will lead to ash better particle size composition distributions. Predictions of particle viscosities are related to the calculated composition of the resultant ash. This subheading shows that although the model was intended for TE partitioning, it has a vast realm of potential for other aspects related to coal combustion modeling.
- Incorporate viscosity calculations of combined mineral groups similar to the Urbain method (Kalmanovitch and Frank 1988).
- Implement other TE species and mineral groups within the program to make it more versatile. Although arsenic, antimony, and selenium are important others TE species are also important. The hazardous air pollutant nickel could be modeled in a similar manner, but parent grain type must taken into account (Bool III et al. 1997). It is feasible that the initial release of other TE species from inclusion or exclusion melts could be modeled using the mass transfer approach used in this model. However, the fate of the TE species will vary depending on relative enrichment class of the elements. Other mineral groups with related TE species can be added as rate transfer through the melt data become available.
- Incorporate ash vaporization subroutines within the model. The motivation for this type of subroutine relates to sub-micrometer particle formation as a function

of furnace conditions as well as the concentration of active sites for TE partitioning (Krishnamoorthy and Veranth 2003). Active sites for TE partitioning can be filled by other species that are released during ash vaporization. Calculating the concentrations of available for TE bonding inhibitors as well as sites for interaction available relates to the ultimate partitioning of the TEs.

- Incorporate aerosol formation subroutines. General dynamics equation can be used to predict the coalescence and coagulation of particles during combustion (McCollor et al. 2003). The particle size distribution of the resultant ash is also a function of aerosol formation.
- Develop subroutines to handle the different types of coal swelling/shrinking fragmentation properties
- Perform future validation of the developed program by using a furnace that can attain a higher peak temperature. Higher-peak temperatures are more representative of full-scale systems.

6.2. Cautionary Considerations

If input data is provided to the program output files will be generated. This illustrates the need for accurate input data. Although some error codes are programmed in the developed model, validity of input data is not always inherent. The only way an output dataset can be correct is if it is based on accurate information.

There is no such thing as a ‘typical’ coal. Any time ‘typical’ coal values are given in coal combustion, a degree of caution should be maintained while interpreting results. The plots shown are provided for trend purposes. Even so, the dataset presented attempted to use the best

information available regarding the coal during calculations. This model provides a tool whereby research regarding TE evolution from pyritic minerals can be explored with greater dynamic ability than previously attained. Parameter sensitivities should be considered during TE modeling.

6.3. Conclusions

Results show that TE release is proportional to the elemental concentration as well as the temperature profiles of the related coal particles and their respective initial size. Trace elements that originated with inclusions, exclusions, or as organically bound materials are modeled. Due to temperature differences, inclusions have higher fractions of TE release than do TEs that originated from exclusions. Organically bound materials are released as a function of the char burnout.

The program enhances previous approaches as it undertakes a semi-random combination of mineral groups based on CCSEM data to provide a generated coal dataset with greater statistical likelihood than alternative methods. Furthermore, one of the distinctive attributes of this research is that it combines kinetic relationships from both previously proven as well as newer methods to obtain the rates of release of arsenic, antimony, and selenium in one computer application.

The model predicts sensitivities to initial coal particle size and particle temperature profile. Larger initial diameter coal particles containing pyritic family mineral inclusions will retain a greater fraction of the initial trace elements present than their smaller particles counterparts due to the surface area to volume ratios of the particles as well as the shorter

durations of which TE mass transfer can occur. Arsenic and antimony show similar trace element release trends, most likely due to similar order of magnitude vapor pressures. Calculations indicate that a larger fraction of the initial selenium contained in pyritic family minerals will be released than either arsenic or antimony. This is likely a function of the volatility of the TEs at the temperatures encountered during combustion.

7. APPENDICES

Appendix A Excerpts from the C⁺⁺ Program Operations Manual

Appendix B Sample Input Files

Appendix C Sample Output Files

Appendix D UND Furnace Diagrams

Appendix E Other Relationships Used

Appendix A Excerpts from the C⁺⁺ Program Operations Manual

TEPCC

TRACE ELEMENT PARTITIONING DURING COAL COMBUSTION

JEHOSHAPHAT

VERSION 1.0

USER MANUAL

University of North Dakota

Department of Chemical Engineering

2013

A.1. Disclaimer of Warranties and Limitation of Liabilities

This program was prepared for the University of North Dakota Department of Chemical Engineering as an account of work sponsored by the U.S. Department of Energy North Dakota Experimental Program to Stimulate Competitive Research Infrastructure Improvement Program. No warranty is expressed or implied nor is any legal liability or responsibility for the accuracy, completeness, or usefulness of any information, apparatus, product, or process disclosed, or represents that its use would not infringe privately owned rights.

This software is copyrighted and the owner of the copyright claims all exclusive rights to such software, except as licensed to users henceforth and subject to strict compliance with the terms of this agreement.

Reference herein to any specific commercial product, process, or service by trade name, trademark, manufacturer, or otherwise does not necessarily constitute or imply its endorsement, recommendation, or favoring by the University of North Dakota or its subsidiaries. It is furthermore noted that even though this program was developed as an account of work sponsored by the U.S. Department of Energy, the U.S. Government makes no warranty, expressed or implied or assumes any legal liability or responsibility for the information contained herein. The views and opinions of the author expressed herein do not necessarily reflect those of the University of North Dakota and its subsidiaries, or the U.S. Government or any agency thereof.

A.2. Acknowledgements

David James developed TEPCC Jehoshaphat as part of a graduate PhD research project. He undertook coding and research relevant to the topic. Committee members of this research project include:

Advisors:

Gautham Krishnamoorthy – contributed to understanding of Fluent and methodology related to that program.

Wayne Seames – provided the TE partitioning modeling project overall goals.

Other Committee Members:

Steven Benson – provided big picture of mineral distribution, methodology of determining organically associated elements, and details regarding CCSEM.

Frank Bowman – contributed insights relating to thermodynamic and kinetics details.

Evguenii Kozliak – contributed chemistry related insights, including details regarding TE speciation and kinetic data used in modeling.

A.3. TEPCC Jehoshaphat Copyright Page

Copyright © 2013, David W. James

University of North Dakota
Department of Chemical Engineering
Harrington Hall, Room 323 Stop 7101
241 Centennial Dr.
Grand Forks, ND 58202

All rights reserved. Neither the TEPCC Jehoshaphat software nor its related user manual may be reproduced or distributed in any form or by any means, or stored in a database or retrieval system without written permission from the author or designated representative,

including but not limited to copies, photocopies, translation, scanning or reduction to any electronic medium or machine-readable format currently in use or that will yet be in use.

Windows and Microsoft Visual Studio 2010 Professional are registered trademarks of Microsoft Corporation.

Fluent is a register trademark of ANSYS

Suggestions, comments, or feedback may be sent to the University of North Dakota, Department of Chemical Engineering, Grand Forks, ND.

A.4. System and Software Requirements

TEPCC Jehoshaphat is a console application, which was written in the C⁺⁺ programming language and compiled using Microsoft Visual Studio 2010 Professional. Windows XP 32 bit platform or higher is required. Memory usage is directly related to the number of points followed in the particle track. This program was developed on a machine that had 4 GB RAM available.

A.5. Usage/Installation

The program is designed to be installed anywhere on a hard drive. The program may be copied and run from anywhere as long as the files are all contained with the program in the same folder. This program is a console application, which must have the application executable file, CCSEMDData.txt, Elements.txt, ExcludedFragmentation.txt, particle.txt, and PSDCoal.txt files within the same working folder to successfully operate the program. All output files will also be saved to this folder.

A.6. Jehoshaphat Model Input File Formats

Text files formatted for the simulation environment form the backbone of the user interface. Data for the text files originates from proximate and ultimate coal analyses, coal PSD, furnace specific geometrical and operational inputs, and CCSEM data, as well as data files from converged computational fluid dynamic software, which describe the time-temperature profiles of coal combustion particles.

The .txt files are written in tab-delimited format and may be modified in Notepad or Microsoft Excel. If Excel is used care must be given to ensure that errant quotation marks are removed before program calculations can begin. Each text line begins with an exclamation mark with its related subsequent data on the next line. Key words found within the line with the exclamation point allow the program to find and retrieve the data. The line of text should not be modified without ensuring the modification will not affect calculations.

The program was written using C⁺⁺. Consistent formatting of numbers must be maintained to ensure values are not truncated inadvertently. This means that values were primarily listed as chars, integers, or doubles. If the values are listed as a double they must have the format of 0.0, whereas integers can be a single whole number.

A.6.1. CCSEM Data

The key components of a CCSEM system that make it possible to image and analyze inorganic particles are the automated scanning electron microscope and related programs used to scan preselected areas of a polished sample to collect backscattered electron images. Backscatter electron imaging can be used in CCSEM due to the fact that the intensity of

the backscattered electrons is a function of the average number of the features on or near the surface (Gardener 2009). The grains are classified into some known mineral, based on heuristics rules, using energy dispersive x-ray spectrums in conjunction with CCSEM, which determine the elemental composition of each grain. The obtained images are used to determine the mineral type and size, and whether the mineral is included or excluded (Gupta et al. 2005; Vassilev and Tascón 2003).

CCSEM provides more quantitative means to determine the abundance, the shape of mineral grains, the size of mineral grains, the chemical form of minerals, and the mode of occurrence associations of inorganic components of coal (Gupta 2007; Gupta et al. 2005; Huggins 2002).

This input file has four key information sets. These sets are comprised of: (1) total mineral weight percent on a coal basis; (2) weight percent mineral basis within size bin 1.0 to 2.2, 2.2 to 4.6, 4.6 to 10.0, 10.0 to 22.0, 22.0 to 46.0, 46.0 to 400.0 (μm); (3) percent excluded of each of the 33 mineral groups listed; and (4) weight percent minerals excluded basis within size bin 1.0 to 2.2, 2.2 to 4.6, 4.6 to 10.0, 10.0 to 22.0, 22.0 to 46.0, 46.0 to 400.0 (μm). The 33 mineral group classifications in order are quartz, iron oxide, periclase, rutile, alumina, calcite, dolomite, ankerite, kaolinite, montmorillonite, KAl-silicate, FeAl-silicate, CaAl-silicate, NaAl-silicate, aluminosilicate, mixed aluminosilicate, Fe-silicate, Ca-silicate, Ca-aluminate, pyrite, pyrrhotite, oxidized pyrrhotite, gypsum, barite, apatite, CaAlP, KCl, gypsum barite, gypsum Al-silicate, Si-rich, Ca-Rich, CaSi-rich, and unclassified compositions. The idealized formulas of the minerals are found in Table 7-1. These values presented are doubles and must have the format of 0.0 to work properly.

Table 7-1 Idealized formulas of the various mineral groups

Mineral Group	Idealized Formula
<u>Oxides</u>	
quartz	SiO ₂
iron oxide	Fe ₂ O ₃
periclase	MgO
rutile	TiO ₂
alumina	Al ₂ O ₃
<u>Carbonates</u>	
calcite	CaCO ₃
dolomite	CaMg(CO ₃) ₂
ankerite	Ca(Fe ²⁺ ,Mg)CO ₃
<u>Silicates</u>	
kaolinite	Al ₂ O ₃ *2SiO ₂ *2H ₂ O
Montmorillonite	(OH) ₄ Si ₈ Al ₄ O ₂₀ (OH) ₄ *2H ₂ O
KAl-silicate/orthoclase	KAlSi ₃ O ₈
FeAl-silicate/Almandine	Fe ₃ Al ₂ (SiO ₄) ₃
CaAl-silicate/anorthite	CaAl ₂ Si ₂ O ₈
NaAl-silicate/albite	NaAlSi ₃ O ₈
aluminosilicate	Al ₂ SiO ₅
mixed aluminosilicate	NaAlSi ₂ O ₆ H ₂ O
Fe-silicate/hisingerite	Fe ₂ Si ₂ O ₅ (OH) ₄ *2H ₂ O
Ca-silicate/hillebrandite	Ca ₆ Si ₃ O ₉ (OH) ₆
Si-rich	Si _{0.80} O ₂
CaSi-rich	CaSiO ₄
<u>Sulfides</u>	
pyrite	FeS ₂
pyrrhotite	FeS _{1.14}
oxidized pyrrhotite	14FeO(OH)S _{9.333}
<u>Sulfates</u>	
gypsum	CaSO ₄ *2H ₂ O
barite	BaSO ₄
gypsum barite	CaSO ₄ *2H ₂ O BaSO ₄
gypsum Al-silicate	CaSO ₄ *2H ₂ O Al ₂ SiO ₅
<u>Phosphates</u>	
apatite	Ca ₅ (PO ₄) ₃ (OH,F,Cl)
<u>Other</u>	
CaAlP	CaAlP
potassium chloride	KCl
Ca-aluminate	3CaOAl ₂ O ₃
Ca-Rich	CaAl _{0.15} O ₈
unclassified compositions	unknown

The user may change the size bins within the CCSEM file as needed. However, any bin bound greater than 400.0 μm will automatically classify that mineral as excluded despite what may be given in the CCSEM dataset bins. The model performs calculations, based on the time step, to determine the actual largest bin size that may be used based on the summation of all the mineral free volume available.

A.6.2. Elements

Information related to the periodic table of elements is detailed within this input file. It is provided as a modifiable file as new advances in technology may dictate its change. Information is stored by atomic number symbol, name, reference oxidation state, atomic weight, specific gravity, and fusion temperature. These values are strings, integers, and doubles and must have the format of such to work properly.

A.6.3. Excluded Fragmentation

The excluded fragmentation input file represents the fragmentation based on size and mineral type expected during combustion. This value is an adjustable parameter and may be modified accordingly. It has a direct effect on excluded calculations, as it will dictate the degree to which a particle will fragment during combustion. The number of fragments relates to the number of active sites that will be present for trace elements reactions.

Excluded Particle Fragmentation lists how many particles, based on size, size bin 1.0 to 2.2, 2.2 to 4.6, 4.6 to 10.0, 10.0 to 22.0, 22.0 to 46.0, 46.0 to 400.0 (μm), that an excluded parent

mineral will form once the fragmentation temperature is reached. Particles smaller than 5 μm do not fragment much but are provided for the users' benefit.

The temperature at which fragmentation occurs for each of the 33 mineral groups is next entered. The default value is 5000.0 Kelvin.

The 33 mineral group classifications in order are quartz, iron oxide, periclase, rutile, alumina, calcite, dolomite, ankerite, kaolinite, montmorillonite, KAl-silicate, FeAl-silicate, CaAl-silicate, NaAl-silicate, aluminosilicate, mixed aluminosilicate, Fe-silicate, Ca-silicate, Ca-aluminate, pyrite, pyrrhotite, oxidized pyrrhotite, gypsum, barite, apatite, CaAlP, KCl, gypsum barite, gypsum Al-silicate, Si-rich, Ca-Rich, CaSI-rich, and unclassified compositions. These values are doubles and must have the format of 0.0 to work properly.

A.6.4. Particle

The particle txt file is a summary input file of information related to the coal particle. Values should be the same as those used within the chosen computational fluid dynamics software package (i.e., ANSYS Fluent). This file includes several values needed during calculation, including:

1. The standard ASTM proximate analysis on an as-received basis, including moisture, ash (dry basis), volatile matter (dry basis), and fixed carbon (dry basis) (all mass fractions but moisture should sum to ~ 1.0). These values are doubles and must have the format of 0.0 to work properly.
2. ASTM analysis results are reported on an as-received and dry basis. This analysis details the weight percent of carbon, hydrogen, nitrogen, sulfur, oxygen (by

difference), and percent ash related to a coal sample. This information is necessary for calculations within the model as well as within the computational fluid dynamics package used during preliminary calculations, and the values should be the same as those used in the CFD program. These values are doubles and must have the format of 0.0 to work properly.

3. The hhv higher heating value or gross calorific value as received (BTU/lb). This value is a double and must have the format of 0.0 to work properly.
4. Forms of sulfur - pyritic, sulfatic, organic, mass fraction of total sulfur (should sum to 1.0). These values are doubles and must have the format of 0.0 to work properly. Currently these values are not used in the vaporization portion of the program but will be useful for the subsequent heterogeneous reaction phase of model development.
5. Ash chemistry in alphabetical order by oxide formula (SiO_2 , Al_2O_3 , TiO_2 , Fe_2O_3 , CaO , MgO , K_2O , Na_2O , SO_3 , P_2O_5 , BaO , MnO_2 , unknown) mass fraction of ash dry basis (should sum to 1.0). These values are doubles and must have the format of 0.0 to work properly.
6. Ash fusion temperature, reducing - initial, softening, hemispherical, and fluid - followed by oxidizing - initial, softening, hemispherical, and fluid. These values are doubles and must have the format of 0.0 to work properly. This portion of the file is currently not used but will be important in the coalescence of particles and subsequent aerosol formation calculations.

Most of the TE content of arsenic, antimony, and selenium in coal has been shown to be associated with three major mineral groups. These groups include pyrite, kaolinite, and illite

(Davidson and Clarke 1996; Kolker et al. 1998). Distribution of minerals is not uniform among a single coal seam and varies greatly between originating sources. General rules are not available to give the relative amounts of TEs within coal based on coal rank. Lateral differences within the same coal seam are attributed to the coalification processes. The current model is set up for pyritic family minerals.

7. Weight percent arsenic in pyrite fraction, organically bound, other inorganically bound - mass fraction of total arsenic (should sum to 1.0). These values are doubles and must have the format of 0.0 to work properly.
8. Weight percent antimony in pyrite fraction, organically bound, other inorganically bound - mass fraction of total antimony (should sum to 1.0). These values are doubles and must have the format of 0.0 to work properly.
9. Weight percent selenium in pyrite fraction, organically bound, other inorganically bound, sulfides and selenides - mass fraction of total selenium (should sum to 1.0). These values are doubles and must have the format of 0.0 to work properly.
10. Weight percent arsenic, antimony, and selenium in pyrite (should be less than 0.05 (only in really bad coal seams is it that high) and the elemental form). These values are doubles and must have the format of 0.0 to work properly.
11. Initial total mass flow rate of the all coal streams combined (kg/s). This value includes moisture. This must be the same total value of all particle tracks used in the CFD program. These values are doubles and must have the format of 0.0 to work properly.

12. Initial density of raw coal (kg/m^3), this must be the same value used in the CFD program. These values are doubles and must have the format of 0.0 to work properly.
13. Number of particle rows in the particleTrackinfo.txt file - this should be the number of lines/rows of numbers in the files and should not include the exclamation point lines. The user can adjust this value in Fluent by coarsening an output file. This line should have the same number of columns as bins in PSD file i.e. 33. It is recommended that these values be in the range of 3000 to 6000 rows for most standard PC operational capabilities and initial estimates. Greater values can be used but calculations will take longer. These values are integers and must have the format of a whole number without a decimal to work properly.
14. Time step of pulse (s). Due to the fact that you have multiple injections files you have to choose one time step to have coal flow rates based upon. All other time calculations will read off of the individual files. These values are doubles and must have the format of 0.0 to work properly.
15. Surface area per gram of coal (m^2/kg). This value is a double and must have the format of 0.0 to work properly.
16. Porosity of the coal. This value is a double and must have the format of 0.0 to work properly.

A.6.5. Particle Track

Computational fluid dynamic (CFD) modeling of coal combustion within a furnace is first undertaken to determine the temperature histories experienced by the individual coal

particles during the combustion process. Any computational fluid dynamics software package may be used as long as the particle tracks have the format provided.

This user manual is written with the expectation that the reader has some familiarity with Fluent, Gambit, their related software packages, and their basic purpose/function. The intention of this manual does not include providing a user manual for Fluent. Numerous tutorials are readily available for the interested reader. For information specific to Fluent software see the user's manual (ANSYS 2012). It is assumed that the reader can converge coal-related combustion environment models, export particle track data to a file, and combine the information in a format readily needed as a model input.

This file should contains particle properties including time (s), particle temperature (K), particle diameter (m), particle mass (kg), particle char mass fraction, particle volatile mass fraction, particle time step (s), particle x position (m), particle radial position (m), particle theta position, static temperature (K), static pressure (Pa), mol fraction CO₂, mol fraction CO, mol fraction N₂, mol fraction O₂, mol fraction H₂O, mol fraction H₂, mol fraction SO₂, mol fraction Vol. The number of lines used in the Particle.txt file must be the same as the number of lines of data and should not include the header line in that number.

Additional gaseous species may be used. However, the Lennard-Jones parameters of only CO₂, CO, N₂, O₂, H₂O, H₂, SO₂, and vol are included in the model. If the value is 0.0 such as would be the case of N₂ during oxy-combustion that column must still be included with 0.0 placeholders.

A.6.6. Coal PSD

The particle size distribution of pulverized coal input file has details relating to the size of the particles. Columns include the diameter of particle micrometers and the cumulative percent passing-volumetric basis. No more than 33 size bins are allowed in the current state of the model. If a bin is unnecessary a diameter greater than the value necessary and a percent passing of 100.1 is acceptable. Unnecessary bins, if any, should be at the end of the list.

A.7. Output File Formats

TEPCC Jehoshaphat produces .txt files listing calculated data related to the project. These output files include organic, excluded, and included vaporization output files for each particle track, the mineral distribution, Coal elemental distribution, and Fluent injection requirements.

A.7.1. Organic Vaporization Output

Use of data from Raeva et al. is provided for informational use only and may provide insights into trends but should not be used for quantitative purposes. For details relating to the obtainment of kinetic parameters used, see related publications (Raeva 2011; Raeva et al. 2012; Raeva, Klykov, et al. 2011; Raeva, Pierce, et al. 2011). Kinetic data parameters were regressed using nonlinear statistical methods. The other columns provided in the organic output file represent a linearly defined release of organically bound materials determined as a proportion of the char mass fraction initially present.

A.7.2. Excluded Vaporization Output

The excluded vaporization output file provides the overall moles of arsenic, antimony, and selenium released from pyritic family minerals at the initial particle x coordinate, particle radial coordinate, and particle that coordinate provided in the original particle track injection file. These values are the overall moles for excluded minerals that have an initial radius similar to that provided for that size bin in the PSD of the coal. The degree of fragmentation of the coal particles is that provided in the excluded fragmentation file, and calculations for kinetic parameters are based on the approach taken by Zeng et al (Zeng, Sarofim, and Senior 2001).

When kinetic parameters from experiments are incorporated into the model, both subsets will be provided for comparison purposes. Kinetic data from experiments can only be provided as a means of comparison and should be used with at least the degree of caution expressed in related publications. Kinetic data parameters will be regressed using nonlinear statistical methods when they become available.

A.7.3. Included Vaporization Output

The included vaporization output file provides the overall moles of arsenic, antimony, and selenium released from pyritic family minerals at the initial particle x coordinate, particle radial coordinate, and particle that coordinate provided in the original particle track injection file. These values provided are the overall moles for included minerals found within coal particles of the size bin with the provided in the particle track file. Calculations for kinetic parameters are based on the approach described by Zeng et al (Zeng, Sarofim, and Senior 2001).

When kinetic parameters from experiments are incorporated into the models both subsets will be provided for comparison purposes. Kinetic data from experiments can only be provided as a means of comparison and should be used with at least the degree of caution expressed in related publications. Kinetic data parameters will be regressed using nonlinear statistical methods when they become available.

A.7.4. Mineral Distribution Output

The mineral distribution output file is comprised of 198 columns of data with a number of rows related to the number of coal particles described by the coal PSD, pulse time step, and coal mass flow rate. The datum in each of the first 198 columns represents the number of mineral particles within that coal particle of the given size and type; i.e., the first 33 columns represent the minerals (quartz, iron oxide, periclase, rutile, alumina, calcite, dolomite, ankerite, kaolinite, montmorillonite, KAl-silicate, FeAl-silicate, CaAl-silicate, NaAl-silicate, aluminosilicate, mixed aluminosilicate, Fe-silicate, Ca-silicate, Ca-aluminate, pyrite, pyrrhotite, oxidized pyrrhotite, gypsum, barite, apatite, CaAlP, KCl, gypsum barite, gypsum Al-silicate, Si-rich, Ca-Rich, CaSI-rich, and unclassified compositions) found in size bin 1.0 to 2.2. The next 33 columns are the minerals within size bin 2.2 to 4.6 (μm). The next 33 columns are the minerals within size bin 4.6 to 10.0 (μm). The next 33 columns are the minerals within size bin 10.0 to 22.0 (μm). The next 33 columns are the minerals within size bin 22.0 to 46.0 (μm). The next 33 columns are the minerals within size bin 46.0 to 400.0 (μm). The next column identifies the total number of minerals in this coal particle, and the last column is the coal particle identifier.

A.7.5. Coal Element Output

The first 17 columns of the coal element output file provide the mass (kg) of the elements—Na, Mg, Al, Si, P, S, Cl, K, Ca, Fe, Ba, Ti, Mn, unknown, As, Sb, Se—within each coal particle. The total number of rows is related to the number of coal particles described by the coal PSD, pulse time step, and coal mass flow rate. The next column is the coal particle identifier. Columns of the coal total original mass (kg) and coal original diameter (m) are also provided.

A.7.6. Fluent Injection Requirements

The Fluent injection requirements file is given as a check for the user and is based on the coal PSD, the mass flow rate of coal, and the initial time step of the pulse. It may be ignored if already properly applied. In 2-D space, the mirror image in Fluent means you need half the mass flow rate which is why the $0.5 \times \text{Mass}$ column is provided. The columns of the file include the following: injection number, mass (kg/s), $0.5 \times \text{Mass}$ (kg/s), min (m), max (m), mean diameter (m).

A.8. TEPCC Jehoshaphat Operation

This console application was designed in a modular format so that the user can specify which sub-models are used during operation. The first section of the program will generate the Mineral Distribution and the Coal Elemental Distribution files. This file is run for every particle track used in the series regardless if it was previously calculated. Subsequent use of the organically bound, inclusion and exclusion portion of the program is only calculated by user

request. All data displayed on the console screen is for the users' benefit and is not necessarily written to a file.

A.8.1. Particle Track

As a console application, double clicking on the Jehosaphat.exe icon found in the folder, which contains the related input files, can activate the TEPCC Jehoshaphat program. Figure 7-1 shows the program icon.



Figure 7-1 TEPCC Jehoshaphat program icon

After double clicking the program icon, a console application will open which will display a message similar to that found in Figure 7-2.

```
Beginning Pulverized Coal Combustion Trace Element Partitioning Simulation
UND PhD project of David James
All Rights Reserved
Copyright 2011, 2012, 2013, David James

Jehosaphat.cpp is now in progress

Reading periodic table of elements information - Element.txt
Reading particle information - particle.txt
Reading CCSEM information - CCSEMdata.txt
Reading Fragmentation file of excluded minerals - ExcludedFragmentation.txt
Reading PSD of raw Coal data - PSDCoal.txt

Which particle track to you want to run?
Enter a whole number from 0 through 32 followed by a hard return.

The name of the file should have the format: particletrackinjection_#.txt
```

Figure 7-2 Opening program example screen

The user is required to input a number, which designates which particle track is being used during calculations. Calculations are based on the initial diameter and not necessarily on the

number provided by the user in this step. However, the value given must have an accompanying particle track with the same number of lines entered into the particle.txt file.

A.8.2. Mineral Distribution Data

The program performs a series of operations which checks the values entered into the input files as well as determines if the appropriate files exist. The names of the files with appropriate formatting include:

Table 7-2 TEPCJ Jehoshaphat required input file names

CCSEMData.txt	Elements.txt	ExcludedFragmentation.txt
particle.txt	particletrackinjection_#.txt	PSDCoal.txt

The program then proceeds with calculating the Fluent injection requirements. This file is given as a check for the user and is based on the coal PSD, mass flow rate of coal, and initial time step of the pulse.

CAUTION: There is a fine balance that must be considered when dictating the pulse time step used in the developed program. If the time step is too short a duration, then the combined total V_{mfree} may not actually be great enough to be able to contain the volume required to accurately model the larger mineral particles. The program will abort if the pulse is not long enough. Alternatively if the pulse is too great then the computer memory may not be sufficient to be able to perform the calculations. If an error occurs after the mineral distribution of the program is calculated, try different pulse durations. This is strictly related to the computer used to perform the calculations.

Next, the program will display the number of particles for each size bin as is shown in Figure 7-3. The columns shown depict: (1) the total coal particle volume of the given coal particle size bin; (2) the total bin included mineral volume; (3) the number of coal particles the pulse time step requires; (4) a whole number integer depicting how many place holders must be generated in the array which will be used to perform the mineral distribution; and (5) the fraction of the last particle is given. This fraction is used to ensure that the mass balance is complete.

```

Finished writing the Fluent Injection Requirements output file
you made it past the:
total bin coal part vol-m^3, total bin included mineral vol-m^3, num coal part,
num spaces allocated, size bin's last particle portion
0 0 0
2.27499e-014 6.45331e-016 24224.4 24225 0.373037
1.1375e-014 3.22665e-016 2414.13 2415 0.134035
3.41249e-014 9.67996e-016 4627.23 4628 0.231559
5.68748e-014 1.61333e-015 4895.56 4896 0.560572
7.96247e-014 2.25866e-015 4429.96 4430 0.955268
1.25125e-013 3.54932e-015 4477.64 4478 0.639523
1.59249e-013 4.51732e-015 3657.01 3658 0.0144416
2.27499e-013 6.45331e-015 3363.7 3364 0.704992
2.61624e-013 7.42131e-015 2476.71 2477 0.710073
2.61624e-013 7.42131e-015 1589.1 1590 0.104589
2.72999e-013 7.74397e-015 1063.55 1064 0.549071
2.84374e-013 8.06664e-015 710.134 711 0.133929
3.52624e-013 1.00026e-014 563.854 564 0.854338
4.20874e-013 1.19386e-014 431.954 432 0.954272
4.66373e-013 1.32293e-014 307.816 308 0.815615
5.00498e-013 1.41973e-014 212.79 213 0.790496
5.68748e-013 1.61333e-014 155.891 156 0.891087
6.14248e-013 1.74239e-014 107.95 108 0.950324
6.14248e-013 1.74239e-014 69.5157 70 0.515722
6.48373e-013 1.83919e-014 47.029 48 0.0289551
6.14248e-013 1.74239e-014 28.5685 29 0.568528
6.25623e-013 1.77466e-014 18.6696 19 0.669561
6.02873e-013 1.71013e-014 11.5259 12 0.525859
6.14248e-013 1.74239e-014 7.55457 8 0.55457
6.14248e-013 1.74239e-014 4.86326 5 0.863255
5.68748e-013 1.61333e-014 2.89209 3 0.892094
4.89123e-013 1.38746e-014 1.59596 2 0.59596
3.86749e-013 1.09706e-014 0.811819 1 0.811819
2.95749e-013 8.3893e-015 0.396705 1 0.396705
2.27499e-013 6.45331e-015 0.195501 1 0.195501
1.81999e-013 5.16265e-015 0.100958 1 0.100958
1.81999e-013 5.16265e-015 0.0648571 1 0.0648571

totals
coal part vol-m^3, mineral vol -m^3, num coal part, num coal spaces generated
1.13863e-011 3.22988e-013 59903.2 59918
extracted mineral portion particle size distribution <m> - this is just the

```

Figure 7-3 Program example display of number of particles in each size bin

A.8.3. Organic Distribution Data

The organic distribution data is displayed on the screen for the users' benefit as is shown in Figure 7-4. The data describe the total organically associated mass of the coal for the given pulse time step for the species Na, Mg, Al, Si, P, S, Cl, K, Ca, Fe, Ba, Ti, Mn, Unknown, As, Sb, and Se. The coal mass for the pulse time step is provided. The mass fraction of the organic portion of the coal of each of the listed species is also shown. Within the organic fraction all species are considered uniformly distributed.

```
Finished writing the Mineral Distribution output file
Determining Organic Associations and the Coal particle elemental compositions
through mass balances ... This could take a while.
organically associated mass (kg), Na, Mg, Al, Si, P, S, Cl, K, Ca, Fe, Ba, Ti, M
n, Unknown, As, Sb, Se
3.55541e-010  1.28136e-010  4.22193e-012  2.78745e-011  1.23509e-010
2.23397e-011  0  3.35651e-012  2.28809e-011  5.17397e-011  4.4002e-
012  2.63596e-012  8.68284e-013  3.49001e-011  4.82606e-013  9.47976e
-014  1.66844e-013
Coal mass (based on timestamp) 1.38383e-008 (kg)
Coal mass fraction Na, Mg, Al, Si, P, S, Cl, K, Ca, Fe, Ba, Ti, Mn, Unknown, As,
Sb, Se
0.0256926  0.00925953  0.000305091  0.00201431  0.0089252
0.00161434  0  0.000242552  0.00165345  0.00373888  0.000317
973  0.000190483  6.27451e-005  0.002522  3.48747e-005  6.85039e
-006  1.20567e-005
```

Figure 7-4 Program example display of coal organically bound elemental total mass for pulse and mass fraction of organically associated metals

A.8.4. Organically Associated

As shown in Figure 7-5, after the mineral and elemental distribution files are written the user is prompted to determine if they would like to continue with the program's trace element portion. A 'Y' or 'N' must be input. The user is also prompted to determine if the user wants to run the Organically Bound TE vaporization portion of the program. A 'Y' or 'N' must be input as is also shown in Figure 7-5.


```
Finished writing the Coal Element Distribution output file

At this point, you have only performed the mass balances to generate the
Mineral_Distribution_Output.txt and Coal_Elemental_Dist_Output.txt output files.

Do you want to continue to the TE vaporization portion of the program? (Y or N)
any key other than Y or y followed by a hard return will end the program.
y

Do you want to run the Organically Bound TE vaporization portion of the program?
type (Y or N) followed by a hard return to continue
```

Figure 7-5 Program example screen to determine if the trace element and organically bound sections of the program should be executed

A.8.5. Included

The user is also prompted to determine if the user wants to run the included TE vaporization portion of the program. A 'Y' or 'N' must be input as is shown in Figure 7-6. After the total surface area of the pyritic family minerals of the bin has been calculated for the current particle bin, a message will appear on the screen to prompt the user to determine if the user wants to continue to run the Included TE vaporization portion of the program. A 'Y' or 'N' must be input as is also shown in Figure 7-6. This message will appear regardless of the amount of pyritic family member particles present within the particle bin, meaning that even if the amount is 0 m² the message will still appear. If the value is 0 m² this indicates that the mineral distribution did not place a pyritic family member in the given particle size bin.

If an affirmative desire to continue with the program is given then the program will iterate through the particle track providing the appropriate k values for each step in the particle track. If Y is entered, the program will still continue but will not perform calculations if pyritic family mineral surface area is 0 m².

```

Do you want to run the Inclusion TE vaporization portion of the program?
type <Y or N> followed by a hard return to continue
y
Working on Trace Element Vaporization of Included Minerals ... This could take a
while.
calculating variables for Coal Particle size_bin/Track 20
Of the 48 coal spaces generated for coal-PSD bin 20, only 2, contain: pyrite, py
rrhotite, or oxidized pyrrhotite minerals
Total hypothetical FeS included mineral family surface area by non-uniform
distribution for working bin 2.83004e-010 (m^2)
At this point, you have the surface area this is a break unless you want to cont
inue.
Do you want to continue to the TE vaporization inclusion portion of the program?
<Y or N> any key other than Y or y followed by a hard return will end the progr
am.
y

```

Figure 7-6 Program example screen to determine if the inclusion section should be continued

The user is prompted to determine if they want to run (0) all three trace elements, (1) arsenic only, (2) antimony only, or (3) selenium only. This option is added to the program to allow for multiple computers to be used when a large number of particles are being calculated, as datasets can be run on differing machines and then recombined during post processing. This should help prevent the loss of larger quantities of data as well as speed up the calculation process.

For arsenic, antimony, and selenium, k values are provided on the console as shown in Figure 7-7.

```

TE = As i = 1924      Koverall As = 1.14189e-007
PSD Bin = 23      Coal Particle = 2      Mineral = 0      Mineral Size Bin = 4
TE = As i = 1925      Koverall As = 1.11958e-007
PSD Bin = 23      Coal Particle = 2      Mineral = 0      Mineral Size Bin = 4
TE = As i = 1926      Koverall As = 1.12127e-007
PSD Bin = 23      Coal Particle = 2      Mineral = 0      Mineral Size Bin = 4
TE = As i = 1927      Koverall As = 1.09634e-007
PSD Bin = 23      Coal Particles = 2      Mineral = 0      Mineral Size Bin = 4
TE = As i = 1928      Koverall As = 1.09577e-007
PSD Bin = 23      Coal Particle = 2      Mineral = 0      Mineral Size Bin = 4
TE = As i = 1929      Koverall As = 1.09574e-007
PSD Bin = 23      Coal Particle = 2      Mineral = 0      Mineral Size Bin = 4
TE = As i = 1930      Koverall As = 1.0986e-007

```

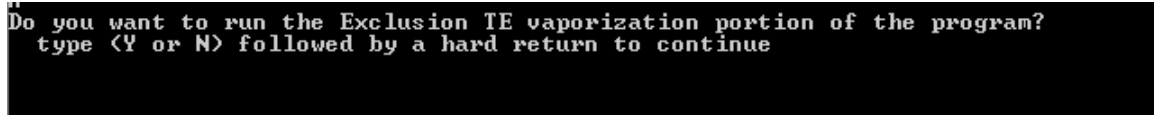
Figure 7-7 Example console messages shown from the program depicting k values of arsenic release from the specified particle

Values given on the screen describe the current particle bin, the coal particle which has the pyritic family mineral grain of the current particle size bin, the mineral ((0) is pyrite, (1) is pyrrhotite, and (2) is oxidized pyrrhotite), the size bin of that mineral, the TE species (arsenic, antimony, or selenium), the current particle track line; and the overall k of that line.

In the event that the user inputs a value (on the particle.txt file) indicating a great number of particle track points than is available in the file, an error message will appear on the screen, which will cancel the program. The number of lines indicated in the particle txt file may be less than the actual number, but never greater. The program checks to ensure that the datum points make sense, and temperature, on an absolute scale, must be greater than 0. However, the program reads a void location as 0. Although the error message will indicate that the particle track should be checked, the particle.txt file should also be checked to ensure that temperature values are greater than 0.

A.8.6. Excluded

Finally, the user is also prompted to determine if the user wants to run the excluded TE vaporization portion of the program. A 'Y' or 'N' must be input as is shown in Figure 7-8.



```
Do you want to run the Exclusion TE vaporization portion of the program?  
type <Y or N> followed by a hard return to continue
```

Figure 7-8 Program example screen to determine if the exclusion section should be executed

In the event that the user inputs a value (on the particle.txt file) indicating a greater number of particle track points than is available, an error message will appear on the screen, which will cancel the program. The number of lines indicated in the particle txt file may be less than the

actual number, but never greater. The program checks to ensure that the datum points make sense. Temperature is on an absolute scale and must be greater than 0. However, the program reads a void location as 0. Although the error message will indicate that the particle track should be checked, the particle.txt file should also be checked to ensure that temperature values are greater than 0.

A.8.7. Post Processing (Potential Methodology)

After the program has been run, the data must be reviewed by the user to determine the usefulness of the data, appropriate significant figures the data should have, and appropriate ways to visualize any trends (which may or may not be present). One methodology that may be beneficial to the user is to use the CFD package to display the results. This can be accomplished in Fluent by interpolating the results. A brief methodology is described here but is not intended to be overly detailed. This is one option but is by no means an all-inclusive answer to how to visualize the generated data sets. The data must be put in the appropriate format to be useful. In Fluent this format of the interpolation file is provided in Section 4.19.2 of the Fluent user manual (ANSYS 2012). For specific details on Fluent, see the users manual.

CAUTION: The combined particle tracks cannot have duplicate coordinates. If swirl is used, then the particle tracks may have a theta coordinate or the same coordinates at differing times, but this will not be apparent in the 2-D format. The input will fail if coordinates are duplicated in the x and y coordinates of a 2-D simulation. Care must be given to see any trends when displaying more than one particle track in this manner.

A.8.8. Common Causes of Error Message and Possible Solutions

The program is designed to check that the data generated are appropriate on a limited basis. Sometimes user input will cause error messages to appear on the console or to cause windows to present an error message window. Some commonly seen places where errors have occurred include the following:

1. If txt files are manipulated in excel for ease with the tab-delimited nature the program. Excel will often leave residual quotation mark around the lines of txt. If the quotation marks are present an error message from Windows will appear that indicates it is searching for a solution to the problem. To rectify open the txt files and check the lines of text for an errand quotation mark at the beginning of the line. Do this in a notepad or txt edit application. Re-save the file from the text program.
2. It has been noticed that during manipulation of the txt file data in Excel, truncation of the data, or the loss of decimals places, may occur if the data are not handled correctly. Opening the original file and changing the numbers to the 'general' format and then moving the decimal place to show all values before saving can remedy this issue. If values are too far from what is expected for a particle track diameter, the program may cause a Windows based error message to appear which indicates that Windows is searching for the solution to the problem. Wherever the input files indicate that the data should add to 1 but they do not add to 1, with the tolerance of the program this type of message may also appear. The best method is to check the entered values and be sure that they make sense.

3. During the calculations of the vaporization subsection of the program, an error may be reported to the console that indicates temperature must be greater than 0 for coal combustion. Upon review of the particle track txt file, the user may believe they have not input any values less than or equal to 0. However, the particle.txt file may indicate a value for the number of lines that is greater than that actually available. Null values are read as 0.0 (double format) for the program, and the particle.txt file should be amended to have what is actually available.

A.8.9. Advisories

The program was not built to make multiple names for the same file in the folder. This means it will not amend the file of the same name but that it will clear the contents at the point in the program that the file is called, and then write data into a file of the name of the output file. Any output files within the folder may be copied over if they are left during a new set of calculations.

Each inclusion, exclusion, and organically bound output file will save the file with the number originally entered by the user for the current particle track. Ensure that older files are not mistakenly written over if multiple cases are run.

Although the mineral distribution and elemental distribution file is written each time the program is run, the contents only change if the informational inputs into the program change.

If the time step is too short a duration, then the combined total V_{mfree} may not actually be great enough to be able to contain the volume required to accurately model the larger mineral particles. The program will abort if the pulse is not long enough.

If the pulse is too great, then the computer memory may not be sufficient to perform the calculations. If an error occurs after the mineral distribution, try a shorter pulse. The value needed is related to the computer used to perform the calculations. The program is tracking the particle composition of each particle generated for both the mineral distribution and the elemental composition, which can be memory intensive. Ninety thousand particles have been tracked using a computer with 4GB RAM; however, only 25,000 were contained in the bin with the largest number of particles.

Appendix B Sample Input Files

B.1. CCSEM Data

```
! coal name (string - arbitrary)
PRB Subbituminous
! total mineral area on a coal basis
1.878
! total mineral wght % on a coal basis
6.451
! weight_percent mineral basis within size bin 1.0 to 2.2, 2.2 to 4.6, 4.6 to 10.0, 10.0 to 22.0,
22.0 to 46.0, 46.0 to 400, sum of columns A to F and all rows therein should add to 100
0.8  3.5  4.5  9.4  5.5  1.3  ! QUARTZ
0.0  0.0  0.2  0.1  0.2  0.0  ! IRON_OXIDE
0.0  0.0  0.0  0.0  0.0  0.0  ! PERICLASE
0.0  0.0  0.0  0.0  0.0  0.0  ! RUTILE
0.0  0.0  0.0  0.1  0.0  0.0  ! ALUMINA
0.1  0.9  2.5  4.6  9.5  7.9  ! CALCITE
0.0  0.1  0.0  0.1  0.1  0.0  ! DOLOMITE
0.0  0.0  0.0  0.0  0.0  0.0  ! ANKERITE
0.8  2.5  5.4  6.1  2.9  1.1  ! KAOLINITE
0.0  0.0  0.4  0.3  0.0  0.1  ! MONTMORILLONITE
0.0  0.2  0.3  0.3  0.1  0.0  ! K_AL_SILICATE
0.0  0.0  0.1  0.1  0.0  0.1  ! FE_AL_SILICATE
0.0  0.1  0.2  0.0  0.1  0.0  ! CA_AL_SILICATE
0.0  0.0  0.1  0.0  0.0  0.0  ! NA_AL_SILICATE
0.0  0.2  0.4  0.2  0.1  0.0  ! ALUMINOSILICATE
0.0  0.0  0.0  0.1  0.0  0.0  ! MIXED_AL_SILICA
0.0  0.0  0.1  0.0  0.0  0.0  ! FE_SILICATE
0.0  0.0  0.0  0.0  0.0  0.1  ! CA_SILICATE
0.0  0.0  0.0  0.0  0.0  0.0  ! CA_ALUMINATE
0.2  0.8  3.3  4.7  5.7  1.2  ! PYRITE
0.0  0.0  0.1  0.4  0.2  0.0  ! PYRRHOTITE
0.0  0.0  0.0  0.0  0.1  0.0  ! OXIDIZED_PYRRHO
0.0  0.0  0.0  0.0  0.0  0.0  ! GYPSUM
0.0  0.0  0.2  0.2  0.0  0.0  ! BARITE
0.0  0.0  0.1  0.1  0.0  0.0  ! APATITE
```


0.0	0.0	0.0	0.0	0.0	0.0	! CA_AL_P
0.0	0.0	0.0	0.0	0.0	0.0	! KCL
0.0	0.0	0.0	0.0	0.0	0.0	! GYPSUM_BARITE
0.0	0.0	0.0	0.0	0.0	0.0	! GYPSUM_AL_SILIC
0.0	0.1	0.4	0.2	0.2	0.1	! SI_RICH
0.0	0.1	0.3	0.2	0.4	0.3	! CA_RICH
0.0	0.0	0.0	0.0	0.0	0.0	! CA_SI_RICH
0.1	0.5	1.6	2.0	1.1	0.7	! UNKNOWN

! percent_excluded, should sum to some number between 0 and 3300 for have 33 mineral groups listed.

55.90	0.00	0.00	19.00	0.00	0.00	0.00	0.00	54.30	76.60	0.00	0.00	100.00
	0.00	44.40	0.00	0.00	0.00	0.00	99.10	21.30	100.00	0.00	86.90	0.00
	15.50	0.00	0.00	0.00	10.80	0.00	0.00	36.90				

! Weight percent mineral_excluded basis within size bin 1.0 to 2.2, 2.2 to 4.6, 4.6 to 10.0, 10.0 to 22.0, 22.0 to 46.0, 46.0 to 400, sum of all columns A to F within a single row should add to a number between 0 and 100

0.00	0.00	0.05	59.39	30.42	10.14	! QUARTZ
0.00	0.00	0.00	0.00	0.00	0.00	! IRON_OXIDE
0.00	0.00	0.00	0.00	0.00	0.00	! PERICLASE
0.00	0.00	100.00	0.00	0.00	0.00	! RUTILE
0.00	0.00	0.00	0.00	0.00	0.00	! ALUMINA
0.00	0.00	0.00	0.00	0.00	0.00	! CALCITE
0.00	0.00	0.00	0.00	0.00	0.00	! DOLOMITE
0.00	0.00	0.00	0.00	0.00	0.00	! ANKERITE
0.00	0.00	0.00	45.46	23.71	30.83	! KAOLINITE
0.00	0.00	9.28	53.10	13.28	24.34	! MONTMORILLONITE
0.00	0.00	0.00	0.00	0.00	0.00	! K_AL_SILICATE
0.00	0.00	0.00	0.00	0.00	0.00	! FE_AL_SILICATE
0.00	0.00	36.36	60.61	3.03	0.00	! CA_AL_SILICATE
0.00	0.00	0.00	0.00	0.00	0.00	! NA_AL_SILICATE
0.00	0.00	0.00	0.00	19.56	80.44	! ALUMINOSILICATE
0.00	0.00	0.00	0.00	0.00	0.00	! MIXED_AL_SILICA
0.00	0.00	0.00	0.00	0.00	0.00	! FE_SILICATE
0.00	0.00	0.00	0.00	0.00	0.00	! CA_SILICATE
0.00	0.00	0.00	0.00	0.00	0.00	! CA_ALUMINATE
6.41	8.77	20.47	23.30	17.55	23.50	! PYRITE
0.00	0.00	0.00	100.00	0.00	0.00	! PYRRHOTITE
0.00	0.00	0.00	0.00	0.00	100.00	! OXIDIZED_PYRRHO
0.00	0.00	0.00	0.00	0.00	0.00	! GYPSUM
0.00	4.10	38.36	57.54	0.00	0.00	! BARITE
0.00	0.00	0.00	0.00	0.00	0.00	! APATITE
0.00	0.00	0.00	83.24	16.76	0.00	! CA_AL_P
0.0	0.0	0.0	0.0	0.0	0.0	! KCL
0.0	0.0	0.0	0.0	0.0	0.0	! GYPSUM_BARITE
0.00	0.00	0.00	0.00	0.00	0.00	! GYPSUM_AL_SILIC
0.00	0.00	0.00	0.00	0.00	100.0	! SI_RICH

```

0.00 0.00 0.00 0.00 0.00 0.00 ! CA_RICH
0.00 0.00 0.00 0.00 0.00 0.00 ! CA_SI_RICH
0.00 0.00 0.00 84.32 4.48 11.20 ! UNKNOWN!
! mineral_density of the 33 minerals listed in CCSEM dataset. Default value is taken as that of
2300.1 or some other num.1 value when no other value is known. i.e. decimals used to identify
approximations
2650.0 5300.0 3610.0 4900.0 4000.0 2800.0 2860.0 3000.0 2650.0 2500.0 2600.0 2800.0 2650.0
2600.0 2650.0 2650.0 4400.0 2950.0 2800.0 5000.0 4600.0 5300.0 2500.0 4500.0 3200.0
2800.0 1990.0 3500.0 2600.0 2650.0 2600.0 2600.0 2700.0
! mineral_meltingpoint of the 33 minerals listed in CCSEM dataset. Default value is set at 500 K
when no other value can be found. Decimals are used to identify approximations
1996.0 1838.0 3125.0 4200.0 2345.0 1196.0 1050.0 1000.0 2086.0 500.0 873.0 1593.0 1873.0
1373.0 883.1 800.1 1473.0 1803.1 1648.1 1076.0 1296.0 1356.0 1725.0 1855.0 1803.0
1973.1 1043.0 2082.1 1596.1 1813.1 2845.1 1473.1 500.0
! Bin_bounds in micrometers these numbers should be increasing and must be greater than or
equal to 0.0 and less than or equal to 0.0004000 meters any size greater than 0.000400 will not
be used. This is a fence post type problem meaning that you need 7 points for 6 bins, the average
size of the bins will be between these numbers i.e. (1.6 3.4 7.3 16.0 34.0 223.0 )
for (1.0 to 2.2, 2.2 to 4.6, 4.6 to 10.0, 10.0 to 22.0, 22.0 to 46.0, 46.0 to 400)
0.0000010 0.0000022 0.0000046 0.0000100 0.0000220 0.0000460
0.0004000

```

B.2. Excluded Fragmentation

! coal name (string - arbitrary) The program looks for numbers greater than 1.0

PRB Subbituminous

! Excluded Particle Fragmentation to how many particles based on size, size bin 1.0 to 2.2, 2.2 to 4.6, 4.6 to 10.0, 10.0 to 22.0, 22.0 to 46.0, 46.0 to 400, particles smaller than 5 microns don't fragment much

1.0	1.0	2.0	2.0	2.0	2.0	! QUARTZ
1.0	1.0	1.0	1.0	1.0	1.0	! IRON_OXIDE
1.0	1.0	1.0	1.0	1.0	1.0	! PERICLASE
1.0	1.0	1.0	1.0	1.0	1.0	! RUTILE
1.0	1.0	1.0	1.0	1.0	1.0	! ALUMINA
1.0	1.0	10.0	10.0	10.0	15.0	! CALCITE
1.0	1.0	10.0	10.0	10.0	15.0	! DOLOMITE
1.0	1.0	1.0	1.0	1.0	1.0	! ANKERITE
1.0	1.0	20.0	20.0	20.0	20.0	! KAOLINITE
1.0	1.0	1.0	1.0	1.0	1.0	! MONTMORILLONITE
1.0	1.0	1.0	1.0	1.0	1.0	! K_AL_SILICATE
1.0	1.0	1.0	1.0	1.0	1.0	! FE_AL_SILICATE
1.0	1.0	1.0	1.0	1.0	1.0	! CA_AL_SILICATE
1.0	1.0	1.0	1.0	1.0	1.0	! NA_AL_SILICATE
1.0	1.0	1.0	1.0	1.0	1.0	! ALUMINOSILICATE
1.0	1.0	1.0	1.0	1.0	1.0	! MIXED_AL_SILICA
1.0	1.0	1.0	1.0	1.0	1.0	! FE_SILICATE
1.0	1.0	1.0	1.0	1.0	1.0	! CA_SILICATE
1.0	1.0	1.0	1.0	1.0	1.0	! CA_ALUMINATE
1.0	1.0	3.0	4.0	5.0	7.0	! PYRITE
1.0	1.0	3.0	4.0	5.0	7.0	! PYRRHOTITE
1.0	1.0	3.0	4.0	5.0	7.0	! OXIDIZED_PYRRHO
1.0	1.0	1.0	1.0	1.0	1.0	! GYPSUM
1.0	1.0	1.0	1.0	1.0	1.0	! BARITE
1.0	1.0	1.0	1.0	1.0	1.0	! APATITE
1.0	1.0	1.0	1.0	1.0	1.0	! CA_AL_P
1.0	1.0	1.0	1.0	1.0	1.0	! KCL
1.0	1.0	1.0	1.0	1.0	1.0	! GYPSUM_BARITE
1.0	1.0	1.0	1.0	1.0	1.0	! GYPSUM_AL_SILIC
1.0	1.0	1.0	1.0	1.0	1.0	! SI_RICH
1.0	1.0	1.0	1.0	1.0	1.0	! CA_RICH
1.0	1.0	1.0	1.0	1.0	1.0	! CA_SI_RICH
1.0	1.0	1.0	1.0	1.0	1.0	! UNKNOWN

! Temperature in which fragmentation has occurred, Quarts, Iron Oxide, Periclase, Rutile, Alumina, Calcite, Ankerite, Kaolinite, Montmorillonite, K_Al_Silicate, Fe_Al_Silicate, Ca_Al_Silicate, Na_Al_Silicate, Aluminosilicate, Mixed_Al_Silica, Fe_Silicate, Ca_Silicate, Pyrite, Pyrrhotite, Oxidized_Pyrrho, Gypsum, Barite, Apatite, Ca_Al_P, KCL, Gypsum_Barite, Gypsum_Al_Silic, Si_Rich, Ca_rich, Ca_Si_Rich, Unknown

1400.0 5000.0 5000.0 5000.0 5000.0 900.0 900.0 5000.0 900.0 5000.0 5000.0 5000.0 5000.0
5000.0 5000.0 5000.0 5000.0 5000.0 5000.0 1100.0 1100.0 1100.0 5000.0 5000.0 5000.0
5000.0 5000.0 5000.0 5000.0 5000.0 5000.0 5000.0 5000.0

B.3. Particle

! Coal Name (string - arbitrary)
PRB Subbituminous
! proximate analysis including, moisture, ash (dry basis), volatile matter (dry basis), fixed carbon (dry basis) (all mass fractions but moisture should sum to ~ 1.0)
0.1976 0.1158 0.3939 0.4903
! ultimate analysis C H N S O mass fraction, dry, ash-free basis (should sum to 1.0)
0.7931463 0.0529292 0.008143 0.0091608 0.1366207
! hhv higher heating value or gross calorific value as received (BTU/lb)
11340.0
! forms of sulfur - pyritic, sulfatic, organic, mass fraction of total sulfur (should sum to 1.0)
0.297468355 0.075949367 0.626582278
! ash_chemistry in alphabetical order by oxide formula (SiO₂, Al₂O₃, TiO₂, Fe₂O₃, CaO, MgO, K₂O, Na₂O, SO₃, P₂O₅, BaO, MnO₂, unknown) mass fraction of ash dry basis (should sum to 1.0)
0.3488 0.1551 0.0065 0.0434 0.2065 0.0406 0.004 0.0233 0.1368 0.0054 0.0032 0.001 0.0254
! ash fusion temperature, reducing - Initial, Softening, Hemispherical, and Fluid - followed by oxidizing - Initial, Softening, Hemispherical, and Fluid
879.9606994 912.5738683 906.8125517 922.5532922 965.5574072 1008.561523
1003.829012 1015.454527
! weight_percent_arsenic in pyrite fraction, organically bound, other inorganically bound - mass fraction of total arsenic (should sum to 1.0)
0.88 0.1 0.02
! weight_percent_antimony in pyrite fraction, organically bound, other inorganically bound - mass fraction of total antimony (should sum to 1.0)
0.8 0.1 0.1
! weight_percent_selenium in pyrite fraction, organically bound, other inorganically bound, sulfides and selenides - mass fraction of total selenium (should sum to 1.0)
0.075 0.8 0.1 0.025
! weight_percent_arsenic, antimony, and selenium in pyrite (should be less than 0.05 (only in really bad coal seams is it that high) and the elemental form)
0.028 0.005 0.0001
! initial_total_mass_flowrate of the all coal streams combined kg/s includes moisture
0.000315
! initial_density of raw coal kg/m³, this must be the same value used in the CFD program
1300.0
! number_of_particle_rows in the particleTrackinfo file this should be the number of rows of numbers in the files not including the exclamation point lines. you can adjust this value in fluent by coarsening an output file, should have the same number of columns as bins in PSD file i.e. 33
3000 3000 3000 3000 3000 3000 3000 3000 3000 3000 3000 3000 3000
3000 3000 3000 3000 3000 3000 3000 3000 3000 3000 3000 3000 3000
3000 3000 3000 3000 3000 3000 3000 3000 3000

! time_step of calculations in seconds due to the fact that you have multiple injections files you have to choose one timestep to have coal flowrates based on all other time calculations will read off of the individual files

4.69442932e-05

! surface_area per gram of coal m²/kg

10000.0

! porosity of the coal

0.5

B.4. Particle Track – Truncated

! ParticleTrack This file contains the particle properties including: 0 Time (s), 1 particle temperature (K), 2 Particle Diameter (m), 3 Particle Mass (kg), 4 Particle Char Mass Fraction, 5 Particle Volatile Mass Fraction, 6 particle timestep (s), 7 ParticleXPosition (m), 8 ParticleRadialPosition (m), 9 ParticleThetaPosition, 10 Static Temperature (K), 11 Static Pressure (Pa), 12 mol fraction CO2, mol fraction CO, mol fraction N2, mol fraction O2, mol fraction H2O, mol fraction H2, mol fraction SO2, mol fraction Vol

```
3.9439962017E-07  3.7801205332E+02  2.5000000000E-07  1.0651962591E-17
    4.9027916789E-01  3.9394316077E-01  3.9439962017E-07  -1.1999901045E-01
    5.1182669804E-07  8.0398073171E-01  3.1318276596E+02  7.2787578702E+00
    0.0000000000E+00  1.2356270582E-32  7.9131599888E-01  2.0868401509E-01
    0.0000000000E+00  0.0000000000E+00  4.3692766377E-40  1.1295529628E-37
1.7169192001E-06  3.7773908508E+02  2.5000000000E-07  1.0651962591E-17
    4.9027916789E-01  3.9394316077E-01  9.2811995973E-07  -1.1999410303E-01
    4.4692958662E-06  8.1570691466E-01  3.1323139763E+02  7.2718263566E+00
    0.0000000000E+00  1.2368029750E-32  7.9131595790E-01  2.0868400857E-01
    0.0000000000E+00  0.0000000000E+00  4.3682396769E-40  1.1306252644E-37
3.3556896717E-05  3.7773879345E+02  2.5000000000E-07  1.0651962591E-17
    4.9027916789E-01  3.9394316077E-01  1.2549074435E-05  -1.1987374197E-01
    1.0229348779E-04  8.2065723866E-01  3.1450982857E+02  7.1266036332E+00
    0.0000000000E+00  1.2677472393E-32  7.9131594300E-01  2.0868400950E-01
    0.0000000000E+00  0.0000000000E+00  4.3410965256E-40  1.1588212953E-37
9.0241993185E-05  3.7773879360E+02  2.5000000000E-07  1.0651962591E-17
    4.9027916789E-01  3.9394316077E-01  1.4546800382E-05  -1.1966034395E-01
    2.6699897479E-04  8.2084912543E-01  3.1706510162E+02  6.9573405385E+00
    0.0000000000E+00  1.3297003834E-32  7.9131591320E-01  2.0868400671E-01
    0.0000000000E+00  0.0000000000E+00  4.2897529499E-40  1.2151968357E-37
```

etc.....

B.5. Coal PSD

! Coal name (string - arbitrary)

PRB Subbituminous

! particle size distribution of pulverized coal diameter of particle micrometers, Cumulative Percent Passing-volumetric basis. No more than 33 size bins without recoding

0.50	0.0
1.93	0.2
2.23	0.3
2.60	0.6
3.02	1.1
3.48	1.8
4.05	2.9
4.68	4.3
5.43	6.3
6.30	8.6
7.30	10.9
8.47	13.3
9.82	15.8
11.4	18.9
13.2	22.6
15.3	26.7
17.7	31.1
20.5	36.1
23.8	41.5
27.5	46.9
32.0	52.6
37.0	58.0
43.0	63.5
49.8	68.8
57.7	74.2
66.8	79.6
77.5	84.6
89.8	88.9
104.0	92.3
121.0	94.9
140.0	96.9
162.0	98.5
188.0	100.1

Appendix C Sample Output Files

C.1. Mineral Distribution Output – Truncated

Qua_0	Iro_1	Per_2	Rut_3	Alu_4	Cal_5	Dol_6	Ank_7	Kao_8	Mon_9	KAlSi_10		
	FeAlSi_11		CaAlSi_12		NaAlSi_13		AlSi_14		MixAlSi_15	FeSi_16		
	CaSi_17		CaAl_18		Pyr_19	Pyrr_20		OxPyrr_21	Gyp_22	Bar_23		
	Apa_24		CaAlP_25		KCl_26		GypBa_27		GypsAlSi_28	SiRi_29		
	CaRi_30		CaSiRi_31		Unk_32		Qua_33		Iro_34	Per_35	Rut_36	Alu_37
	Cal_38	Dol_39		Ank_40		Kao_41		Mon_42		KAlSi_43		
	FeAlSi_44		CaAlSi_45		NaAlSi_46		AlSi_47		MixAlSi_48	FeSi_49		
	CaSi_50		CaAl_51		Pyr_52	Pyrr_53		OxPyrr_54	Gyp_55	Bar_56		
	Apatite_57		CaAlP_58		KCl_59		GypBa_60		GypAlSi_61	SiRi_62		
	CaRi_63		CaSiRi_64		Unk_65		Qua_66		Iro_67	Periclase_68		
	Rutile_69		Alu_70		Cal_71	Dol_72		Ank_73		Kao_74		
	Mon_75		KAlSi_76		FeAlSi_77		CaAlSi_78		NaAlSi_79	AlSi_80		
	MixAlSi_81		FeSi_82		CaSi_83		CaAl_84		Pyr_85	Pyrr_86		
	OxPyrr_87		Gyp_88		Bar_89	Apatite_90		Ca_Al_P_91		KCl_92		
	GypBa_93		GypAlSi_94		Si_Rich_95		CaRi_96		CaSiRi_97	Unkn_98		
	Qua_99		Iro_100		Per_101		Rut_102		Alu_103	Cal_104		
	Dol_105		Ank_106		Kao_107		Mon_108		KAlSi_109	FeAlSi_110		
	CaAlSi_111		NaAlSi_112		AlSi_113		MixAlSi_114		FeSi_115	CaSi_116		
	CaAl_117		Pyr_118		Pyrr_119		OxPyrr_120		Gyp_121	Bar_122		
	Apa_123		CaAlP_124		KCl_125		GypBa_126		GypAlSi_127	SiRi_128		
	CaRi_129		CaSiRi_130		Unk_131		Qua_132		Iro_133	Per_134		
	Rut_135		Alu_136		Cal_137		Dol_138		Ank_139	Kao_140		
	Mon_141		KAlSi_142		FeAlSi_143		CaAlSi_144		NaAlSi_145	AlSi_146		
	MixAlSi_147		FeSi_148		CaSi_149		CaAl_150		Pyr_151	Pyrr_152		
	OxPyrr_153		Gyp_154		Bar_155		Apa_156		CaAlP_157	KCl_158		
	GypBa_159		GypAlSi_160		SiRi_161		CaRi_162		CaSiRi_163	Unk_164		
	Qua_165		Iro_166		Per_167		Rut_168		Alu_169	Ca_170		
	Dol_171		Ank_172		Ka_173		Mon_174		KAlSi_175	FeAlSi_176		
	CaAlSi_177		NaAlSi_178		AlSi_179		MixAlSi_180		FeSi_181	CaSi_182		
	CaAl_183		Pyrite_184		Pyrr_185		OxPyrr_186		Gyp_187	Bar_188		
	Apa_189		CaAlP_190		KCl_191		GypBa_192		GypAlSi_193	SiRi_194		
	CaRi_195		CaSiRi_196		Unk_197							
												Number of minerals in this particle
												Coal

particle identifier

C.2. Coal Elemental Distribution Output – Truncated

Sodiu_0	Magne_1	Alumi_2	Silic_3	Phosp_4	Sulfu_5	Chlor_6	Potas_7	Calci_8	Ferri_9	Bariu_10	Titan_11	Manga_12	Unkno_13	Arsen_14	Antim_15	Selen_16	Coal particle identifier	Coal total original mass (kg)	Coal original diameter (m)
2.55716e-019	9.21595e-020	3.03654e-021	3.30191e-017	8.88319e-020	1.60674e-020	0	2.41411e-021	1.64567e-020	3.72128e-020	3.16476e-021	1.89586e-021	6.24497e-022	2.51012e-020	3.47106e-022	6.81814e-023	1.19999e-022	number_0	9.95293e-018	2.5e-007
2.55716e-019	9.21595e-020	3.03654e-021	2.00483e-020	8.88319e-020	1.60674e-020	0	2.41411e-021	1.64567e-020	3.72128e-020	3.16476e-021	1.89586e-021	6.24497e-022	7.19524e-017	3.47106e-022	6.81814e-023	1.19999e-022	number_1	9.95293e-018	2.5e-007
2.55716e-019	9.21595e-020	3.03654e-021	2.00483e-020	8.88319e-020	7.12081e-017	0	2.41411e-021	1.64567e-020	6.20438e-017	3.16476e-021	1.89586e-021	6.24497e-022	2.51012e-020	8.51099e-020	8.33174e-020	5.11495e-021	number_2	9.95293e-018	2.5e-007

etc...

C.3. Organic Vaporization Output – Truncated

IMPORTANT Raeva's data does not describe/support real coal. These values are only given for comparison purposes only and should not be trusted until further investigations have been undertaken it is a ballpark estimate only and the ballpark is idealized at best. The first three columns are the dataset generated using the parameters from Raeva's dataset.

Initial cumulative			of the particle track					
As_mol	Sb_mol	Se_mol	As mol Linear	Sb mol Linear	Se mol Linear			
Particle_x_coord	Particle_radial_coord	Particle_theta_coord						
1.12279e-013	2.7754e-014	2.88497e-014						
0	0	0	1.12279e-013	2.7754e-014	2.88497e-014	-0.12	2.12e-005	0.45
0	0	0	1.12279e-013	2.7754e-014	2.88497e-014	-0.12	0.000105	0.734
0	0	0	1.12279e-013	2.7754e-014	2.88497e-014	-0.119	0.000318	0.786
0	0	0	1.12279e-013	2.7754e-014	2.88497e-014	-0.119	0.000399	0.578
0	0	0	1.12279e-013	2.7754e-014	2.88497e-014	-0.119	0.000444	0.0647

C.4. Example Output Files for Included/Excluded Vaporization – Truncated

Initial cumulative			Se_mol of the particle track			
As_mol	Sb_mol	Se_mol	Particle_x_coord	Particle_radial_coord	Particle_theta_coord	
1.12279e-013	2.7754e-014	2.88497e-014				
0	0	0	-0.119711	1.85217e-005	0.803981	
0	0	0	-0.119081	7.14623e-005	0.047851	
0	0	0	-0.118539	0.00018203	0.809714	
0	0	0	-0.118082	0.000315338	0.944133	
0	0	0	-0.118072	0.0003175	0.944133	
0	0	0	-0.117737	0.0003852	0.868832	
0	0	0	-0.117175	0.000391178	0.696314	
0	0	0	-0.116832	0.0003175	0.561961	

Appendix D UND Furnace Diagrams

The mesh used to model the UND furnace with Fluent consists of 129971 cells, 261314 faces, and 131344 nodes. A portion of the mesh is shown in Figure 7-9.

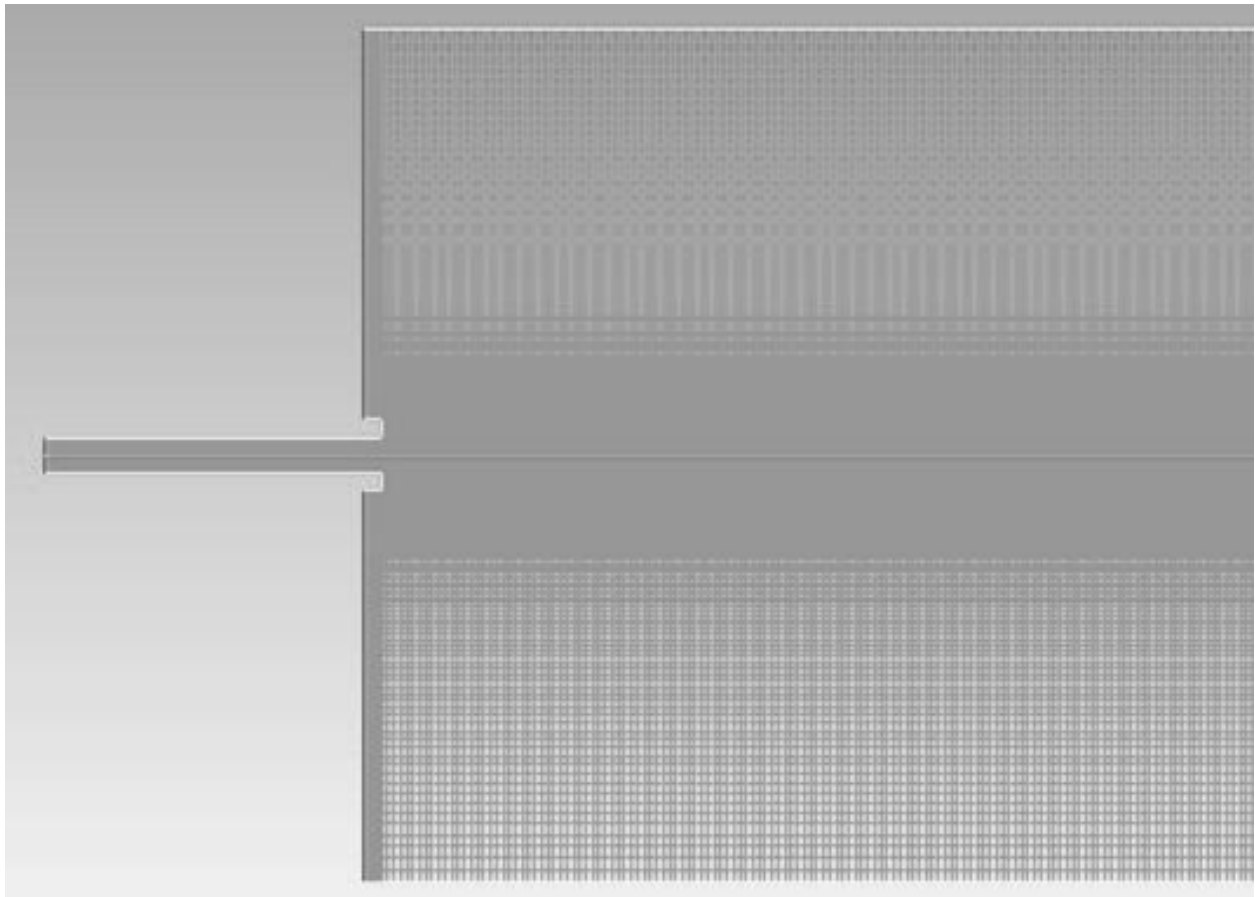


Figure 7-9 Example mesh of the UND 19kW down-fired furnace inlet

A diagram of the UND furnace, as shown in the work of Lentz et al, is found in Figure 7-10 (Lentz et al. 2012).

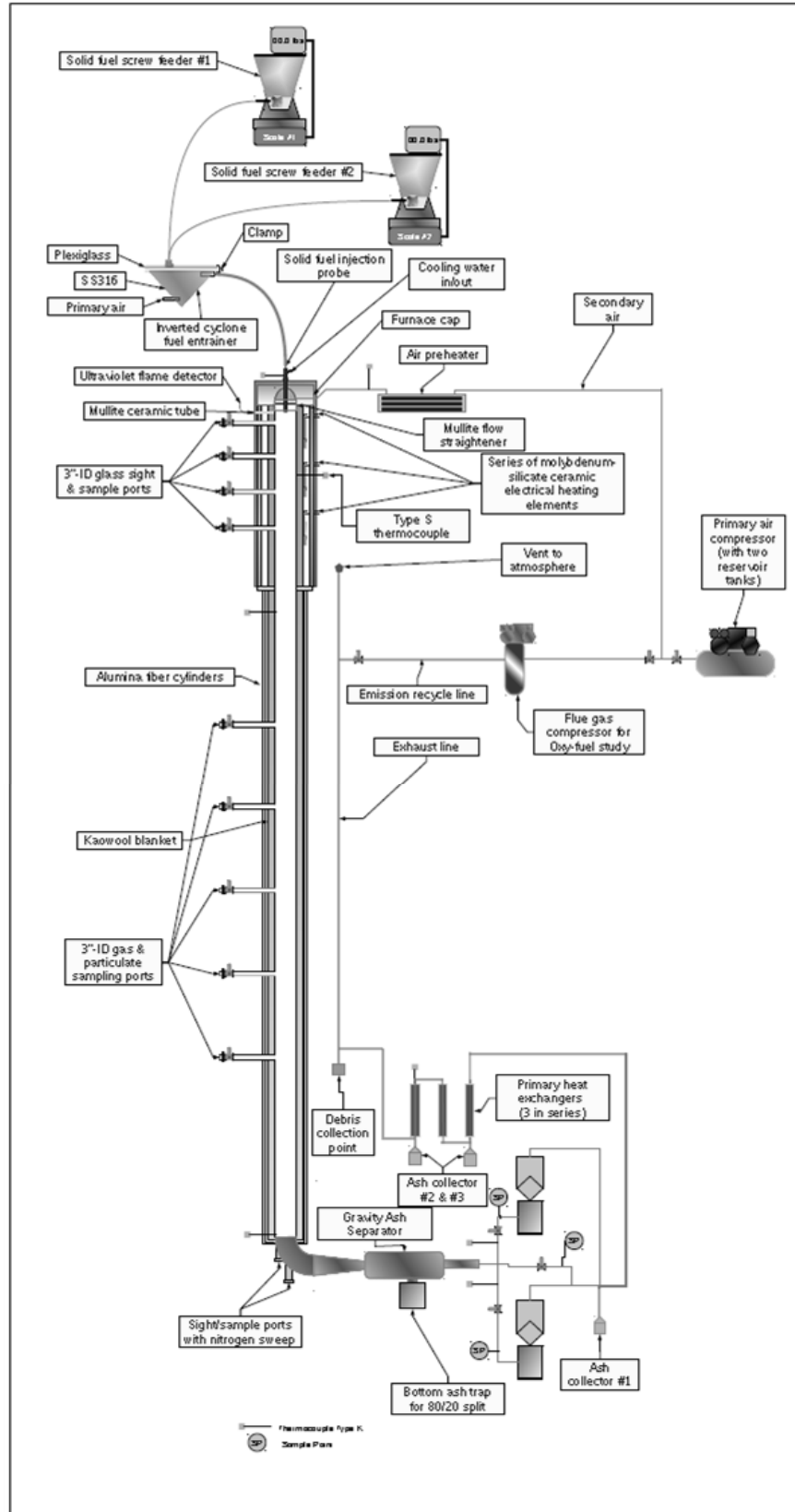


Figure 7-10 Illustration of the UND 19kW down-fired furnace (Lentz et al. 2012)

Appendix E Other Relationships Used

E.1. Molecular Weight

The molecular weight of the gas and particle mixtures (Turns 2000):

$$M_{mix} = \sum_i y_i M_i \quad 7-1$$

E.2. Mole Fraction

The mole fractions of the gas and particle mixtures:

$$y_i = \frac{n_i}{\sum_i n_i} \quad 7-2$$

E.3. Geometry

E.3.1. Particle Volume

$$V = \frac{\pi}{6} d_p^3 \quad 7-3$$

E.3.2. Particle Surface Area

$$SA = \pi d_p^2 . \quad 7-4$$

E.4. Gas Viscosity

E.4.1. Lennard Jones Parameters

$$\mu = \frac{5}{16} \frac{\sqrt{MT}}{\sigma^2 \Omega_\mu}.$$

7-5

E.4.2. Collision Integral

$$\Omega_\mu = \Omega_k = \frac{1.16145}{T^{*0.14874}} + \frac{0.52487}{e^{0.77320T^*}} + \frac{2.16178}{e^{2.437870T^*}}.$$

7-6

E.4.3. T^*

$$T^* = \frac{\kappa T}{\varepsilon}.$$

7-7

E.4.4. Gas Mixture Viscosity

$$\mu_{mix} = \sum_{\alpha=1}^N \frac{x_\alpha \mu_\alpha}{\sum_{\beta} x_\beta \Phi_{\alpha\beta}}.$$

7-8

E.4.5. Dimensionless $\Phi_{\alpha\beta}$

$$\Phi_{\alpha\beta} = \frac{1}{\sqrt{8}} \left(1 + \frac{M_\alpha}{M_\beta} \right)^{-1/2} \left[1 + \left(\frac{\mu_\alpha}{\mu_\beta} \right)^{1/2} \left(\frac{M_\alpha}{M_\beta} \right)^{1/4} \right]^2.$$

7-9

According to Curtis and Hirschfelder, as cited in Bird et al., the above relationship “has been shown to reproduce measured values of the viscosities of mixtures within an average deviation of about 2%.”

E.5. Diffusion Coefficient

E.5.1. Effective Diffusion Coefficient – a-mix

(Wilke 1950; Richard 1996)

$$D_{ab} = D_{1,mix} = \frac{1}{\frac{y'_2}{D_{1,2}} + \frac{y'_3}{D_{1,3}} + \dots + \frac{y'_n}{D_{1,n}}} \cdot$$

7-10

E.5.2. y'_n

$$y'_n = \frac{y'_n}{y_2 + y_3 + \dots + y_n} \cdot$$

7-11

8. REFERENCES

- 101st Congress. 1990. Title 42, Chapter 85. edited by United States House of Representatives. Washington D.C.: United States House of Representatives.
- Ake, Terence, Clayton Erickson, William Medeiros, Linton Hutcheson, Mark Barger, and Scott Rutherford. 2003. Limestone Injection for Protection of SCR Catalyst. Duke Energy, Riley Power Inc, Cormetech Inc.
- ANSYS. 2006. *Fluent 6.3 UDF Manual*. Lebanon, HN: Fluent Inc.
- . 2009. *ANSYS Fluent 12.0 UDF Manual*. Lebanon, NH: Fluent Inc.
- . 2012. *FLUENT 6.3 User's Guide*. ANSYS FLUENT 2012 [cited February 2012].
- Attalla, M. I., C. Chao, and P. F. Nelson. 2003. *A Review of Tools for the Modelling and Prediction of Trace Element Deposition in Combustion Processes*. Edited by Cooperative Research Center for Coal in Sustainable Development: QCAT Technology Transfer Center.
- Attalla, M. I., S. Morgan, K. Riley, G. W. Bryant, and P.F. Nelson. 2007. Trace Element Deposition in Combustion Processes. Cooperative Research Center for Coal in Sustainable Development.
- Babu, S.P. 1975. "Trace Elements in Fuel." *Advances in Chemistry* no. 141:223.
- Baxter, Larry L. 2005. Biomass Impacts on SCR Catalyst Performance. In *IEA Biomass Task 32*.
- . 2009. A Method for Separating CO₂ from Light Gases Provo, UT: Sustainable Energy Solutions, LLC.
- . 2010. Energy Facility Contractor's Group. Provo, UT.
- Benson, S. A. 1984. Distribution of Inorganics in Low-Rank Coals. United States.
- Benson, S. A., T. A. Erickson, C. A. O'Keefe, K. Katrinak, and S. E. Allan. 1995. Trace Metal Transformations in Gasification. United States.

- Benson, Steven A. 2011. *Fuels Technology*. Grand Forks, ND: University of North Dakota Department of Chemical Engineering.
- Benson, Steven A., Thomas A. Erickson, Robert R. Jenen, and Jason D. Laumb. 2002. "Transformations Model for Predicting Size and Composition of Ash During Coal Combustion." *Fuel Chemistry Division Preprints* no. 47 (2).
- Benson, Steven A., Jason D. Laumb, Donald P. McCollor, and Jim Tibbetts. 2007. *Methods for the Production of Low-Density Microspheres*. edited by University of North Dakota Energy and the Environment Research Center. USA.
- Benson, Steven A., Edward N. Steadman, Arun K. Mehta, and Charlse E. Schmidt. 1994. *Trace Element Transformations in Coal-Fired Power Systems*. 1-3 vols. Vol. 39, *Fuel Processing Technology*. Scottsdale, AZ, USA, 19-22 April 1993, Amsterdam: Elsevier.
- Bird, R. B., W. E. Stewart, and E. N. Lightfoot. 2002. *Transport Phenomena*. Edited by Wayne Anderson. Second Edition ed. New York, NY: John Wiley & Sons, Inc.
- Bool III, Lawrence E., and Joseph J. Helble. 1995. "Laboratory Study of the Partitioning of Trace Elements During Pulverized Coal Combustion." *Energy and Fuels* no. 9:880-887.
- Bool III, Lawrence E., Connie L. Senior, F. Huggins, Gerald P. Huffman, and N. Shah. 1996. Toxic Substances from Coal Combustion -- A Comprehensive Assessment. Quarterly Technical Progress Report, 1 April 1996--30 June 1996. In *Other Information: PBD: Jul 1996*.
- Bool III, Lawrence E., Connie L. Senior, Frank E. Huggins, Gerald P. Huffman, N. Shah, Jost O. L. Wendt, T. W. Peterson, Adel Sarofim, I. Olmez, Taofang Zeng, S. Crowley, and Rober B. Finkelman. 1996. Toxic Substances from Coal Combustion: A Comprehensive Assessment: Quarterly report, 1 July 1996-30 September 1996. In *Other Information: PBD: Oct 1996*.
- Bool III, Lawrence E., Constance L. Senior, Frank E. Huggins, Gerald P. Huffman, Naresh Shah, Jost O. L. Wendt, Adel F. Sarofim, and Taofang Zeng. 1996. Toxic Substances from Coal Combustion -- A Comprehensive Assessment. Quarterly report number 2, January 1-- March 31, 1996. In *Other Information: PBD: Apr 1996*.
- Bool III, Lawrence E., Constance L. Senior, Frank E. Huggins, Gerald P. Huffman, Naresh Shah, Jost O. L. Wendt, F. Shadman, T. W. Peterson, Wayne S. Seames, Adel F. Sarofim, I. Olmez, Taofang Zeng, S. Crowley, Robert B. Finkelman, Joseph J. Helble, and M. J. Wornat. 1997. Toxic Substances from Coal Combustion - A Comprehensive Assessment. edited by U.S. Department of Energy. Pittsburgh, PA.
- Bool III, Lawrence E., Constance L. Senior, Adel F. Sarofim, and Taofang Zeng. 1996. Toxic Substances from Coal Combustion -- A comprehensive Assessment. Quarterly report number 1, 1 October 1995--31 December 1995. In *Other Information: PBD: Jan 1996*.

- Clarke, L. B., and L. L. Sloss. 1992. Trace Elements. International Organization.
- Clean Air Act. 1963. In *Title 42, Chapter 85, U.S.C.* United States of America: U.S. House of Representatives. Original edition, Air Quality Act of 1967 (81 Stat. 485, P.L. 90-148)
- Clean Air Act Extension of 1970 (84 Stat. 1676, P.L. 91-604)
- Clean Air Act Amendments of 1977 (91 Stat. 685, P.L. 95-95)
- Clean Air Act Amendments of 1990 (104 Stat. 2468, P.L. 101-549).
- Cramer, H. 1986. *VGB Powertech/VGB Kraftwekstechnik* no. 66 (8):648-651.
- Crowley, S. S., Curtis A. Palmer, Allan Kolker, Robert B. Finkelman, K. C. Kolb, and H. E. Belkin. 1996. Toxic Substances from Coal Combustion -- Forms of Occurrence Analyses. Technical progress report, April 30--November 1, 1996. In *Other Information: PBD: 6 Dec 1996*.
- Davidson, R. M., and L. B. Clarke. 1996. Trace Elements in Coal: Perspectives. International Organization.
- Diaz-Somoano, M., and M. R. Martinez-Tarazona. 2003. "Trace Element Evaporation During Coal Gasification Based on a Thermodynamic Equilibrium Calculation Approach." *Fuel* no. 82 (2):137-145. doi: 10.1016/s0016-2361(02)00251-x.
- Dismukes, Edward B. 1994. "Trace Element Control in Electrostatic Precipitators and Fabric Filters." *Fuel Processing Technology* no. 39 (1-3):403-416. doi: 10.1016/0378-3820(94)90195-3.
- Field, M. A. 1969. "Rate of Combustion of Size-Graded Fractions of Char from a low-Rank Coal Between 1200K and 2000K." *Combustion and Flame* no. 13 (3):237-252. doi: 10.1016/0010-2180(69)90002-9.
- Finkelman, Robert B. 1980. *Modes of Occurrence of Trace Elements in Coal*, Chemistry, University of Maryland.
- . 1994. "Modes of Occurrence of Potentially Hazardous Elements in Coal: Levels of Confidence." *Fuel Processing Technology* no. 39 (1-3):21-34. doi: 10.1016/0378-3820(94)90169-4.
- Fletcher, Thomas H., Alan R. Kerstein, Ronald J. Pugmire, and David M. Grant. 1990. "Chemical Percolation Model for Devolatilization. 2. Temperature and Heating Rate Effects on Product Yields." *ENERGY & FUELS* no. 4 (1):54-60. doi: 10.1021/ef00019a010.

- Fremer, Fred. 2010. U.S. Coal Supply and Demand: 2009 Review. edited by DOE U.S. Energy Information Administration. Washington, DC: U.S. Department of Energy.
- Gardener, John. 2009. Scanning Electron Microscopy. Provo, UT: Brigham Young University.
- Giere, R., and P Stille. 2004. *Energy, Waste and the Environment: A Geochemical Perspective*. Bath BAI 3JN, UK: The Geological Society.
- Grant, David M., Ronald J. Pugmire, Thomas H. Fletcher, and Alan R. Kerstein. 1989. "Chemical Model of Coal Devolatilization Using Percolation Lattice Statistics." *ENERGY & FUELS* no. 3 (2):175-186. doi: 10.1021/ef00014a011.
- Green, Don W., and Robert H. Perry. 2008. *Perry's Chemical Engineers' Handbook*. 8th ed. Chicago, IL: McGraw-Hill.
- Groves, S. J., Jim Williamson, and A. Sanyal. 1987. "Decomposition of Pyrite During Pulverized Coal Combustion." *Fuel* no. 66 (4):461-466. doi: 10.1016/0016-2361(87)90148-7.
- Gupta, Parthapratim, Anup Kumar Sadhukhan, and Ranajit Kumar Saha. 2007. "Analysis of the Combustion Reaction of Carbon and Lignite Char with Ignition and Extinction Phenomena: Shrinking Sphere Model." *International Journal of Chemical Kinetics* no. 39 (6):307-319. doi: 10.1002/kin.20245.
- Gupta, Raj P., Li. Yan, S. K. Gupta, Terry F. Wall, T. Kiga, and S. Watanabe. 2005. "CCSEM Analysis of Minerals in Coal and Thermal Performance of PC-Fired Boilers." *Clean Air* no. 6:157-170.
- Gupta, Rajender. 2007. Advanced Coal Characterization: A Review, at 2540 Olentangy River Road, P.O. Box 3337, Columbus, OH 43210-3337, United States.
- Halder, P. K., A. Datta, and R. Chattopadhyay. 1993. "Combustion of Single Char Particle in a Turbulent Fluidized Bed." *The Canadian Journal of Chemical Engineering* no. 71 (1):3-9. doi: 10.1002/cjce.5450710102.
- Helble, Joseph J., Srivats Srinivasachar, and Arthur A. Boni. 1990. "Factors Influencing the Transformation of Minerals During Pulverized Coal Combustion." *Progress in Energy and Combustion Science* no. 16 (Compendex):267-279.
- Hino, Mitsutaka, Shei-Bin Wang, Tetsuya Nagasaka, and Shiro Ban-Ya. 1994. "Evaporation Rate of Zinc in Liquid Iron." *ISIJ International* no. 34 (6):491-497.
- Huffman, Gerald P., Frank E. Huggins, Naresh Shah, and Jianmin Zhao. 1994. "Speciation of Arsenic and Chromium in Coal and Combustion Ash by XAFS Spectroscopy." *Fuel Processing Technology* no. 39 (1-3):47-62. doi: 10.1016/0378-3820(94)90171-6.

- Huggins, Frank E. 2002. "Overview of Analytical Methods for Inorganic Constituents in Coal." *International Journal of Coal Geology* no. 50 (1-4):169-214. doi: 10.1016/s0166-5162(02)00118-0.
- Hurley, John P., Steven A. Benson, Thomas A. Erickson, Sean E. Allan, and Jay Bieber. 1992. Project Calcium. Grand Forks, ND: Energy and Environmental Research Center.
- Ilyushechkin, Alexander, Daniel Roberts, David Harris, and Riley Kenneth. 2011. "Trace Element Partitioning and Leaching in Solids Derived from Gasification of Australian Coals." *Coal Combustion and Gasification Products* no. 3.
- Jassim, Esam. 2009. Model of Coal Devolatilization and Char Combustion Including Inorganic Minerals. Grand Forks, ND: University of North Dakota.
- Jassim, Esam, Steven A. Benson, Frank M. Bowman, and Wayne Seames, S. 2010. "The Influence of Fragmentation on the Behavior of Pyrite Particles During Pulverized Coal Combustion." *Fuel Processing Technology*. doi: 0.1016/j.fuproc.2010.12.018
- Jassim, Esam, Steven A. Benson, Wayne S. Seames, and Michael D. Mann. 2009. Modeling Pyrite Behavior in Gasification Environments. Paper read at 2009 AIChE Annual Meeting, 09 AIChE, November 8, 2009 - November 13, 2009, at Nashville, TN, United states.
- Jones, W. P., and R. P. Lindstedt. 1988. "Global Reaction Schemes for Hydrocarbon Combustion." *Combustion and Flame* no. 73 (3):233-249. doi: 10.1016/0010-2180(88)90021-1.
- Kalmanovitch, David P, and Melvin Frank. 1988. "An effective model of viscosity for ash deposition phenomena." In *Proceedings of Mineral Matter and Ash Deposition from Coal*, edited by Richard W. Bryers and Karl S. Vorres, 22-26. Santa Barbara, California: United Engineering Trustees, Inc.
- Kang, Shin G. 1991. *Fundamental Studies of Mineral Matter Transformation During Pulverized Coal Combustion: Residual ash Formation*, Massachusetts Institute of Technology. Dept. of Chemical Engineering, Massachusetts Institute of Technology.
- Kang, Shin G., A. R. Kerstein, J. J. Helble, and A. F. Sarofim. 1990. "Simulation of Residual ash Formation During Pulverized Coal Combustion: Bimodal ash Particle Size Distribution." *Aerosol Science and Technology* no. 13 (Compendex):401-412.
- Kobayashi, H., J. B. Howard, and A. F. Sarofim. 1977. "Coal Devolatilization at High Temperatures." *Symposium (International) on Combustion* no. 16 (1):411-425. doi: 10.1016/s0082-0784(77)80341-x.

- Kolker, Allan , Stanley J. Mroczkowski, Curtis A. Palmer, Kristen O. Dennen, Robert B. Finkelman, and John H. Bullock Jr. 2002. Toxic Substances From Coal Combustion -- A Comprehensive Assessment, Pahse II; Element Modes of Occurrence for the Ohio 5/6/7, Wyodak and North Dakota Coal Samples. In *Other Information: PBD: 30 May 2002*.
- Kolker, Allan , Stanley J. Mroczkowski, Curtis A. Palmer, and Robert B. Finkelman. 1999. USGS Toxic Substances From Coal Combustion -- Forms of Occurrence Analysis. In *Other Information: PBD: 1 Apr 1999*.
- Kolker, Allan, Curtis A. Palmer, Harvey E. Belkin, Jason Willet, Kathleen C. Kolb, Robert B. Finkelman, Sharon S. Crowley, and Stanley J. Mroczkowski. 1998. Toxic Substances from Coal Combustion - Forms of Occurrence Analyses.
- Kolker, Allan, Adel F. Sarofim, Curtis A. Palmer, Frank E. Huggins, Gerald P. Huffman, JoAnn S. Lighty, Joseph J. Helble, Jost O. L. Wendt, M. R. Ames, N. Yap, Robert B. Finkelman, R. Mamani-Paco, S. J. Mroczkowsky, T. Panagiotou, and Wayne S. Seames. 1999. Toxic Substances from Coal Combustion a Comprehensive Assessment. United States.
- Krishnamoorthy, Gautham, and John M. Veranth. 2003. "Computational modeling of CO/CO₂ ratio inside single char particles during pulverized coal combustion." *Energy and Fuels* no. 17 (Compendex):1367-1371.
- Lentz, Nicholas B., Charles K. Thumbi, Dan Madche, Prasanna Seshadri, and Steven A. Benson. 2012. Characterization of Ash Particle Formation during Air-Fired and Oxycombustion Operation. Paper read at Clearwater Clean Coal Conference, June 3-7, 2012, at Clearwater, Florida.
- Lide, David R. 2002. *CRC Handbook of Chemistry and Physics*. 83rd ed. New York, NY: CRC Press.
- Linak, William P., and Jost O. L. Wendt. 1994. "Trace Metal Transformation Mechanisms During Coal Combustion." *Fuel Processing Technology* no. 39 (1-3):173-198. doi: 10.1016/0378-3820(94)90179-1.
- Lockwood, F. C., and S. Yousif. 2000. "Model for the particulate matter enrichment with toxic metals in solid fuel flames." *Fuel Processing Technology* no. 65 (Compendex):439-457.
- Ma, Z. H. 2007. "A comprehensive slagging and fouling prediction tool for coal-fired boilers and its validation/application." *Fuel Processing Technology* no. 88 (11-12):1035-1043.
- Maloney, Daniel J., Ramanathan Sampath, and John W. Zondlo. 1999. "Heat Capacity and Thermal Conductivity Considerations for Coal Particles During the Early Stages of Rapid Heating." *Combustion and Flame* no. 116 (1-2):94-104. doi: 10.1016/s0010-2180(98)00044-3.

- McCollor, Donald P., Steven A. Benson, Bernard Hamel, and Robin Rhodes. 2003. Method and apparatus for capturing gas phase pollutants such as sulfur trioxide. USA: Energy & Environmental Research Center, Marsulex Environmental Technologies Corporation, Alstom Technolog Ltd.
- Meij, R. 1994. "Trace Element Behavior in Coal-Fired Power Plants." *Fuel Processing Technology* no. 39 (1-3):199-217.
- Miller, Robert N., Richard F. Yarzab, and Peter H. Given. 1979. "Determination of the mineral-matter contents of coals by low-temperature ashing." *Fuel* no. 58 (1):4-10. doi: 10.1016/0016-2361(79)90044-9.
- Murarks, I. P., S. V. Mattigod, and Robert F. Keefer. 1993. "An Overview of Electric Power Research Institute (EPRI) Research Related to Effective Management of Coal Combustion Residues." In *Trace Elements in Coal and Coal Combustion Residues*, edited by Rober F. Keefer and Kenneth S. Sajwan. Boca Raton, FL: Lewis Publishers.
- Nelson, Peter F. 2007. Trace Metal Emissions in Fine Particles from Coal Combustion, at 2540 Olentangy River Road, P.O. Box 3337, Columbus, OH 43210-3337, United States.
- Neville, M., and A. F. Sarofim. 1982. The Stratified Composition of Inorganic Submicron Particles Produced During Coal Combustion. Paper read at Nineteenth Symposium (International) on Combustion, at Pittsburgh, PN.
- Ohno, Reiichi. 1991. "Kinetics of Removal of Bismuth and Lead from Molten Copper Alloys in Vacuum Induction Melting." *Metallurgical and Materials Transactions B* no. 22 (4):447-465. doi: 10.1007/bf02654283.
- Quann, R. J., M. Neville, and A. F. Sarofim. 1990. "A Laboratory Study of the Effect of Coal Selection on the Amount and Composition of Combustion Generated Submicron Particles." *Combustion science and technology* no. 74 (1-6):245-265. doi: 10.1080/00102209008951691.
- Quann, R. J., and A. F. Sarofim. 1982. "Vaporization of Refractory Oxides During Pulverized Coal Combustion." *Symposium (International) on Combustion* no. 19 (1):1429-1440. doi: 10.1016/s0082-0784(82)80320-2.
- Quann, Richard J., Matthew Neville, Morteza Janghorbani, Charles A. Mims, and Adel F. Sarofim. 1982. "Mineral matter and trace-element vaporization in a laboratory-pulverized coal combustion system." *Environmental Science & Technology* no. 16 (11):776-781. doi: 10.1021/es00105a009.
- Quann, Richard J., and Adel F. Sarofim. 1986. "A Scanning Electron Microscopy Study of the Transformations of Organically Bound Metals During Lignite Combustion." *Fuel* no. 65 (1):40-46. doi: 10.1016/0016-2361(86)90139-0.

- Raask, Erich. 1985. *Mineral impurities in Coal Combustion: Behavior, Problems, and Remedial Measures*. Washington: Hemisphere Pub. Corp.
- Raeva, Anna A. 2011. *Trace Element Partitioning During Coal Combustion Using New/in situ Direct Method*, Chemistry, University of North Dakota, Grand Forks, ND.
- Raeva, Anna A., Nagaraju Dongari, Evgenii I. Kozliak, David T. Pierce, and Wayne S. Seames. 2012. "Modeling Trace Element Partitioning During Coal Combustion in the Excluded Mineral Fraction Using GFAAS and TGA-DSC."
- Raeva, Anna A., Oleg V. Klykov, Evgenii I. Kozliak, David T. Pierce, and Wayne S. Seames. 2011. "In Situ Evaluation of Inorganic Matrix Effects on the Partitioning of Three Trace Elements (As, Sb, Se) at the Outset of Coal Combustion." *ENERGY & FUELS* no. 25 (10):4290-4298. doi: 10.1021/ef200879j.
- Raeva, Anna A., David T. Pierce, Wayne S. Seames, and Evgenii Kozliak. 2011. "A Method for Measuring the Kinetics of Organically Associated Inorganic Contaminant Vaporization During Coal Combustion." *Fuel Processing Technology* no. 92:1333-1339.
- Ratafia-Brown, Jay A. 1994. "Overview of Trace Element Partitioning in Flames and Furnaces of Utility Coal-Fired Boilers." *Fuel Processing Technology* no. 39 (1-3):139-157. doi: 10.1016/0378-3820(94)90177-5.
- Ratafia-Brown, Jay A., Lynn Manfredo, Jeffrey Hoffman, and Massood Ramezan. 2002. *Major Environmental Aspects of Gasification-Based Power Generation Technologies*. edited by U.S. Department of Energy. Pittsburgh, Pa: National Energy Technology Laboratory.
- Richard, Tom. 1996. "Calculating the Oxygen Diffusion Coefficient in Air."
- Roberts, Warren B. 2006. *Black Liquor Droplet Combustion and Modeling*, Department of Chemical Engineering, Brigham Young University, Provo, UT.
- Sadhukhan, Anup Kumar, Parthapratim Gupta, and Ranajit Kumar Saha. 2008. "Analysis of the Dynamics of Coal Char Combustion with Ignition and Extinction Phenomena: Shrinking Core Model." *International Journal of Chemical Kinetics* no. 40 (9):569-582. doi: 10.1002/kin.20343.
- Sarofim, A. F., and J. J. Helble. 1993. Mechanisms of ash and Deposit Formation Paper read at Engineering Foundation Conference - The Impact of ash deposition on coal fired plants.
- Seames, Wayne S. 2000. *The Partitioning of Trace Elements During Pulverized Coal Combustion* Chemical Engineering, University of Arizona, Tuscon, AZ.
- . 2005. *The North Dakota DOE EPSCoR Infrastructure Improvement Program: Advances in the Fundamental Understanding of Coal Combustion Emission Mechanisms*. University of North Dakota, Grand Forks, ND: DOE.

- . 2008. The North Dakota DOE EPSCoR IIP Phase 2 - Performance Impacts of Impurities in Clean Coal Systems Equipped with Carbon Capture Technologies. University of North Dakota, Grand Forks, ND: DOE EPSCoR.
- Seames, Wayne S., Mandar Gadgil, Chunmei Wang, and Joshua Fetsch. 2006. Impacts on Trace Metal Leaching from fly ash due to the Co-Combustion of Switchgrass with Coal. Paper read at 23rd International Pittsburgh Coal Conference, at Pittsburgh, Pennsylvania.
- Seames, Wayne S., Essam I. Jassim, and Steve A. Benson. 2010. Modeling Trace Element Release from Included and Excluded Pyrite during Pulverized Coal Combustion. In *International Pittsburgh Coal Conference*. Istanbul, Turkey.
- Seames, Wayne S., and Jost O. L. Wendt. 2000a. The Partitioning of Arsenic During Pulverized Coal Combustion. Paper read at Proceedings of the Combustion Institute,.
- . 2000b. "Partitioning of Arsenic, Selenium, and Cadmium During the Combustion of Pittsburgh and Illinois #6 Coals in a Self-Sustained Combustor." *Fuel Processing Technology* no. 63 (Compendex):179-196.
- . 2000c. "The Partitioning of Radionuclides During Coal Combustion." *Advances in Environmental Research* no. 4 (Compendex):45-58.
- . 2001. "The Partitioning of Arsenic, Selenium, Cadmium, and Cesium During Pulverized Coal Combustion in a 17 kW Downflow Combustor." *4th International Symposium on Coal Combustion, August 18, 1999 - August 21, 1999* no. 9:219-231.
- . 2007. "Regimes of Association of Arsenic and Selenium During Pulverized Coal Combustion." *31st International Symposium on Combustion, August 5, 2006 - August 11, 2006* no. 31 II:2839-2846.
- Sen, S. 2010. "An Overview of Clean Coal Technologies I: Pre-Combustion and Post-Combustion Emission Control." *Energy Sources, Part B: Economics, Planning and Policy* no. 5 (Compendex):261-271.
- Senior, Constance L. 2000. "Emissions of Mercury, Trace Elements, and Fine Particles from Stationary Combustion Sources." *Fuel Processing Technology* no. 65:263-288.
- Senior, Constance L., Lawrence E. Bool III, Gerald P. Huffman, and Frank E. Huggins. 1996. A Fundamental Investigation of Toxic Substances From Coal Combustion. PSI Technologies, Andover, MA (United States), Univ. of Kentucky, Lexington, KY (United States).

- Senior, Constance L., Frank E. Huggins, Gerald P. Huffman, Naresh Shah, N. Yap, Jost O. L. Wendt, Wayne S. Seames, M. R. Ames, Adel F. Sarofim, Swenson S., JoAnn S. Lighty, Allan Kolker, Robert B. Finkelman, Curtis A. Palmer, Stanley J. Mroczkowski, Joseph J. Helble, R. Mamani-Paco, R. Sterling, G. Dunham, and S. Miller. 2001. *Toxic Substances From Coal Combustion - A Comprehensive Assessment*.
- Senior, Constance L., David O. Lignell, Adel F. Sarofim, and Arun Mehta. 2006. "Modeling Arsenic Partitioning in Coal-Fired Power Plants." *Combustion and Flame* no. 147 (Compendex):209-221.
- Senior, Constance L., Brydger Van Otten, Jost O. L. Wendt, and Adel Sarofim. 2010. "Modeling the Behavior of Selenium in Pulverized-Coal Combustion Systems." *Combustion and Flame* no. 157 (Compendex):2095-2105.
- Senior, Constance L., T. Panagiotou, Jost O. L. Wendt, Wayne S. Seames, Frank E. Huggins, Gerald P. Huffman, N. Yap, M. R. Ames, I. Olmez, Taofang Zeng, Adel F. Sarofim, A. Kolker, R. Finkelman, and Joseph J. Helble. 1998. *Toxic Substances From Coal Combustion: A Comprehensive Assessment*. In *Other Information: PBD: 16 Jul 1998*.
- Senior, Constance L., Taofang Zeng, J. Che, M. R. Ames, Adel F. Sarofim, I. Olmez, Frank E. Huggins, N. Shah, Gerald P. Huffman, A. Kolker, S. Mroczkowski, C. A. Palmer, and R. Finkelman. 2000. "Distribution of Trace Elements in Selected Pulverized Coals as a Function of Particle Size and Density." *Fuel Processing Technology* no. 63 (Compendex):215-241.
- Seshadri, Prasanna, Dennis Sisk, Frank M. Bowman, Steven A. Benson, and Wayne Seames. 2011. *Leachability of Arsenic and Selenium in Submicron Coal Fly Ash*. In *World of Coal Ash* Denver, CO, USA.
- Shah, Pushan, Vladimir Strezov, Chris Stevanov, and Peter F. Nelson. 2007. *Speciation of Arsenic and Selenium in Coal Combustion Products, at 2540 Olentangy River Road, P.O. Box 3337, Columbus, OH 43210-3337, United States*.
- Sheng, Changdong, and Yi Li. 2008. "Experimental Study of ash Formation During Pulverized Coal Combustion in O₂/CO₂ Mixtures." *Fuel* no. 87 (7):1297-1305. doi: 10.1016/j.fuel.2007.07.023.
- Sheng, Changdong, Jun Lin, Yi Li, and Chao Wang. 2010. "Transformation Behaviors of Excluded Pyrite During O₂/CO₂ Combustion of Pulverized Coal." *Asia-Pacific Journal of Chemical Engineering* no. 5 (Compendex):304-309.
- Sidgwick, Nevil Vincent. 1950. *The Chemical Elements and their Compounds*. 2 vols. London, Great Britain: Clarendon Press.

- Sisk, Dennis. 2011a. Characterization of Impurities of Subbituminous Pulverized Coal Combustion to Investigate Ash Formation Mechanisms. Paper read at CleanTech, at Grand Forks, North Dakota.
- . 2011b. Studying the Effects of Blending Coal to Reduce Emission s of Inorganic Particulate Materials. Paper read at Energy, Utility & Environment Conference, 31 January to 2 February 2011, at Phoenix, Arizona.
- Smoot, L. Douglas. 1997. "A Decade of Combustion Research." *Progress in Energy and Combustion Science* no. 23 (3):203-232. doi: 10.1016/s0360-1285(97)00014-2.
- Spears, D. A., and C. A. Booth. 2002. "The Composition of Size-Fractionated Pulverised Coal and the Trace Element Associations." *Fuel* no. 81 (5):683-690. doi: 10.1016/s0016-2361(01)00156-9.
- Spears, D. A., L. I. Manzanares-Papayanopoulos, and C. A. Booth. 1999. "Distribution and Origin of Trace Elements in a UK Coal; the Importance of Pyrite." *Fuel* no. 78 (Compendex):1671-1677.
- Spencer, L J. 1910. "On the Occurence of Alstonite and Ullmanite (a Species new to Britain) in Barytes-Witherite Vein at the New Brancepeth Colliery Near Durham." *Mineralogical Magazine* no. 15.
- Srinivasachar, Srivats, and Arhur A. Boni. 1989. "A Kinetic Model for Pyrite Transformations in a Combustion Environment." *Fuel* no. 68 (July, 1989):829 - 836. doi: 0016-2361/89/070829-08.
- Srinivasachar, Srivats, Joseph J. Helble, and Arhur A. Boni. 1990. "Mineral Behavior During Coal Combustion. 1. Pyrite Transformations." *Progress in Energy and Combustion Science* no. 16 (Compendex):281-292.
- Srinivasachar, Srivats, Joseph J. Helble, Arthur A. Boni, Naresh Shah, Gerald P. Huffman, and Frank E. Huggins. 1990. "Mineral Behavior During Coal Combustion. 2. Illite Transformations." *Progress in Energy and Combustion Science* no. 16 (Compendex):293-302.
- Swaine, Dalway J. 1977. "Trace Elements in Coal." In *Trace Substances in Environmental Health-XI*, edited by Hemphill, 107-116. Columbia, Missouri: University of Missouri.
- . 1990. *Trace Elements in Coal*: Butterworth.
- . 1994. "Trace Elements in Coal and their Dispersal During Combustion." *Fuel Processing Technology* no. 39 (1-3):121-137. doi: 10.1016/0378-3820(94)90176-7.
- Swaine, Dalway J., and F. Goodarzi. 1995. *Environmental Aspects of Trace Elements in Coal*: Kluwer Academic Publishers.

- Thompson, D., and B. B. Argent. 2002. "Thermodynamic Equilibrium Study of Trace Element Mobilisation Under Pulverised Fuel Combustion Conditions." *Fuel* no. 81 (Compendex):345-361.
- Turns, Stephen R. 2000. "An Introduction to Combustion, Concepts and Applications."704.
- U.S. Department of Energy. 2013. International Energy Statistics. Washington, DC: U.S. Department of Energy Energy Information Administration,.
- U.S. Environmental Protection Agency. 2009. "Climate Change, Proposed Endangerment and Cause or Contribute Findings for Greenhouse Gases under the Clean Air Act." no. 2009 (17 August).
- . 2011. Mercury and Air Toxics Standards.
- United States Geological Survey. 1998. Toxic Substances from Coal Combustion-forms of Occurrence Analyses. includes semiannual report for march 31, 1998. United States.
- Valković, V. 1983. *Trace elements in coal*: CRC Press.
- Vassilev, Stanislav V., Kunihiro Kitano, and Christina G. Vassileva. 1996. "Some Relationships Between Coal Rank and Chemical and Mineral Composition." *Fuel* no. 75 (13):1537-1542. doi: 10.1016/0016-2361(96)00116-0.
- Vassilev, Stanislav V., and Juan M. D. Tascón. 2003. "Methods for Characterization of Inorganic and Mineral Matter in Coal: A Critical Overview." *ENERGY & FUELS* no. 17 (2):271-281. doi: 10.1021/ef020113z.
- Vassilev, Stanislav V., and Christina G. Vassileva. 1996. "Occurrence, abundance and origin of minerals in coals and coal ashes." *Fuel Processing Technology* no. 48 (2):85-106. doi: 10.1016/s0378-3820(96)01021-1.
- Vejahati, Farshid, Zhenghe Xu, and Rajender Gupta. 2010. "Trace Elements in Coal: Associations with Coal and Minerals and their Behavior During Coal Utilization - A Review." *Fuel* no. 89 (Compendex):904-911.
- Wang, Qunying, Lian Zhang, Atsushi Sato, Yoshihiko Ninomiya, and Toru Yamashita. 2007. "Interactions Among Inherent Minerals During Coal Combustion and Their Impacts on the Emission of PM10. 1. Emission of Micrometer-Sized Particles." *ENERGY & FUELS* no. 21 (2):756-765. doi: 10.1021/ef0603075.
- . 2008. "Effects of Coal Blending on the Reduction of PM10 During High-Temperature Combustion 1. Mineral Transformations." *Fuel* no. 87 (13–14):2997-3005. doi: <http://dx.doi.org/10.1016/j.fuel.2008.04.013>.

- . 2009. "Effects of Coal Blending on the Reduction of PM10 During High-Temperature Combustion 2. A Coalescence-Fragmentation Model." *Fuel* no. 88 (1):150-157.
- Wewerka, E. M., J. M. Williams, P. O. Wanek, and J. D. Olsen. 1976. *Environmental Contamination from Trace Elements in Coal Preparation Wastes. A Literature Review and Assessment*. United States.
- Wibberley, Louis J., and Terry F. Wall. 1982. "Alkali-ash reactions and deposit formation in pulverized-coal-fired boilers: the thermodynamic aspects involving silica, sodium, sulphur and chlorine." *Fuel* no. 61 (1):87-92. doi: [http://dx.doi.org/10.1016/0016-2361\(82\)90298-8](http://dx.doi.org/10.1016/0016-2361(82)90298-8).
- Wigley, Fraser, Jim Williamson, and Will H. Gibb. 1997. "The Distribution of Mineral Matter in Pulverised Coal Particles in Relation to Burnout Behaviour." *Fuel* no. 76 (13):1283-1288. doi: 10.1016/s0016-2361(97)00139-7.
- Wilke, C. R. 1950. *Chemical Engineering Progress* no. 46:95-104.
- Xu, Minghou, Rong Yan, Chuguang Zheng, Yu Qiao, Jun Han, and Changdong Sheng. 2004. "Status of trace element emission in a coal combustion process: A review." *Fuel Processing Technology* no. 85 (Compendex):215-237.
- Xu, Minghou, Chuguang Zheng, Rong Feng, Yu Qiao, and Rong Yan. 2001. "Overview of Trace Elements Research in Coal Combustion Process." *Zhongguo Dianji Gongcheng Xuebao/Proceedings of the Chinese Society of Electrical Engineering* no. 21 (Compendex):33-38.
- Yan, Li. 2000. *CCSEM Analysis of Minerals in Pulverised Coal and Ash Formation Modeling*, Chemical Engineering, University of Newcastle, Newcastle, NSW, AU.
- Yan, Rong, Xiaohua Lu, and Hancui Zeng. 1999. "Trace elements in Chinese coals and their partitioning during coal combustion." *Combustion science and technology* no. 145 (Compendex):57-81.
- Yinghui, Liu, Zheng Chuguang, and Wang Quanhai. 2003. "Speciation of most Volatile Toxic Trace Elements During Coal Combustion." *Developments in Chemical Engineering and Mineral Processing* no. 11 (Compendex):381-394.
- Yudovich, Ya E., and M. P. Ketris. 2005. "Arsenic in Coal: A Review." *International Journal of Coal Geology* no. 61 (Compendex):141-196.
- Zeng, Taofang. 1998. *Transformation of Iron and Trace Elements During Coal Combustion*. 0801177, Mechanical Engineering, Massachusetts Institute of Technology, United States -- Massachusetts.

Zeng, Taofang, Adel F. Sarofim, and Constance L. Senior. 2001. "Vaporization of Arsenic, Selenium and Antimony During Coal Combustion." *Combustion and Flame* no. 126 (Compendex):1714-1724.